INVESTIGATING THE RELATIONSHIP BETWEEN MICROSACCADES AND OSCILLATIONS IN THE HUMAN VISUAL CORTEX

by Kacper Wieczorek

Supervisors: Krish D. Singh & Petroc Sumner

A thesis submitted to Cardiff University

for the degree of Doctor of Philosophy.

Summary

Neural oscillations play important roles in vision and attention. Most studies of oscillations use visual fixation to control the visual input. Small eye movements, called microsaccades, occur involuntarily ~ 1-2 times per second during fixation and they are also thought to play important roles in vision and attention. The aim of the work described in this thesis was to explore the relationship between microsaccades and oscillations in the human visual cortex.

In Chapter 2, I describe how remote video eye tracking can be used to detect and characterize microsaccades during MEG recordings. Tracking based on the pupil position only, without corneal reflection, and with the participant's head immobilized in the MEG dewar, resulted in high precision gaze tracking and enabled the following investigations.

In Chapter 3, I investigated the relationship between induced visual gamma oscillations and microsaccades in a simple visual stimulation paradigm. I did not find evidence for the relationship. This finding supports the view that sustained gamma oscillations reflect local processing in cortical columns. In addition, early transient gamma response had a reduced amplitude on trials with microsaccades, however the exact nature of this effect will have to be determined in future studies.

In Chapter 4, I investigated the relationship between alpha oscillations and microsaccades in covert spatial attention. I did not find evidence for a relationship between hemispheric lateralization of the alpha amplitude and the directional bias of microsaccades. I propose that microsaccades and alpha oscillations represent two independent attentional mechanisms - the former related to early attention shifting and the latter to maintaining sustained attention.

In Chapter 5, I recorded, for the first time, microsaccade-related spectral responses. Immediately after their onset, microsaccades increased amplitude in theta and beta bands and this effect was modulated by stimulus type. Moreover, microsaccades reduced alpha amplitude ~ 0.3 s after their onset and this effect was independent of stimulus type.

These results have important implications for the interpretation of the classical oscillatory effects in the visual cortex as well as for the role of microsaccades in vision and attention.

DECLARATION

This work has not been submitted in substance for any other degree or award at this or any other university or place of learning, nor is being submitted concurrently in candidature for any degree or other award.

Signed …… (candidate) Date: 30/09/2015

STATEMENT 1

This thesis is being submitted in partial fulfillment of the requirements for the degree of PhD.

Signed …… (candidate) Date: 30/09/2015

STATEMENT 2

This thesis is the result of my own independent work/investigation, except where otherwise stated.
Other sources are acknowledged by explicit references. The views expressed are my own.

Signed …… (candidate) Date: 30/09/2015

STATEMENT 3

I hereby give consent for my thesis, if accepted, to be available online in the University's Open Access repository and for inter-library loan, and for the title and summary to be made available to outside organisations.

Signed …… (candidate) Date: 30/09/2015

STATEMENT 4: PREVIOUSLY APPROVED BAR ON ACCESS

I hereby give consent for my thesis, if accepted, to be available online in the University's Open Access repository and for inter-library loans **after expiry of a bar on access previously approved by the Academic Standards & Quality Committee.**

Signed …… (candidate) Date: 30/09/2015

NOTICE OF SUBMISSION OF THESIS: POSTGRADUATE RESEARCH DEGREES

Please TYPE or write in BLACK ink and use BLOCK capitals

SECTION A: TO BE COMPLETED BY THE CANDIDATE AND SUBMITTED WITH THE THESIS

CANDIDATE'S LAST NAME	WIECZOREK		
CANDIDATE'S FIRST NAME(S)	KACPER		
CANDIDATE'S ID NUMBER	C1128494		
SCHOOL	PSYCHOLOGY		
TITLE OF DEGREE	PHD		
FULL TITLE OF THESIS	INVESTIGATING THE RELATIONSHIP BETWEEN MICROSACCADES AND OSCILLATIONS IN THE HUMAN VISUAL CORTEX		
IS THIS A RESUBMISSION?	NO		
IS A BAR ON ACCESS OR LIBRARY DEPOSIT REQUIRED?	Bar on access: NO Library Deposit: NO		
THESIS SUBMITTED FOR EXAMINATION IN	Permanent binding: X Temporary binding:		
CANDIDATE SIGNATURE		DATE	

Acknowledgments

I would like to say a huge thank you to both of my supervisors, Krish Singh and Petroc Sumner. Thank you for your encouragement and helpful guidance during my time as a PhD student in Cardiff. Thank you for allowing me to explore my own ideas and for providing support with the problems I encountered. I hope we can collaborate again in the future.

I would like to thank Wellcome Trust for funding my PhD and for providing me with excellent experience in different branches of neuroscience.

I would like to thank Suresh Muthukumaraswamy, Gavin Perry, Mark Drakesmith, and Loes Koelewijn for their help with MEG data analysis. Time-frequency decomposition, gradient transformation, source localization, and cluster-based statistics are now much more familiar topics to me.

I would like to thank Olaf Dimingen from Humbold University in Germany for his advice on eye tracking data analysis.

I would like to thank Cyril Charron and Spiro Stathakis, 'the IT guys', for always being helpful and fixing things within five minutes.

I would like to thank Mike Cohen for writing 'Analysing neural time series data' and György Buzsáki for writing 'Rhythms of the brain' – two books I found very useful and stimulating while doing my PhD.

I would like to thank all the staff members and students at CUBRIC for their friendliness, support, and for the really good times on Fridays at the Pen&Wig. Special thanks go to Alberto Merola and Lorenzo Magazzini who were always keen to grab a coffee after lunch and discuss many non-research related topics. I hope you guys submit your PhD theses soon and then go on to have successful research careers.

I would like to thank all my participants. Thanks for sitting perfectly still in the MEG and looking at black and white lines during my long experiments. It all worked out thanks to your brain waves and your microsaccades.

I would like to thank my family for their continuous support, encouragement and love. Submitting this thesis would not be possible without your help.

Finally, I dedicate this thesis to Ilona Lipp – an amazing basketball player, a board game champion, an unparalleled baker, a tireless traveller, and an outstanding scientist. Although she does not know much about studying actual brain activity (she does fMRI), discussing research with her has been very stimulating. Kocham Cię!

Impact of this thesis

Parts of Chapter 1, 2 and the Appendix from this thesis have been presented as posters at international conferences:

Kacper Wieczorek, Petroc Sumner & Krish Singh. (2013). Detecting and characterising microsaccades during MEG recordings using video eye tracking and radial electrooculography. *17th European Conference on Eye Movements*, Lund, Sweden.

Kacper Wieczorek, Suresh D. Muthukumaraswamy, Petroc Sumner, Krish D. Singh. (2014) Visual gamma oscillations recorded with MEG are not affected by the microsaccadic spike artefact. *19th International Conference on Biomagnetism*, Halifax, Canada

Parts of Chapter 1, 2 and the Appendix from this thesis were presented during a talk at a national conference:

Kacper Wieczorek, Petroc Sumner, Krish Singh. (2013). Cortical gamma oscillations and the microsaccadic spike artefact. *MEG-UK*, Nottingham, United Kingdom

Abbreviations

BOLD	Blood oxygen level dependent
ECoG	Electrocorticography
EEG	Electroencephalography
EMG	Electromyography
EOG	Electrooculography
ERF	Event-related field
ERP	Event-related potential
fMRI	Functional magnetic resonance imaging
LGN	Lateral geniculate nucleus
MEG	Magnetoencephalography
MRI	Magnetic resonance imaging
SAM	Synthetic aperture magnetometry
SC	Superior colliculus
TMS	Transcranial magnetic stimulation
V1	Visual area 1, primary visual cortex
V4	Visual area 4

Contents

1 Chapter 1: General Introduction 1

1.1 Overview 2

1.2 Neural oscillations 4

1.3 Microsaccades 12

1.4 Rationale behind the studies 19

2 Chapter 2: Studying microsaccades during MEG recordings using video based pupil tracking 23

2.1 Abstract 24

2.2 Introduction 26

2.3 Important specifications for studying microsaccades 32

2.4 Measuring precision 35

2.5 General eye tracking methods 38

2.6 Discussion 45

3 Chapter 3: Visual gamma oscillations and microsaccades. 47

3.1 Abstract 48

3.2 Introduction 49

3.3 Methods 52

3.4 Results 57

3.5 Discussion 65

4 Chapter 4: Visual alpha oscillations and microsaccades in spatial attention 69

4.1 Abstract 70

4.2 Introduction 71

4.3 Methods 73

4.4 Results 80

4.5 Discussion 90

5 Chapter 5: Microsaccade-related spectral responses 95

5.1 Abstract 96

5.2 Introduction 97

5.3 Methods 100
5.4 Results 105
5.5 Discussion 111

6 Chapter 6: General Discussion 114

6.1 Overview 115
6.2 Microsaccade characteristics 115
6.3 Implications and future directions 117
6.4 General implications for the effect of microsaccades on visual oscillations 119

Appendix 122

References 127

Chapter 1:
General Introduction

1.1 Overview

Neural oscillations provide a promising framework for studying how activity in the visual system is related to information processing, cognition and behaviour. Studies of neural oscillations have proposed mechanistic explanations for how such complex processes as information flow (Jensen et al. 2015; Jensen et al. 2014), information integration (Singer 1999), attention (Klimesch et al. 2007; Fries 2001) and top-down processing (Engel et al. 2001) can be implemented in the brain. Neural oscillatory activity reflects how ensembles of neurons work together and internally create emergent states – a process that is more likely to be directly linked to important functions than single neuron activity (Buzsáki & Draguhn 2004; Yuste 2015). The same neural oscillations, such as the visual gamma oscillation, can often be observed in both invasive animal and non-invasive human studies (e.g. Hall et al. 2005) which enables a very effective comparative approach.

Many, if not most, studies in visual and cognitive neuroscience employ gaze fixation in order to control the visual input and to avoid problems related to eye movements. Most of the studies assume that humans can keep their gaze perfectly still at visual fixation. Although it has been well-established for more than 60 years that humans involuntarily make small eye movements during fixation (Rolfs (2009) for a historical review), recent improvements in non-invasive high-speed video eye tracking have contributed to our current understanding that visual fixation is a dynamically rich process during which a few types of fixational eye movements play an active role in visual processing and attention (Martinez-Conde et al. 2004; Martinez-Conde et al. 2013). Most prominent of these fixational eye movements are microsaccades - jerk-like flicks of the eye that occur ~ 1 -2 times per second. Microsaccades have recently received much attention regarding their functions in vision and attention as well as their causal role in important observations that had previously been attributed to central neural mechanisms (e.g. Yuval-Greenberg et al. 2008; Hafed 2013).

Given that both microsaccades and visual oscillations play important roles in vision and attention, it is surprising that the relationship between two is relatively unexplored. The experiments in this thesis were designed to investigate the interplay between the two. In this introductory chapter, I will first focus on neural oscillations. I will then explain what neural oscillations are and describe some of their important characteristics. Then, I will give some reasons for the recent growing interest in the topic. Subsequently, I will review studies that contributed to our understanding of the functional roles of alpha, beta and gamma oscillations in vision. Lastly, I will present how neural oscillations can be recorded non-invasively in humans with magnetoencephalography (MEG).

In the second part of this chapter, I will focus on microsaccades. First, I will explain the difference between microsaccades and other fixational eye movements. Then, I will review evidence on how microsaccade characteristics can be affected by stimulus properties. Subsequently, I will describe studies that linked microsaccades to visual spatial attention. Lastly, I will explain what important roles microsaccades were proposed to play in visual processing.

In the third part of this chapter I will briefly explain the motivation behind each of the studies described in this thesis. In short, Chapter 2 describes the method to detect and characterise microsaccades during MEG recordings. Chapter 3 is motivated by the suggestions that microsaccade-related activity (muscle and cortical) can contaminate recordings of stimulus-driven gamma oscillations. Chapter 4 explores the potential relationship between microsaccades and visual alpha oscillations in mediating visual spatial attention. Chapter 5 stems from our lack of knowledge about oscillatory responses related to microsaccades in the human visual system.

1.2 Neural oscillations

1.2.1 What are neural oscillations?

The term ‘neural oscillations’ is most frequently used in reference to the temporal rhythmicity of measures of neuronal population field activity at different spatial scales such as LFP, ECoG, EEG and MEG. These continuous signals, commonly viewed in the time-domain as waveforms, can be transformed to the frequency domain using Fourier analysis. This process enables illustration of the signal as a power spectrum that provides a quantitative power relationship between the frequencies. Oscillations are identified as peaks in the power spectrum that deviate from the typical spectrum of pink noise (1/f) or as increases in amplitude from baseline activity at specific frequencies. Because the power spectrum representation ignores the temporal variation, time-frequency methods, for instance wavelet or Hilbert transforms, have been developed to illustrate how the power spectrum dynamically changes over time.

The term neural oscillation is also used in reference to periodic patterns of action potentials (spikes). While spiking activity of single cortical neurons generally follows a Poisson distribution (Bair et al. 1994), spiking activity of a neuronal assembly (recorded with multiunit activity) often displays oscillatory properties (Gray & Singer 1989; Wang 2006). Oscillations of these discrete signals are commonly presented in the form of auto-correlograms and cross-correlograms.

Neuronal networks in the mammalian cortex generate oscillations in several distinct bands, covering frequencies from < 0.05 Hz to >500 Hz (Buzsáki 2006). The first and still most popular classification of oscillatory rhythms was introduced by the International Federation of Societies for Electroencephalography and Clinical Neurophysiology: 0.5-4 Hz (delta), 4-8 Hz (theta), alpha 8 – 12 Hz (alpha), 12-30 Hz (beta), > 30Hz (gamma). More recently, Buzsáki & Draguhn (2004) proposed a taxonomy of neural oscillations based on three most prominent hippocampal rhythms in the rat. Other

frequency bands were interpolated from these rhythms. As a result, the mean frequencies of distinct oscillatory bands formed a linear progression on a natural logarithmic scale with a constant ratio between neighbouring frequencies. However, this taxonomy does not include the alpha rhythm - the most prominent oscillation in the awake human brain. Classification of oscillatory rhythms in frequency bands is therefore, to some extent, arbitrary and there are considerable inconsistencies in the exact ranges of these bands across studies. Moreover, the classical frequency bands often do not capture the true oscillatory dynamics underlying specific functions. For instance, identified oscillatory effects can span multiple classical bands (e.g. from theta to beta during perceptual suppression - Maier et al. 2008) and different processes can occur in different sub-bands of the classical bands (e.g. in distinct gamma sub-bands for attention and target detection (Wyart & Tallon-Baudry 2008)). Currently, functional frequency bands tend to be defined in a data-driven fashion (Donner & Siegel 2011), however, classical frequency bands are still being used.

Functional frequency bands for neural oscillations are often related to information processing, behaviour and cognitive tasks. However, a power spectrum of a field recording from a resting mammal shows a general pattern of amplitude being inversely related to frequency: the amplitude increases as the frequency decreases ($A \sim 1/f$), with no distinct peaks (except for alpha ~10 Hz). Signals with this power spectrum are called pink noise. This spectral pattern is remarkably consistent across spatial scales (from microelectrode LFP recordings from a few hundred neurons to scalp EEG recordings from millions of neurons) and cross mammals (Buzsáki 2006). The pink noise characteristic of field activity may be to some extent explained by filtering properties of the brain tissue. Specifically by the low-pass frequency filtering property of dendrites and the extracellular medium (Buzsáki et al. 2012). However, the skull is now not thought to filer neural signals up to several kHz (Oostendorp et al. 2000). Faster oscillations are attenuated more than slow

rhythms. However, a more attractive explanation from a neuroscientist's perspective is that low frequency oscillations recruit larger populations of neurons because they allow longer axon conduction and synaptic delays while for the same reasons only a small group of neurons can follow fast rhythms. As a consequence widespread slow oscillations may modulate faster local oscillations (Buzsáki 2006).

1.2.2 Why are neural oscillations important?

The recent growing interest in neural oscillations (Buzsáki & Draguhn 2004; Fries 2009) stems from a number of factors. First, in the past, strong oscillatory EEG patterns were mainly observed during states of idling such as during rest, sleep (Crunelli & Hughes 2010), and anaesthesia or associated with neurological disorders such as epilepsy (Steriade 2001). Conscious behaviour was associated with low-amplitude desynchronised patterns. More recently, however, neural oscillations have been linked to many information processing and cognitive functions. For instance, alpha frequency, previously associated with idling, has been recently shown to play an active role in such processes as attention, memory and consciousness (Jensen & Mazaheri 2010; Klimesch 2012; Palva & Palva 2007). Moreover, high frequency rhythms in the beta (15-30 Hz) and gamma (>30 Hz) bands in the waking brain were robustly characterised and are now thought to play important roles in cognition and behaviour (Engel & Fries 2010; Fries et al. 2007). In contrast to the slow oscillations that tend to have a more global character (Steriade et al. 1993), these fast oscillatory states are more often local and relatively transient (a few hundreds of milliseconds; Donner & Siegel (2011)).

Second, it became possible to create neural oscillations under controlled conditions. Experiments carried out in brain slice preparations in vitro exclude variables that are uncontrollable in the intact brain and allow for systematic changes, for instance using pharmacological manipulations, of various parameters that play a role in

emergence, maintenance and termination of neural oscillations (Buzsáki 2006; Khalilov et al. 1997). More recently, neural oscillations were entrained in vivo in rodents using optogenetic tools (Sohal 2012) and in humans using TMS (Thut et al. 2012). These methods further enabled investigations into the mechanisms of oscillations and, most importantly, helped to establish a more causal link between oscillations and behaviour.

Third, analysing neural signals within an oscillations framework allows for richer signal characterisation. Instead of being constrained to the event-related average spike rate or the time-domain averaged amplitude modulations of field activity, one can also look at time-frequency and phase dynamics (Cohen 2011; Makeig et al. 2004). Moreover, the oscillatory approach to brain signals also enables more effective investigations into ongoing, spontaneous, activity and neural connectivity. In general, the oscillatory framework provides more ways in which information in the brain can be represented and processed. Systematic investigations of these oscillatory characteristics of neural signals on a global scale (all sensors/electrodes (M/EEG) or multiple sites on high-density silicone probes) became possible with recent improvements in computational power and in neural signal processing algorithms (Le Van Quyen & Bragin 2007).

1.2.3 Functional role of neural oscillations in the visual system

Alpha oscillations (~ 10 Hz) at occipital and parietal sites are the strongest and most readily-observed electrophysiological signals that can be measured from the awake human brain. Early studies found the alpha rhythm to be attenuated by eye opening, visual stimuli presentation and by increased attentiveness. These observations lead to the formulation of the hypothesis that alpha oscillations function as an 'idling rhythm' that is characteristic for a resting but alert state (Adrian & Matthews 1934). Observations that alpha oscillations are stronger during internal tasks such as mental arithmetic and visual imagery than during attention to one's environment, inspired the idea that this rhythm

reflects disengagement from the environment (Ray & Cole 1985). However, more recent studies showed that alpha oscillations play an active role in information processing. This function of alpha oscillations was first based on observations that low alpha amplitudes are associated with regions of active neuronal processing, whereas large-amplitude alpha oscillations reflect the inhibition of stimulus and task-irrelevant cortical areas (Pfurtscheller 2001; Klimesch 1996). Apart from being modulated by the stimulus in a bottom-up manner, alpha oscillations amplitude is also modulated by attention. Visual and auditory spatial cues are followed by alpha suppression that is larger in the occipital cortex contralateral than ipsilateral to the attended visual hemifield (Worden et al. 2000; Thut et al. 2006). This effect is thought to reflect the 'spotlight of attention' mechanism that acts by releasing the task-relevant areas from inhibition and by suppressing task-irrelevant regions with large-amplitude alpha oscillations (Klimesch et al. 2007). In a recent striking demonstration of this mechanism, Zumer et al. (2014) observed that the alpha lateralisation predicted increases of fMRI BOLD signal to attended objects and decreases to unattended objects in ventral object-selective regions. This observation provided evidence for a related proposal that alpha band activity serves to route information to downstream regions by inhibiting neuronal processing in task-irrelevant regions and therefore allowing task-relevant regions to communicate (Jensen & Mazaheri 2010).

The role of visual beta oscillations (~ 15-30 Hz) is not well-studied and beta oscillations, outside the primary motor cortex, are arguably the least studied classical frequency band of all neural oscillations. However, a recent review article suggested a unifying hypothesis based on the limited evidence. Engel & Fries (2010) proposed that beta-band activity is related to the maintenance of the current sensorimotor, cognitive or perceptual state, and that oscillations and coupling in the beta-band should be stronger for endogenous, self-generated brain states and are weaker if a change occurs triggered by external exogenous factors. Although this proposed function is rather vague, there is a

fair amount of evidence that supports their claim. First, it is a well-established effect in vision that stimulus-driven processing that does not have an endogenous, top-down, component, causes a reduction in beta-band activity. Recent evidence suggests that this general effect in extrastriate cortex may be dependent on intact primary visual cortex. Schmiedt et al. (2014) showed that visual stimuli surprisingly elicited large increases in beta amplitude in V4 but only when the stimulus was presented in locations that corresponded to parts of V1 affected by a lesion. Second, tasks that strongly involve endogenous top-down processes, such as for instance when a stimulus is constant but perception of the stimulus fluctuates, were linked to beta oscillations. Beta amplitude increases were reported around the time of perceptual switch in ambiguous figure perception (Okazaki et al. 2008), illusory motion reversal (Piantoni et al. 2010), and binocular rivalry (Piantoni et al. 2010). Moreover, beta amplitude increases were also associated with bound (as opposed to unbound) perception of ambiguous moving objects (Aissani et al. 2014), illusory perception in the sound induced-flash illusion (Keil et al. 2014), and subjective visibility of a visual target (Wilke et al. 2006). Aside from Engel & Fries's (2010) proposal, beta activity in the human dorsal visual pathway predicted correct choices in a visual motion detection task and was proposed to control the efficiency of neural computations in simple perceptual decisions (Donner et al. 2007). In summary, it appears that visual beta oscillations are suppressed by bottom-up stimulus processing, an effect that in extrastriate areas may be controlled by V1, and are enhanced by switches in perception of ambiguous figures and states of subjective visibility.

Gamma oscillations in the visual cortex were first recorded by Gray & Singer (1989) and their observations had a great impact on the entire neuroscience community. They found that LFP and multi-unit activity in anesthetized cat's primary visual cortex displayed oscillations in the 30 – 60 Hz band in response to moving bars. Unit activity was phase-locked to the trough of the field oscillation, but the units and the field were not time

locked to the onsets or other aspects of the visual stimuli, providing striking evidence that oscillatory neuronal ensemble activity can result from an emergent local state. Also, the observation that synchronization of the discharges of spatially segregated neurons depended on them being activated by contours that of the same object that were either continuous or moved coherently with the same speed in the same direction lead the binding-by-synchrony hypothesis. The hypothesis states that cerebral cortex synchronises discharges of neurons to bind responses for further joint processing to encode relations (reviewed in Singer (1999)). Gamma oscillatory synchrony is now thought to represent a fundamental cortical computation (Fries 2009). Gamma oscillations are now routinely recorded in humans using EEG and MEG but it is unclear to what extent muscle artefacts contaminate these recordings (Whitham et al. 2007; Yuval-Greenberg et al. 2008; Muthukumaraswamy 2013).

1.2.4 Neural oscillations can be recorded in humans non-invasively with MEG

Although much has been learnt from invasive animal studies of visual oscillations, the ultimate goal is to understand their mechanisms and their functions in perception, cognition and behaviour in the human brain. Activity of the human brain can only be recorded from outside the scalp (with the exception of rare cases when EEG electrodes are placed on the cortical surface (ECoG) or when depth electrodes are implanted inside the brains of neurological patients undergoing brain surgery). This poses a substantial problem for the recording of electrical signals with such methods as scalp-EEG because these signals are smoothed due to the distorting and attenuating effects of the soft and hard tissues between the current source and the recording electrodes (Buzsáki et al. 2012). However, any electrical current generates an associated magnetic field perpendicular to the direction of the current and this magnetic field can be measured with MEG.

An advantage of MEG is that magnetic signals are much less dependent on the conductivity of the extracellular space than EEG, resulting in greater spatial discrimination of neural contributions. This enables a more accurate neural source localization. The frequency versus power relationship is different for EEG and MEG, typically in the higher frequency bands. These differences may be partly explained by the capacitive properties of the extracellular medium (such as skin and scalp muscles) that distort the EEG signal but not the MEG signal (Dehghani et al. 2010). What is more, MEG measures are absolute – they are not dependent on the choice of a reference.

However, because magnetic fields produced by the brain are several orders of magnitude smaller the environmental electromagnetic noise, their measurement is challenging. It is routinely done using very sensitive magnetic sensors called SQUIDs (super-conducting quantum interference devices) that are immersed in liquid helium at -269 ^{o}C. The latest generation of MEG scanners contain 275 – 300 sensors that cover the entire head. To protect the neural measurements from environmental noise, scanners are placed in multi-layered magnetically shielded rooms and recordings are done using combinations of pick-up coils (known as 'gradiometers') that render the sensors differentially sensitive to the closer neural signals. MEG has excellent temporal resolution because SQUIDs can operate at acquisition rates higher than the highest frequency in the brain signals.

It is unlikely that action potentials will give rise to a magnetic field measureable with MEG because they are temporally brief events and therefore the probability that action potentials synchronise precisely is rather low. Also, magnetic fields of two closely spaced opposing current sources (one depolarising and one repolarising), that arise when an action potential is travelling down an axon, falls off rapidly with distance. Therefore it is more likely that MEG signal is generated by postsynaptic potentials in the dendrites of neuronal populations (Hämäläinen et al. 1993). The weakest measureable cortical signals

can be produced by around fifty thousand synchronously active neurons (Lopes da Silva 2013), however, signals related to cognition that can be modulated by experimental factors would normally involve synchronous firing of millions of neurons from approximately 25 mm^2 of the cortical surface (Singh 2006). Moreover, dendritic processes need to be spatially aligned in order to generate a measureable magnetic field such as for instance apical dendrites of pyramidal cells.

Although MEG only gives us access to spatially smoothed synchronous activity of large numbers of neurons, this is not necessarily a disadvantage. The most efficient way to establish synchrony in neuronal populations is by creating oscillations (Buzsáki 2006). As many perceptual and cognitive process are related to synchronous oscillations it is likely that MEG gives us access to one of the most important types of brain activity.

1.3 Microsaccades

1.3.1 What are microsaccades?

In many animals, including humans, photoreceptors are not uniformly distributed across the retina. Instead, photoreceptor density rapidly declines from a small region approximately at the centre of the fovea, where the density is the highest. As a consequence, human vision relies on sequences of rapid eye movements, called saccades, which align the fovea with objects of interest enabling high-resolution processing during so called fixations.

However, human eyes are never completely still. When we attempt to fix our gaze, our eyes nevertheless produce so-called 'fixational eye movements', which include microsaccades, drift and tremor. In fact, a recent analysis of fixational eye movements in a large sample of untrained observers revealed that fixational dispersion of gaze was much larger than previously thought (Cherici et al. 2012). During fixation, our eyes slowly

drift (< 0.5 deg/s) in an erratic manner that can approximated with random walk models. Simultaneously with drift, our eyes exhibit small (< 0.01 deg) aperiodic, wave-like motion with a frequency of ~90 Hz, known as tremor. Microsaccades are small saccades that interrupt the simultaneous drift and tremor motion around 1-2 times per second during attempted fixation. Small saccades the size of microsaccades can also be made voluntarily, for instance in order to precisely relocate gaze in high-acuity tasks (Ko et al. 2010). Since it is difficult to distinguish between voluntary and involuntary movements (but see Sinn & Engbert 2015), microsaccades are commonly defined as saccades smaller than threshold size (1 - 2 deg in video eye tracking studies) that occur during attempted fixation. An average microsaccade size is ~0.35 deg. Microsaccades differ from drift and tremor because they result in larger gaze displacements and have higher velocity. The time-course of velocity for each microsaccade is highly stereotypical and approximately symmetric around its peak. A key property of microsaccades is that they share a fixed relation between peak velocity and movement amplitude with regular saccades (Zuber et al. 1965). This relation is a consequence of the ballistic nature of microsaccades. To underline the importance of this fixed relation between peak velocity and amplitude, it is often referred to as the ‘‘main sequence’’ (Bahill et al. 1975). Microsaccades are generally considered binocular movements. A vast majority of microsaccades in humans have horizontal directions and oblique directions in all species with foveal vision are observed very rarely. The growing interest in microsaccades and their role in vision is reflected in a large number of recent review articles on the topic (Martinez-Conde et al. 2013; Martinez-Conde et al. 2009; Rolfs 2009; Poletti & Rucci 2015; Collewijn & Kowler 2008; Engbert 2006).

1.3.2 Microsaccades are modulated by stimulus

A number of factors have been reported to affect microsaccade characteristics. For instance, McCamy, Najafian Jazi, et al. (2013) found that as fixation spot size increased microsaccade rates and preference for horizontal direction decreased while microsaccade amplitudes increased. Thaler et al. (2013) studied the effect of fixation spot shape and found that a combination of bull's eye and crosshair yielded lower microsaccade rates than other commonly used fixation spot shapes. Surprisingly, it was found that an instruction to keep relaxed fixation in the centre of the screen without a fixation marker (during presentation of grayscale natural images) resulted in lower microsaccade rates than fixation on a marker (Poletti & Rucci 2010).

The most striking modulation of microsaccade characteristics is triggered by stimulus and cue onsets. Microsaccade rate first drops to a minimum shortly after stimulus onset (at ~ 0.15 s, 'microsaccadic inhibition') and then increases to a higher rate (at ~0.25 s, 'microsaccadic rebound') before returning to baseline. Rolfs et al. (2008) found that microsaccadic inhibition occurred sooner after auditory than after visual stimuli and after luminance-contrast than after colour-contrast visual stimuli. The latency of microsaccadic inhibition increased with decreasing luminance contrast. Moreover, microsaccade amplitude strongly decreased during microsaccadic inhibition. They concluded that microsaccadic inhibition it mediated via the fast retinotectal pathway from the retina to the superior colliculus and results from suppression of activity at the central part of the superior colliculus motor map. However, this conclusion is not in line with the observation that cognitive factors can affect the duration of the inhibition period, for instance that oddball stimuli in a visual oddball tasks substantially prolonged the inhibition period and abolished the microsaccadic rebound (Valsecchi et al. 2007). According to Hafed & Ignashchenkova (2013) the suppression-rebound sequence after stimulus onset can be explained by phase resetting of an ongoing microsaccadic oscillatory rhythm. In their framework, stimulus

onsets cancel the upcoming microsaccade and resume the microsaccadic rhythm anew. Stimulus parameters were also found to modulate the microsaccadic rebound: arrow cues produced stronger microsaccadic rebound than colour cues (Engbert & Kliegl 2003); visual object familiarity, object-coherence, and number of object-masking bars modulated microsaccade amplitudes and rates in the rebound period (Yuval-Greenberg et al. 2008).

What is more, latency of the first microsaccade in the rebound interval robustly decreased as contrast of a briefly presented Gabor patch increased (Bonneh et al. 2015). Spatial frequency in this contrast detection experiment had the same effect on accuracy of behavioural responses as on latency of microsaccades and the same contrast sensitivity function could be obtained from both measures.

While the bulk of research focused on the stimulus-triggered microsaccade modulations, there are also some reports of modulations in other scenarios. For instance, during free-viewing of natural scenes microsaccade rates were increased during fixations on highly informative regions (M. B. McCamy et al. 2014). Two moving contrast bars triggered sustained decreases in microsaccade rates (Hipp & Siegel 2013). The complexity of visual stimulation has also been shown to increase inter-microsaccadic-intervals (Amit & Greenberg 2015). However, little is known about microsaccadic dynamics during sustained presentation of stimuli and whether stimulus parameters such as contrast or spatial frequency affect microsaccade characteristics during these sustained presentations.

1.3.3 Microsaccades and attention

Despite the common assumption that covert orienting occurs in the absence of eye movements (Carrasco 2011), it is now clear that microsaccades are present during covert attention and that attentional allocation influences microsaccade dynamics. The most robust effect of attention on microsaccades is observed in classic Posner-style (Posner

1980) spatial cueing paradigms during the cue-triggered rebound interval (~ 0.25 s after cue onset) when microsaccade rates are increased. In this interval, most microsaccade are generated towards the cued location (Hafed & Clark 2002; Engbert & Kliegl 2003; Laubrock et al. 2010). It is important to note here that microsaccades do not relocate the gaze all the way to the attentional target as targets are usually placed a few degrees of visual angle away from the fixation spot and the average size of a microsaccade is ~0.3. The effect of is the strongest for first microsaccades after cue-onset in each trial and, appear not to be present after the rebound-interval in the classic spatial-cueing paradigm (Laubrock et al. 2010). However, in other more complex covert attention paradigms it appears that the microsaccades are biased towards the cue-direction during the sustained periods between cue and target onset (Hafed et al. 2011; Pastukhov & Braun 2010).

Hafed (2013) showed a relationship between the biasing of microsaccade directions towards the cued location and behavioural performance. Performance was found to be higher on trials where microsaccades directed towards the target occurred immediately after target onset (and up to ~75 ms after target onset). This observation was explained as a pre-microsaccadic compression of space phenomenon, described for the first time in the same article. There are no reports of significant relationship between the directions of microsaccades in the cue-triggered rebound period to behavioural performance. Microsaccades, regardless of direction, can have a negative impact on accuracy and reaction times of behavioural responses in attention tasks when they occur just before or exactly at target onset (Pastukhov & Braun 2010; Hafed 2011). This effect is probably due to the 'microsaccadic suppression' phenomenon whereby visual responsiveness is transiently supressed during microsaccades in order to provide perceptual stability and avoid blurring due to retinal motion, similarly to saccadic suppression (Herrington et al. 2009; Zuber & Stark 1966). Interestingly, spontaneous microsaccades occurring during fixation without any attentional tasks also lead to or reflect

shifts of covert attention. In a demonstration of this phenomenon Yuval-Greenberg et al. (2014) showed that targets appearing immediately after microsaccade onsets (controlled with gaze-contingent stimulus presentation) in the locations consistent with microsaccade direction were discriminated better than targets appearing in the opposite location.

1.3.4 Functions of microsaccades in visual processing

Given how ubiquitous microsaccades are (1-2 times per second) during fixation, a number of studies investigated what roles these eye movements may play in vision. Microsaccades have been shown play a number of roles similar in nature to those of regular saccades that involve relocating the centre of gaze. Microsaccades control fixation position (Engbert & Kliegl 2004), scan small regions of space (Otero-Millan et al. 2008), and relocate gaze in high acuity tasks (Ko et al. 2010). Do microsaccades, however, have a more fundamental function in central visual processing?

In the early history of eye movement research several groups demonstrated, using retinal stabilisation techniques, that the visual perception of stationary objects faded in the absence of eye movements (Ditchburn & Ginsborg 1952; Riggs & Ratliff 1952). As a consequence, fixational eye movements were related to the prevention of visual fading and to the restoration of visibility during fixation. More recent studies directly tested these hypothesis and found that microsaccades counteracted visual Troxler fading of peripheral targets (Martinez-Conde et al. 2006), restored visibility of foveal targets that extended to the periphery (McCamy et al. 2012) and of exclusively foveal targets of minute size (Costela et al. 2013). Crucially, the effect of microsaccades on restoring vision and counteracting visual adaptation was also present during a more ecologically valid condition of free head movement, demonstrating that the observed effect is not a laboratory artefact (Martinez-Conde et al. 2006). Despite these rather convincing findings, some authors have argued that fixation drift movements can account for the counteracting

visual fading function and that microsaccades do not play a significant role in vision (Collewijn & Kowler 2008; Poletti & Rucci 2010). Two recent studies that quantified the relative contribution of microsaccades and drift to restoring vision after fading concluded that microsaccades contribute the most of all fixational eye movements to restoring normal vision after fading (McCamy et al. 2012), however both microsaccades and drift play equally important roles in preventing fading before it takes place (Michael B McCamy et al. 2014).

As well as counteracting and preventing visual fading, microsaccades may enhance the signal-to-noise ratio of the visual input. This proposal is supported by the fact that moving a stimulus with a frequency and amplitude that resembles microsaccades increases the signal-to-noise ratio of a threshold-level stimulus in cat visual cortex (Funke et al. 2007). Also psychophysical results from human subjects showed that microsaccades improve discrimination of high spatial frequency stimuli that are masked by noise through enhancement of the signal-to-noise ratio (Rucci et al. 2007). Moreover, microsaccades were proposed to constitute a discrete temporal sampling method of the visual system based on the observations that transient firing patterns in visual neurons are similar following microsaccades and stimulus onsets (Martinez-Conde et al. 2002; Martinez-Conde et al. 2004). Others have proposed that the discrete sampling function of microsaccades mediated by the fact that visual processing after microsaccades is enhanced due to corollary activity from the motor system (Melloni, Schwiedrzik, Rodriguez, et al. 2009).

1.4 Rationale behind the studies

1.4.1 Detecting and characterising microsaccades during MEG recordings

Given that both neural oscillations and microsaccades play important roles in visual processing and cognition and that most recordings of visual oscillations in humans are done with participants instructed to fixate a central spot, it is surprising that the relationship between the two remains almost unexplored. Recently, it became possible to study these small eye movements in humans non-invasively using high-speed video eye tracking. MEG compatible remote video eye tracking systems are now available that can be kept at distance to the MEG dewar. However, given a small size of microsaccades (on average ~ 0.3 deg: Martinez-Conde et al. 2013)), detection and characterisation during MEG recordings is still challenging. Remote video eye trackers are designed for setups whereby participants can freely move their head. The on-line process of correcting for head movements in remote eye tracking, even when head movements are almost absent, introduces a substantial proportion of noise to the recording and has a detrimental effect on precision of gaze estimation. In Chapter 2, I show how precision can be boosted by turning off the head movement correction mechanism. The possible downside of small head movements not being corrected for and therefore introducing artefacts in the recording is taken care of by effectively immobilising the participant's head in the MEG dewar with headcuff and chinrest. Chapter 2 illustrates how, using this setup, one can reliably record microsaccades during MEG recordings. In subsequent chapters the method is utilised to study the relationship between visual oscillations and microsaccades.

1.4.2 Visual gamma oscillations and microsaccades

Most of classic and contemporary studies in vision science and cognitive neuroscience require subjects to fixate a target. Target fixation serves as a normalizing factor across studies and a control of the visual input between conditions. However,

because characteristics of microsaccades are modulated by both experimental and group variables it is possible that microsaccade-related signals may appear as task or stimulus-related effects. For instance, it was suggested that increases in fMRI BOLD signal in early visual areas following microsaccades indicate that 'results of fMRI studies may arise because of microsaccades, and not the experimental variables under consideration, forcing a re-evaluation of many past fMRI results' (P. Tse et al. 2010; Martinez-Conde et al. 2009). Also, Dimigen et al. (2009) showed that microsaccade characteristics were modulated by task demands in a visual oddball task and in turn lead to a condition-specific modulation of the P300 ERP component.

Microsaccades can be related to oscillatory signals in the gamma frequency range in two ways. First, the frequency spectrum of muscle activity overlaps entirely with the cortical gamma range and is several orders of magnitude larger. An EEG study found recently that an increase in number of microsaccades (and therefore the related muscle artefacts) between 200 and 300 ms after stimulus onset lead to the microsaccade-related saccadic spike artefact being mistaken for genuine cortical visual gamma (Yuval-Greenberg et al. 2008). This mis-identification appears to be mostly due to the use of a frontal EEG reference that became contaminated with the saccadic spike artefact. The same study also found that experimental conditions that were thought to be modulating visual gamma oscillations were actually modulating microsaccade rates and amplitudes. Another EEG study found that the microsaccadic spike artefact lead to a suppression of task-related gamma oscillations in an experiment where the visual stimulation was non-stationary (two moving contrast bars; Hipp & Siegel 2013). The second potential source of microsaccade-related modulations of gamma activity is of neural origin. Bosman et al. (2009) studied peri-microsaccadic neural activity in monkey visual cortex and reported gamma amplitude increases before and after microsaccades. Similar modulations of gamma oscillations in the occipital cortex were found after regular saccades in monkeys

(Rajkai et al. 2008) and in human epileptic patients studied with ECoG (Nagasawa et al. 2011). In Chapter 3, we test whether MEG-measured sustained visual gamma oscillations are related to microsaccades.

1.4.3 Visual alpha oscillations and microsaccades in spatial attention

Given that covert spatial attention modulates both directions of microsaccades and relative alpha amplitude between the two hemispheres, there is possibility that the two may be related. The existence and the possible nature of the relationship is yet to be investigated. What is more, microsaccades have been shown to explain a link between behaviour and neural activity in a motion detection task (Herrington et al. 2009) and it is possible that this could explain the link between attention and alpha oscillations. In Chapter 4, we aimed to determine whether microsaccades and alpha oscillations represent related or independent attentional processes. We also aimed to investigate whether microsaccades can explain the link between alpha oscillations and attention.

1.4.4 Microsaccade-related spectral responses

To understand how the proposed functions of microsaccades can be implemented at the neural level it is important to study peri-microsaccadic activity in the visual cortex. Most of what we know about peri-microsaccadic activity in the visual system comes from single-neuron recordings in monkeys (Kagan et al. 2008; Leopold & Logothetis 1998; Martinez-Conde et al. 2000; Martinez-Conde et al. 2002). Recently, Melloni et al. (2009) suggested that corollary activity related to saccades and microsaccades interacts with the ongoing oscillations in the visual cortex to enhance the processing of visual signals immediately after eye movements. A recent study observed microsaccades-related modulations of visually induced gamma oscillations in areas V1 and V4 of alert monkeys and that these modulations were correlated with variability in behavioural response speed,

suggesting that microsaccades structure the sampling of the visual environment through transient gamma-band synchronisation of visual neuronal ensembles (Bosman et al. 2009). In Chapter 5, we aimed to characterise, for the first time, spectral responses to microsaccades in humans.

Chapter 2: Studying microsaccades during MEG recordings using video based pupil tracking

2.1 Abstract

A method to reliably study microsaccades during MEG recordings would enable effective investigations into both the related muscle artefact and the fundamental impact these eye movements have on visual processing. However, eye tracking in the MEG environment is challenging. Only systems that do not require physical contact with a participant and are specially designed not to introduce noise in MEG recordings can be used. Remote video eye tracking is currently the best solution as it meets these two criteria and, in addition, is non-invasive and provides rich information about eye movements. In this method, a noisy estimate of the position of the corneal reflection in the video image is used as a reference to correct for head movements. Some remote systems allow for recording in a 'pupil-only' mode, although this is only recommended when the head is kept completely still and data precision is prioritized over accuracy.

Data quality varies dramatically between video eye trackers and it is important to establish what specifications are sufficient and optimal to reliably study microsaccades. Because microsaccades are generally conjugate movements, monocular recordings are sufficient, although data from both eyes is often used to reduce the number of false positives in detection algorithms. A sampling frequency of 200 Hz and higher is recommended; however, faster systems can potentially study microsaccades of shorter durations and estimate their parameters more accurately. High precision quantification of small difference between consecutive position samples when gaze is held constant is critical for studying small eye movements. However, manufacturers rarely disclose how the precision of their systems is calculated and therefore their estimates are difficult to interpret.

Here, I measured precision specifically for our setup and stimuli type during central fixation. I also took advantage of the fact that our system allows pupil-only recordings and that a participant's head can be immobilised in the MEG helmet with a chinrest and a

headcuff to avoid head movement artefacts. I found that median RMS precision was around 0.013 deg when recording in pupil-only mode, which was approximately 2.5 better than when using corneal reflection.

Based on these considerations and measurements, and also subject to practical limitations, eye movement data were recorded monocularly using a 250 Hz remote video eye tracker operating in a pupil-only mode. Microsaccades were detected using a common algorithm with adaptive velocity thresholds based on a median estimator of standard deviation. For a signal to be classified as a microsaccade, three consecutive data samples were required to exceed an elliptical velocity threshold formed from the x and y components.

The magnitude of the detected microsaccades showed a strong correlation with velocity – the so-called 'main sequence' distribution, validating our identification procedures. We conclude that with such a high precision setup we can reliably detect microsaccades and characterise their parameters during MEG recordings while effectively controlling for head movements. This method can be used with any remote video eye tracker that supports gaze estimation using pupil position information only.

2.2 Introduction

2.2.1 Eye tracking in MEG is challenging

Studying eye movements in MEG environment is challenging for a number of reasons. First, the MEG sensors are extremely sensitive and only eye tracking systems specially designed not to introduce magnetic field noise artefacts in MEG recordings can be used. Second, a participant's head must be placed in the MEG helmet during a recording and, because of this, eye tracking systems that require physical contact with, or a close proximity to, a participant's head, are not suitable. As a result many systems that provide good quality data cannot be used and only long-range systems, which in general tend to provide worse data quality (Holmqvist et al. 2011), are suitable. Third, regardless of whether an experimenter's goal is either to limit the vestibulo-ocular reflex by reducing a participant's head movements or to study more natural eye movements by allowing free head movements (Aytekin et al. 2014), MEG is not an optimal environment. Depending on a participant's head size, there is a gap between a participant's head and the MEG helmet ranging from a few millimetres to a few centimetres. Therefore, on one hand there is no complete head stabilization (unless extra equipment is used), and on the other hand a participant cannot freely move their head, which is also desirable from a MEG data quality perspective. Because of these reasons eye tracking in the MEG environment is not commonly done. Exception are studies that do not study eye movements explicitly but use eye tracking techniques, for instance bipolar EOG (usually uncalibrated), to control for large eye movements in experiments that require continuous fixation. A Web of Science literature search for original research articles with keywords and phrases 'MEG' or 'Magnetoencephalography' and 'eye tracking' in a title and abstract, found 11 results on the 25th of March 2015. Furthermore, up to date only one article detected microsaccades during MEG recordings (Carl et al. 2012). In contrast, studying eye movements during EEG recordings is relatively common and has recently received much attention from the

brain imaging community (Yuval-Greenberg et al. 2008; Dimigen et al. 2009; Ossandon et al. 2010; Plöchl et al. 2012). The next section contains a short overview of eye tracking methods that have been used to detect microsaccades and a discussion of their usefulness for combining with MEG.

2.2.2 Which method is most suitable?

The *search coil* is a contact lens method considered to be the gold standard for eye tracking owing to its excellent signal to noise ratio (McCamy, Macknik, et al. 2013). The contact lens is a silicon annulus containing coils of thin copper wire. It is based on the principle that the amount of electric current induced in the coils by an external magnetic field depends on the angle of the coil relative to the direction of the magnetic field, which in turn depends gaze position. It is an invasive method because participants experience painful sensation and it often involves the use of a topical anaesthetic. Subjects can only wear the contact lens for up to 25 minutes before it becomes too uncomfortable. Furthermore, it has been shown to alter saccadic eye movements (Frens 2002) and it might temporarily reduce visual acuity (McCamy, Macknik, et al. 2013). Most importantly, it is currently not suitable for use with MEG because it involves the application of external magnetic field and placing a copper wire close to MEG sensors, both of which would introduce noise in MEG recordings. However, an MRI-compatible search coil system has been recently developed (Oeltermann et al. 2007).

Bipolar electrooculography (EOG) typically involves placing pairs of electrodes above and below the eye as well as to the left and right of the eye. Because the eye is a dipole in which the anterior pole is positive (cornea) and the posterior pole is negative (retina), a potential difference occurs between the two electrodes whenever the dipole rotates, that is whenever the eye moves. EOG has been used extensively for tracking saccadic and smooth pursuit eye movements. However, most microsaccades are too small to lead to a

detectable rotation of the dipole (Keren et al. 2010). For detecting microsaccades, a technique called *radial EOG (REOG)* has been used instead (Croft & Barry 2000; Keren et al. 2010; Carl et al. 2012). Radial EOG, despite its name, is technically an electromyography (EMG) method because it measures an electric potential defection generated by extraocular muscles at an eye movement onset, commonly referred to as the spike potential (Thickbroom & Mastaglia 1985; Keren et al. 2010). It involves averaging signals from a number of electrodes placed around the eyes and referenced to a posterior electrode. Because most MEG systems are also equipped with a compatible EEG system, this technique is readily available in most MEG laboratories and it is relatively easy to use. However, it cannot be used to estimate microsaccadic characteristics such as direction, duration, peak velocity, and amplitude. Moreover, even when used with an optimised filter, this method performs only slightly above chance level at detecting microsaccades smaller than 0.2 deg (Keren et al. 2010).

Feature recognition methods illuminate eyes with infrared light and determine eye orientation from distinct landmarks and optical reflections. The *dual Purkinje image (DPI)* method uses the first Purkinje image (reflection from the outer surface of the cornea, also called the corneal reflex) and the fourth Purkinje image (reflection from the inner surface of the lens) to track the eyes (Crane & Steele 1985). With spatial resolution of around 0.015 deg, DPI is the most precise of feature detection methods. However, it is rarely used due to its elaborate setup and difficult maintenance. Using the DPI system in an MEG environment would require putting it close to the MEG dewar which would in turn result in equipment artefacts. *Video-based eye tracking*, another feature recognition method, is currently the most commonly used method to study microsaccades (Martinez-Conde et al. 2009), and to track eye movements in general (Holmqvist et al. 2011). It involves digital filming of the eyes with a video camera and estimating gaze position from the relative movement of pupil and corneal reflection. Eye tracking systems of this category are non-

invasive, easy to use, and quick to set up. Models specially designed to be MEG-compatible are available from at least two manufacturers. Pupil and corneal reflection tracking provides gaze position information relative to a visual stimulus (for instance pixels on the monitor screen) and eye movements parameters such as amplitude and direction can be calculated based on this information. Despite all these advantages there are no published reports of using remote video eye tracking to detect microsaccades during MEG recordings. Although a recent study found that one remote eye tracker performed as well as the search coil method at detecting microsaccades (Kimmel et al. 2012), in general, technical specifications of remote eye trackers vary dramatically with regards to sampling frequency, precision, and accuracy. In order to be able to critically evaluate these specifications with respect to their impact on detection of small eye movements it is important to understand how remote video eye tracking works.

2.2.3 How does remote video eye tracking work?

Video-based eye tracking involves digital filming of the eyes with one or more video cameras, illuminated with one or more infrared light sources. In remote systems, the cameras and light sources are not in physical contact with a participant, instead they are placed in a certain distance in front of the participant. When remote systems are used, small head movements are possible. The primary reasons for using remote pupil and corneal reflection tracking is that these landmarks are relatively easy to identify as image features, using image analysis, and they can be formally related to gaze, using gaze estimation methods.

A person's gaze direction is determined by the eyeball orientation and head pose (position and orientation). The position of the centre of the pupil, the opening in the centre of the iris (Figure 2-1), is a good indicator of eye orientation because the pupil moves in unison with the eyeball, except for a brief period right after saccades when the pupil moves

inside the iris (Nyström et al. 2013). Head and eye movements will both result in pupil movement in the video image. The corneal reflection (Figure 2-1), on the other hand, stays relatively still during eye movements as long as the light source and head stay still. The movement of the pupil relative to corneal reflection can be used to to estimate eye movements corrected for head movements (Merchant et al. 1974)

The first step in the process of eye tracking is image analysis which, in real time, find the geometric centres of both the pupil and the corneal reflection. This is typically done using feature-based approaches where features in the image are detected by an automatic algorithm or subjectively by the experimenter (Hansen & Ji 2010). For instance a threshold for pixel intensity is specified (pupil is a dark ellipse surrounded by brighter iris, corneal reflection is a bright spot surrounded by darker pupil or iris as shown in Figure 2-1). Another approach looks for gradients (for instance edges and contours that outline regions in the eye image that resemble the target features). The quality of gaze estimation will depend on how robustly these features are detected and tracked.

The corneal reflection is particularly troublesome to track for a number of reasons. First, it is much smaller than the pupil and in the video eye image corneal reflection comprises approximately 25 times less the number of pixels than in the pupil region. As a consequence, the spatial noise inherent in all video systems will be more significant to the estimation of the centre of the CR than to the estimation of the centre of the pupil (Kolakowski & Pelz 2006). Second, the inhomogeneity of the structure of the surface of the cornea or tear layer introduces artefactual movement of the reflection during eye movements (Hansen & Ji 2010). Third, the corneal reflection might sometimes be impractical to track because it tends to roll off the image during calibration for extreme gaze directions. Forth, spurious reflections present in the eye image are often an obstacle for robust tracking of the actual corneal reflection. This results in the corneal reflection estimate jumping around the image and generally has a dramatic effect on data quality.

Once image features are identified, the gaze estimation process takes place. Its goal is to use the position of the identified image features to estimate gaze position (sometimes referred to as point-of-regard or point of gaze) in the calibrated area. There are two main approaches to estimate gaze. Geometrical approaches model the common physical structures of the human eye geometrically to calculate a 3D gaze direction vector (Guestrin & Eizenman 2006). By defining the gaze direction vector and integrating it with information about the objects in the scene, the point of regard is computed as the intersection of the gaze direction vector with the nearest object of the scene (e.g., the monitor). In practice these approaches are not commonly used due to the difficulty in obtaining robust geometrical models of the eye and their elaborate calibration routines (Holmqvist et al. 2011). More commonly used regression approaches assume that the mapping from image features to gaze coordinates have either a particular parametric form such as a polynomial, or a nonparametric form such as in artificial neural networks, where no assumptions about the form of the underlying mapping function are made. (Morimoto & Mimica 2005). These methods avoid explicitly calculating the intersection between the gaze direction and gazed object. A calibration procedure, during which a user is asked to look at several points on the computer screen, one point at a time, is required to compute the mapping from the pupil and corneal reflection position to monitor screen coordinates.

The regression approach also works without corneal reflection information but the subject's head has to stay still to avoid head movement artefacts. While pupil-only gaze estimation is relatively common for head-mounted eye trackers, it is rarely done in remote systems. One common way of estimating gaze from pupil position only involves using a second order polynomial for the x and y coordinates separately (Stampe 1993). From here onwards, we will refer to the combined pupil and corneal reflection method as the 'P-CR method' and to the pupil only method as the 'P-only method'

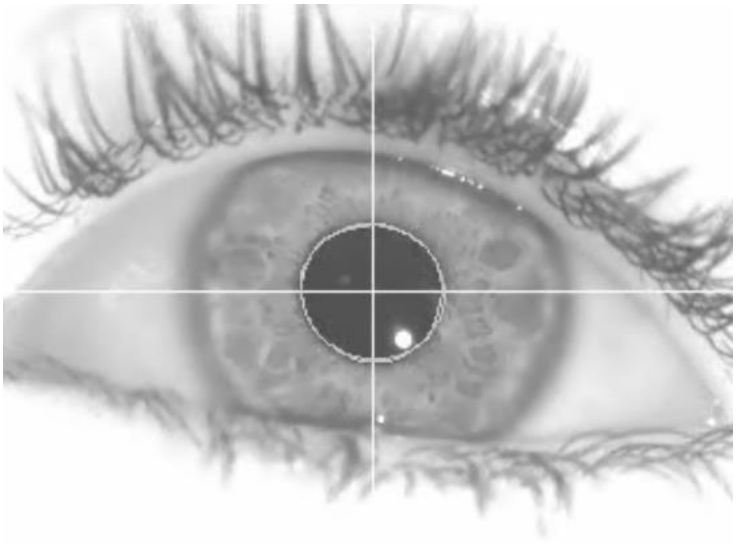

Figure 2-1. Eye image from the eye tracking video camera. The image comes from the experiment described in Chapter 3. The crosshair in the centre of the pupil indicates that the pupil is being tracked. Corneal reflection, in the bottom right part of the pupil, is not being tracked. Therefore, the recording is being done in pupil-only mode. Videos of the eye image were used to verify performance of the microsaccade detection algorithm as microsaacades generally lead to a visible pupil movement.

2.3 Important specifications for studying microsaccades

It is only recently that video eye trackers have been used to study microsaccades (Martinez-Conde et al. 2009). However, data quality varies dramatically between different video eye trackers and it is important to establish what technical specifications are sufficient and optimal to study microsaccades reliably.

2.3.1 One or two eyes?

The vast majority of microsaccades are binocular, conjugate movements with comparable amplitudes and directions in both eyes (Martinez-Conde et al. 2009; Otero-Millan et al. 2014). Therefore monocular tracking is sufficient for studying microsaccades. Nevertheless, many studies made use of binocular recordings in head-mounted eye trackers to reduce the amount of false positives in automatic microsaccade detection

algorithms by only analysing microsaccades detected in both eyes (Engbert & Mergenthaler 2006; Martinez-Conde et al. 2009). Currently there are very few high-speed remote eye trackers that support binocular recordings and only one that is specially designed for MEG, that is the EyeLink 1000 (SR Research, Canada).

2.3.2 Sampling frequency

Video eye tracking systems acquire data at a fixed sampling (frame) rate and, to date, there has been no systematic investigation of the minimum sampling frequency required to accurately characterise microsaccades. However, realistically, it should be that the duration between samples is not longer than the average microsaccade duration. In practice, video eye trackers used in microsaccade studies use sampling frequencies no lower than 200 Hz. A survey conducted by Martinez-Conde et al. (2009) found that between 2004 and 2009 there were 9 publications on microsaccades that used eye trackers with sampling frequency between 200 and 300 Hz, and 25 publications with sampling frequencies of 500 Hz. Almost all of the 25 studies used a head-mounted eye tracker. Although a sampling frequency of 200 Hz is sufficient to reliably detect microsaccades it imposes a limit on the minimum duration, and therefore size, of microsaccades that can be detected. Namely, the minimum number of samples required by a detection algorithm multiplied by the between-sample duration results in the minimum duration. For instance if 3 samples are required by an algorithm, this result in a minimum duration of 6 ms at 500 Hz and 15 ms at 200 Hz. Moreover, microsaccade parameters such as, for instance, peak velocity, can be estimated more accurately with higher higher sampling frequencies (Holmqvist et al. 2011).

2.3.3 Precision

Spatial precision is a crucial eye tracker parameter that determines how well one can detect small eye movements and estimate their parameters. Formally, precision is defined as the ability of an eye tracker to reliably reproduce the same gaze point measurement and is commonly calculated as the root mean square of angular distances between consecutive samples of the gaze position (Holmqvist et al. 2012) and referred to as 'RMS precision'. When there is a sample to sample variability in estimated gaze position with the gaze point being constant (except for involuntary fixational eye movements), movements that are not substantially larger than this average variability will not be detected, because they are smaller or equal to noise. Precision can be calculated using perfectly still artificial eyes (instrument precision) and as such reflects system-inherence noise. Precision can also be calculated using human eyes fixating on a stationary target using a large participant sample with a wide spectrum of eye physiologies (typical precision) and as such it reflects the sum of system-inherent noise and oculomotor noise. Precision can also be measured for different gaze angles and stimuli with different luminance and contrast. Most manufacturers report some precision for their eye trackers. However, they do not commonly disclose the details of how they measured it and, because there are many different ways of how precision can be measured, it is difficult to interpret their estimates. Although precision is not the only factor that determines how well small eye movements can be detected, Holmqvist et al. (2011) suggests that the RMS precision required for studying microsaccades is at least 0.03 deg.

The factors that influence the precision of remote eye trackers most significantly, apart from eye camera resolution, filtering, and averaging data from two eyes in binocular recordings, are related to head movement compensation methods. While using corneal reflection in order to correct for head movements increases the accuracy of gaze position estimation, it is generally thought to reduce the precision because corneal reflection

position in the video image is noisy. For instance, Holmqvist et al. (2011) observed that pupil-only recordings (that is without the corneal reflection) improved precision up to 3 times.

2.3.4 What is the smallest movement that can be detected?

There is no straightforward method for calculating the smallest saccadic eye movement that can be detected with a given eye tracker. Factors that should be taken into account when trying to accomplish this task are: an estimate of the upper limit of the gaze position displacements during fixation (for instance the 95th percentile); the eye tracker's sampling frequency and minimum number of samples required by a detection algorithm; a model of how microsaccadic velocity behaves as a function of duration. Importantly, it is not critical to detect the smallest possible microsaccades, it appears from visual inspection of microsaccade amplitude distribution in research papers that only approximately 5% of microsaccades are smaller than 0.1 deg.

It is therefore important to measure the eye tracker's precision for each specific experimental setup because manufacturers' estimates are difficult to interpret. As described above, corneal reflection tracking is a relatively noisy process that might result in noisy gaze estimation. However, there appears to be only anecdotal evidence of improved precision when recording in the pupil-only mode (Holmqvist et al. 2011). With that in mind, I formally tested the effect of the recording mode (P and P-CR) and head support on precision in our eye tracking setup.

2.4 Measuring precision

Five subjects (3 females, mean age = 26 years) participated in the experiment after giving informed consent, with all procedures approved by the Cardiff University School of Psychology Ethics Committee. The subjects were placed in the same position as during a

typical MEG experiment (see the 'General eye tracking methods' section below for details). Their task was to continuously fixate on a central red spot while the monitor display alternated every 3 s between a uniform grey image and a vertical, square wave grating of 100% contrast that subtended 8 deg both vertically and horizontally. These stimuli are similar to the stimuli used in the other experiments described in this thesis. This way we can arrive at an estimate of precision that applies to the other experiments. There were three conditions that differed with respect to whether pupil only (P) or pupil and corneal reflection (P-CR) were used to estimate gaze position, and whether the participant's head was immobilised in the MEG helmet with head support (chinrest and headcuff). The conditions were as follows: (A) recording in P-CR mode with no head support; (B) recording in P-CR mode with head support; (C) recording in P mode with head support. To avoid order effects, the condition order was counterbalanced using a palindrome design. Each condition was tested in two runs in the following sequence: ABCCBA. Each run lasted 3 minutes and consisted of 60 trials. After each run there was a 2 minute rest period when the participant was allowed to move her eyes. Before the start of each run, the focus of the video camera was adjusted and a calibration routine with a 9-point grid was carried out. A condition with recording in P mode and no head support was not included in the design because it is problematic to run the calibration routine in this configuration.

Trials with blinks, large artefactual corneal reflection displacements, and saccadic eye movements bigger than 1 deg, were removed from the analysis (19% of trials). For each remaining trial and separately for vertical and horizontal coordinates of gaze position, the root-mean-square of the distances between each pair of consecutive gaze position samples was calculated. Figure 2-2 shows medians of these values separately for each subject and each condition. The group-level medians for P-CR mode with no head support, P-CR mode with head support and P mode with head support were 35.3×10^{-3}

deg, 34.2×10^{-3} deg and 13.5×10^{-3} deg for X coordinate and 31.2×10^{-3} deg, 33×10^{-3} deg and 13.2×10^{-3} for Y coordinate respectively. Friedman's tests determined that the RMS of gaze displacements differed significantly between the three conditions for X ($\chi^2(2) = 8.4$, $p = 0.015$) and Y ($\chi^2(2) = 7.6$, $p = 0.022$) coordinates.

The results above show that the precision for both X and Y gaze coordinates is ~ 2.5 times higher (indicated by lower RMS values) when the pupil information only is used to estimate gaze position. When pupil and corneal reflection are used head support does not seem to increase precision but when pupil only is used head support is essential to control for head movements and to successfully run the calibration routine.

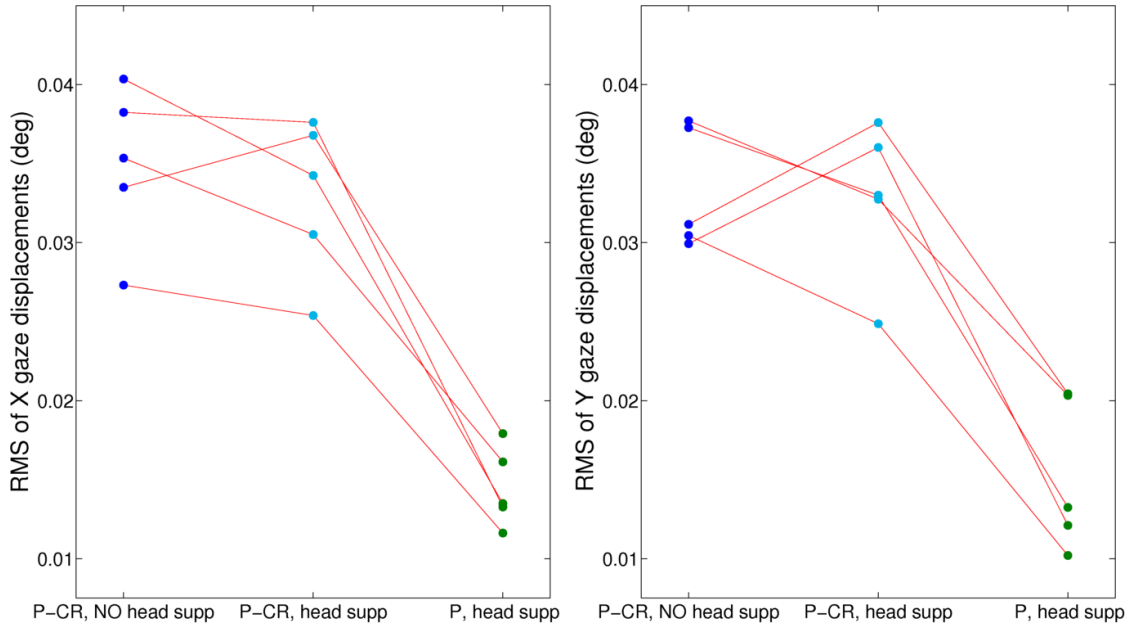

Figure 2-2. Eye tracker RMS precision for three recording conditions. Data is presented separately for the horizontal (**Left**) and vertical (**Right**) gaze coordinates. Note the ~2.5 precision increase (RMS decrease) in the condition recorded in pupil-only mode. Each line represents one participant.

2.5 General eye tracking methods

2.5.1 Hardware and setup

An iViewX MEG250 (SensoMotoric Instruments, Germany) eye tracking system was used to record eye movements in all experiments reported in this thesis. It is a remote dark pupil system with one video camera and one infrared light source positioned away from the optical axis of the camera. The system uses a long-range infrared camera with 320×240 resolution and sampling frequency of 250 Hz. The infrared illuminator was placed 60 cm horizontally to the right of the video camera. The system allows only for monocular recordings, that is recordings of either the left or right eye but not both simultaneously. Typical tracking resolution reported by the manufacturer (measured in the pupil and corneal reflection mode) is 0.15 deg.

The camera and infrared illumination unit were placed on a mount in front of the participant seat in the MEG magnetically shielded room (Figure 2-3) so that the distance between a participant's eyes and the camera lens was 125 cm. The monitor display was situated 15 cm above and 90 cm behind the eye tracker camera. The participants' head was immobilized in the MEG helmet with a headcuff, supplied by the MEG manufacturer, and a custom-built chinrest (Figure 2-3).

The system supports gaze position tracking using either of the two methods: pupil with corneal reflection and pupil-only. As we have shown above that eye-tracking precision is greatest for pupil-only mode, all the experiments described in this thesis use this approach. The eye tracking acquisition software provides optional on-line filtering using heuristic and bilateral filters; however, neither of these filters were used.

Figure 2-3. Experimental setup for simultaneous MEG and eye tracking.
Top, an overview of the MEG magnetically shielded room with the eye tracker placed between the participant and the monitor display. **Bottom left**, view of the eye tracker and the participant from the monitor's perspective. **Bottom right**, view of the eye tracker and the monitor from the participant's perspective. The infrared illumination unit is placed to the right of the eye tracker camera.

2.5.2 Co-registration with MEG

Analysis of simultaneously recorded eye tracking and MEG data require that both data streams are synchronized with millisecond precision. In our setup this was achieved by a visual stimulation computer (1) sending trigger pulses to a MEG acquisition computer via the parallel port and (2) sending a command to the eye tracking acquisition computer to insert an ASCII text message (with the value of the corresponding MEG trigger) into the eye tracking data. In the visual stimulation computer, commands for the two operations were executed frequently (at the beginning of each trial) and in immediate succession.

2.5.3 Microsaccade detection and parameter estimation

The method for microsaccade detection is based on Engbert & Mergenthaler (2006). Microsaccade detection and microsaccade parameter estimation was carried out in MATLAB (The MathWorks, Inc., United States) using custom functions written by the PhD candidate and functions from the EYEEEG plugin (Dimigen et al. 2011). Data for X and Y coordinates were processed separately. First, continuous gaze position (point of regard) data was converted from monitor pixel units to degrees of visual angle (deg). Then the position data was demeaned. Velocity was calculated by dividing distances between consecutive data samples by 4 ms (sample duration). Velocity was then smoothed using a moving average with a window width of two or four velocity samples (corresponding to three and five position samples respectively) to suppress high-frequency noise. Then data was epoched according to triggers received from the visual stimulation computer. Figure 2-4 (*Upper* and *Middle* panels) shows position and velocity data from a representative trial.

Microsaccades can be identified by their velocities, which are clearly separated from the rest of the velocity distribution during fixation, that is microsaccades are ‘‘outliers’’ in velocity space (Engbert & Kliegl 2003) as shown in Figure 2-4 *Lower Right* panel. To this end, detection thresholds (dashed black lines in Figure 2-4 *Upper* and *Middle* panels)

were obtained by calculating a median estimator of the standard deviation of velocity samples and multiplying it by an integer (usually 5). The value of the integer was based on previous reports (Engbert & Kliegl 2003; Engbert & Mergenthaler 2006) and on visual inspection of our own data. While the integer value is consistent for an entire analysis, the median estimator was calculated separately for each trial and independently for the vertical and horizontal components. The horizontal and vertical detection thresholds served as radiuses to obtain an elliptic threshold for microsaccade detection in 2D velocity space (dotted black ellipse in Figure 2-4 *Lower Right* panel). It is important to note that the detection threshold is chosen relative to the noise level in velocities of a single trial. Therefore, the algorithm is robust with respect to different noise levels between different trials and participants. A minimum duration of 12 ms (three data samples) was applied, that is a microsaccade was detected only if three or more velocity samples were outside the elliptic threshold. Additionally, if the distance between any two microsaccades was 16 ms (4 data samples) or shorter only the largest of the two microsaccades was kept for further analysis. This way instances of instability of the pupil relative to the iris, that occur commonly after saccadic movements (Nyström et al. 2013) and mimic small microsaccades, were removed from analysis. Performance of the detection method was validated for each participant and each trial by visual inspection of the gaze position and velocity time-courses as well as by inspection of eye videos (Figure 2-1). Rare instances when head movements, half-blinks or transient pupil occlusion were mistakenly classified as microsaccades were removed.

Microsaccadic amplitude was calculated as the length of a straight line connecting two most extreme points within gaze position samples belonging to the microsaccade. Microsaccade orientation was the angle of this line relative to a horizontal reference. Smoothed velocities are reported in text and figures.

A key property of microsaccades, and also regular saccades, is that they show a fixed linear relation between peak velocity and movement amplitude (Zuber et al. 1965). This finding is a consequence of the ballistic nature of microsaccades. To stress the importance of this relationship, it is often referred to as the ‘‘main sequence’’ (Bahill et al. 1975), a term borrowed from astrophysics, where it is used to describe the relation between colour and brightness of stars. Plots of main sequences appear in all publications on microsaccades to validate data quality and detection routines. Large deviations from the main sequence might reflect noisy data or inadequate parameters used in detection algorithms. Here we also illustrate that microsaccades detected in the precision measurement experiment described above followed the main sequence. Figure 2-5 top panel shows that microsaccades detected in all three conditions followed the main sequence with the correlations coefficients between amplitude and peak velocity: r = 0.90 for the recording in P-CR mode with no head support, r = 91 for the recording in P-CR mode with head support, and r = 0.93 for the recording in P mode with head support. Although microsaccades in all conditions followed the main sequence, the higher precision in the condition without corneal reflection reported in the section above is reflected here by the fact that more microsaccades were detected in this condition (1.18 microsaccades/s) than in the recordings where corneal reflection was used (0.36 microsaccades/s without head support and 0.59 microsaccades/s with head support). The smaller number of detected microsaccades in recordings when corneal reflection was used probably stems from the fact that, due to lower precision, velocity detection thresholds were elevated in many trials.

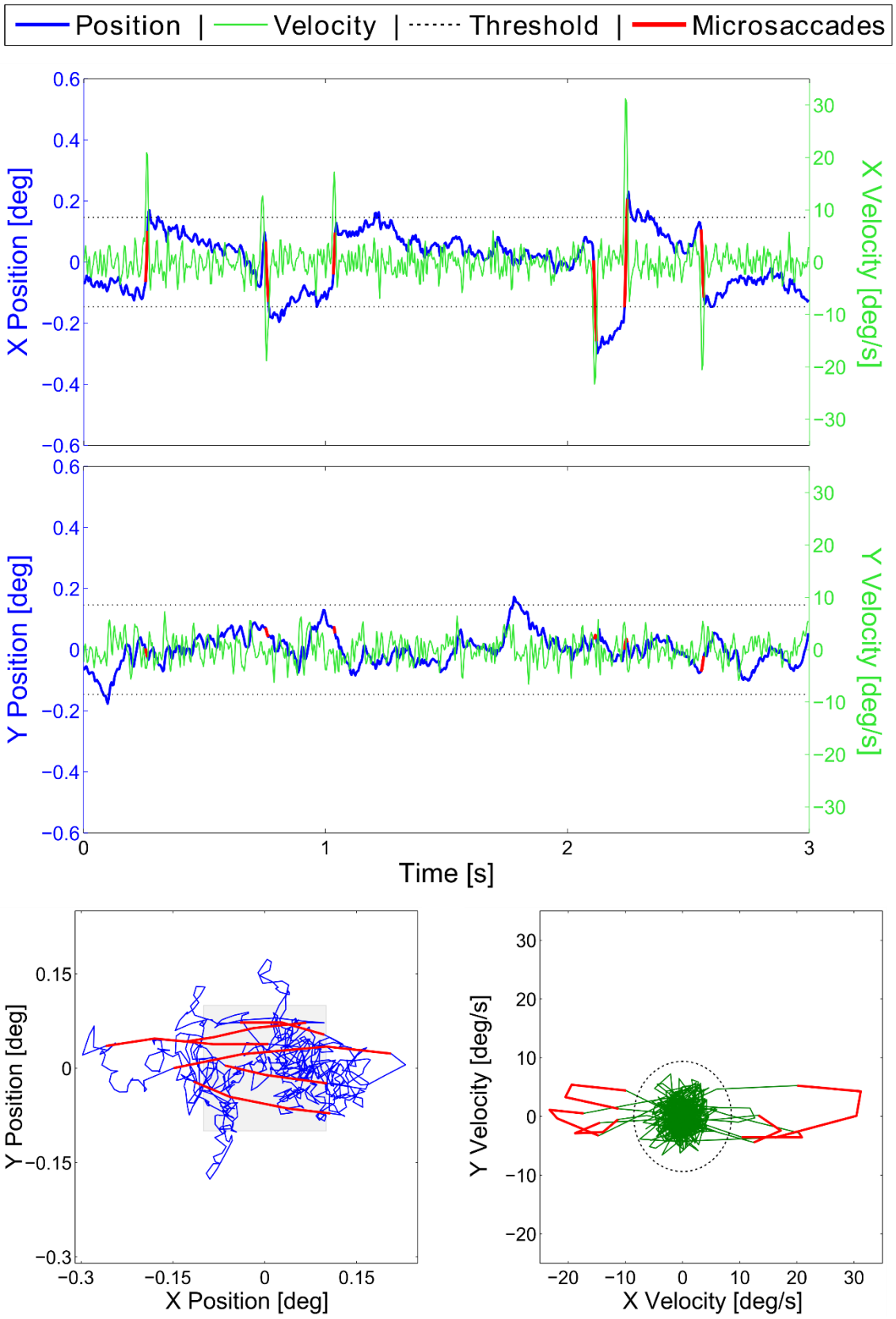
Position | Velocity | Threshold | Microsaccades
X Position [deg]
X Velocity [deg/s]
Y Position [deg]
Y Velocity [deg/s]
Time [s]
Y Position [deg]
X Position [deg]
Y Velocity [deg/s]
X Velocity [deg/s]

Figure 2-4. Representative eye tracking data from one trial during fixation and microsaccade detection procedure. Microsaccades are plotted here in red and range in size from 0.17 to 0.36 deg. **Upper**, vertical gaze position and velocity. **Middle**, horizontal gaze position and velocity. **Lower Left**, gaze position during fixation. The gray square is the same shape and size as the fixation spot. **Lower Right**, 2D velocity space. Independent detection thresholds for horizontal and vertical components (plotted with a dashed black line in ***Upper*** and ***Middle***) constitute an elliptic threshold criterion (dashed black ellipse). The legend in the top part of he figure applies to all the subfigures. Data from the same data is plotted in all subfigures. Note that the absolute position plotted in the figure was demened and therefore does not illustrate the actual gaze position.

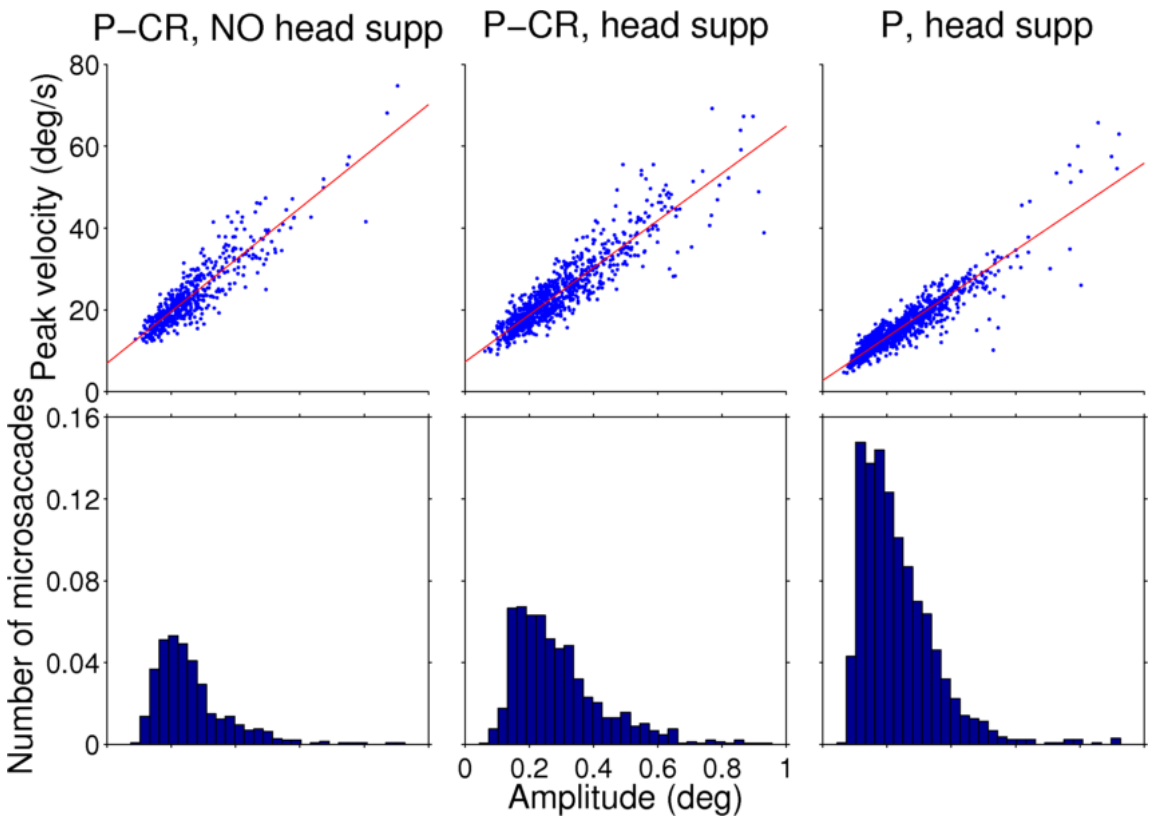

Figure 2-5. Characteristics of microsaccades for three recording conditions. **Top Panel**. A strong relationship between microsaccade peak velocity and amplitude, the so called 'main sequence' was evident for each recording condition. Each microsaccade is represented by one dot in these scatterplots. Lines of best fit are shown in red. **Bottom Panel**. Distribution of microsaccade amplitudes normalised by the time duration of good trials in each condition.

2.6 Discussion

In this chapter, I demonstrated how remote video eye tracking can be used to study microsaccades during MEG recordings. Although microsaccades have been detected during MEG recordings before, using radial EOG technique (Carl et al. 2012), this is the first report that uses a method that provides complete characterisation of eye movements. While radial EOG is good enough for detecting microsaccades larger than 0.2 deg (Keren et al. 2010), it does not reliably provide detailed information about their amplitude, velocity, duration or orientation. The reason is that radial EOG relies on the myographic signal from extraocular muscles rather than on direct measurements of eyeball movements. Microsaccades characteristics are modulated by many factors and being able to precisely measure the characteristics of microsaccades is crucial to study the impact of microsaccades on visual processing (Martinez-Conde et al. 2013). Moreover, it is a standard practise to present microsaccade characteristics in research publications as a validation of the accuracy of the recording method. Finally, in studies of the microsaccade related muscle artefact in EEG/MEG, it is beneficial to detect microsaccades with a technique that is independent from the one that is used to characterise the artefact.

I also measured the precision of our eye tracker specifically for our experimental setup and stimuli. I confirmed earlier anecdotal evidence that estimating gaze position in the pupil-only mode increases precision almost three fold, compared to pupil and corneal reflection mode, due to the fact that corneal reflection tracking is a relatively noisy process. In our setup, RMS precision in the pupil-only mode is approximately 0.013 deg and should enable detection of smaller eye movements and a better classification of their parameters (Holmqvist et al. 2011) than recordings using both the pupil and the corneal reflection. Recording in pupil-only mode is routinely used in head-mounted eye trackers when studying microsaccades (Martinez-Conde et al. 2009; Hermens 2015). This method can be used during MEG recordings with any remote video eye tracker that supports pupil-

only gaze estimation. Given the relatively high precision, our eye tracker's sampling frequency (250 Hz) and minimum three data samples required by the detection algorithm determine that 12 ms is the shortest duration of a microsaccade that can be detected with our setup. Effective recording in the pupil-only mode was possible because participant's head was immobilised in the MEG helmet and head movements were minimised.

Nevertheless, small sporadic head movements were present during the recordings. Head movements artefacts did not lead to false positives in the microsaccade detection algorithm because their velocity is generally too low compared to microsaccades. Moreover, these artefacts mainly affected the vertical component which is consistent with the observation that head movements during MEG recordings are present mainly in the up-down direction (Wehner et al. 2008). Head movements during the attempt to measure precision when recording in pupil-only with no head support lead to gaze position estimate drifting outside of the calibrated monitor area and rendered it impossible to run the calibration routine. This did not happen during experiments when head support was used. This emphasises the need to use head support.

Because both microsaccades and neural oscillations play important roles in vision, one can use the method described in this chapter to study the relationship between the two. One particular problem that this putative relationship may cause is linked to the fact that microsaccade characteristics are modulated by the visual stimulus and task. Given that microsaccades both generate an artefactual muscle activity, in the gamma band, and drive genuine visual cortical activity, it is possible that microsaccade-related activity can directly drive at least part of the visual gamma signal. In the next chapter, I investigate the relationship between visual gamma oscillations and microsaccades. Evidence for a strong relationship between the two would challenge the common interpretation that visual gamma oscillations recorded with MEG reflect stimulus-driven information processing in local cortical circuits.

Chapter 3:
Visual gamma oscillations and microsaccades.

3.1 Abstract

There has been much recent interest in the non-invasive measurement and characterization of gamma oscillations in the human cortex in order to investigate their role in cognition and behaviour. Many studies have demonstrated their measurement using EEG and MEG, together with source localization to estimate their cortical locations. One of the most studied and robustly elicited of these signals is the induced visual gamma oscillation, which is thought to be generated within local cortical columns of primary visual cortex, via coupled populations of inhibitory interneurons and pyramidal cells.

However, there is a possibility that these recordings are contaminated by muscle artefacts and in particular there is a concern that these may be related to microsaccades, as has been demonstrated in a recent EEG study. Moreover, gamma oscillations in the visual cortex have been shown to be evoked by saccadic eye movements suggesting that gamma oscillations recorded in the visual cortex may reflect retinal motion or extraretinal motor signals rather than originating from the local cortical circuit. By detecting microsaccades in a paradigm commonly used in animal and human studies for inducing visual gamma oscillations we here provide the first direct evidence that sustained visual gamma oscillations recorded with MEG are unlikely to be related to microsaccades. We did not find evidence for a relationship at the group or within-subject single-trial level. However, the early transient broadband gamma amplitude was found to be lower in trials with microsaccades. Our results show that sustained gamma oscillations are likley to reflect stimulus processing in local cortical circuits and provide further evidence for a difference between the transient and sustained components of the visual gamma response.

3.2 Introduction

Neuronal oscillations in the gamma frequency band (>30 Hz) have been the focus of a growing research interest because they appear to be an important substrate of cortical information processing, perception and cognition, as well as reflecting local inhibitory-excitatory interactions (Buzsáki & Wang 2012; Fries et al. 2007). Invasive recordings in a number of animal species suggest that these oscillations play a key role in such diverse processes as visual feature integration (Singer & Gray 1995), attentional selection (Fries 2001), episodic memory (Montgomery & Buzsáki 2007), working memory maintenance (Pesaran et al. 2002), and olfactory processing (Wehr & Laurent 1996).

More recently, MEG and scalp EEG studies probed induced gamma oscillations in humans non-invasively with a particular focus on the visual domain. The bulk of the EEG studies reported a transient broadband increase in gamma power between 0.2 and 0.3 s after stimulus onset at occipital and parietal sensors, thought to be related to object representation (Lutzenberger et al. 1995; Muller et al. 1996; Tallon-Baudry et al. 1996). In contrast, most of the MEG studies used simple visual gratings and reported a more narrowband gamma response sustained for stimulus duration and localized to the early visual cortex (Adjamian et al. 2004; Hoogenboom et al. 2006; Muthukumaraswamy et al. 2010). The sustained gamma oscillations reported in the MEG studies resemble closely those reported in invasive animal studies (Ray & Maunsell 2011; Rols et al. 2001; Henrie & Shapley 2005) they are also sensitive to the same stimulus properties such as contrast (Hall et al. 2005; Logothetis et al. 2001; Henrie & Shapley 2005), orientation (Duncan et al. 2010; Frien et al. 2000), velocity (Friedman-Hill 2000; Swettenham et al. 2009), and stimulus size (Gieselmann & Thiele 2008; Perry et al. 2013). Importantly, MEG visual gamma oscillations are highly repeatable within the same individuals between recording sessions (Muthukumaraswamy et al. 2010) and highly heritable (van Pelt et al. 2012). Furthermore, MEG signals are much less dependent on the conductivity of the

extracellular space (such as cerebrospinal fluid, skull and scalp) and therefore MEG signals are less distorted by them. Consequently, MEG is potentially more sensitive to high frequency signals, as demonstrated for visual gratings stimuli (Muthukumaraswamy & Singh 2013), enables a more accurate spatial localization of brain sources, and therefore has a potential to tap into the same mechanisms of oscillatory dynamics as local field potential recordings in invasive animal studies (Buzsáki et al. 2012; Lopes da Silva 2013). Moreover, unlike EEG, MEG measurements are absolute: they are not dependent on the choice of a reference and therefore less likely to be affected by placing reference close to a source of muscle activity. All these characteristics suggest that induced sustained visual gamma oscillations recorded with MEG provide a model paradigm for studying, non-invasively in humans, mechanisms of cortical gamma oscillations and their role in cognition and behaviour.

MEG and EEG recordings of neuronal gamma oscillations, however, may be contaminated by muscle artefacts (~20–300Hz) as their spectral bandwidths overlap and the amplitude of neuronal oscillations is several orders of magnitude smaller than those from muscle (Muthukumaraswamy 2013; Whitham et al. 2007). One type of muscle artefacts, the microsaccadic spike artefact, occurs at the onset of microsaccades: jerk-like eye movements that occur involuntarily at fixation and are typically smaller than 1° (for a recent review on microsaccades see Martinez-Conde et al., 2013). It is particularly problematic because the occurrence of microsaccades is related to visual processing in a complex way, as they are thought to be dynamically triggered in order to prevent visual adaptation and retinal fatigue (Engbert & Mergenthaler 2006; Martinez-Conde et al. 2006). As such, characteristics such as temporal distribution, rate of occurrence, magnitude and direction are modulated by stimulus properties and task demands (Engbert & Kliegl 2003; McCamy, Najafian Jazi, et al. 2013; Rolfs et al. 2008; Valsecchi et al. 2007; Yuval-Greenberg et al. 2008). Moreover, microsaccade characteristics are altered in clinical

populations (Kapoula et al. 2014; Otero-Millan et al. 2011; Willard & Lueck 2014) . Therefore, characteristics of the microsaccadic spike artefact are often modulated with by both experimental and group variables and consequently may appear as modulations of genuine cortical oscillations.

In one striking demonstration Yuval-Greenberg et al. (2008) suggested that a transient increase in induced broadband gamma power observed in posterior EEG electrodes around 200 – 300 ms after stimulus presentation reflects concentration of microsaccade-related spike artefacts rather than, as previously thought, neural activity associated with visual cognitive functions such as object representation. Since then it has been discussed under what conditions visual gamma oscillations can be studied with scalp EEG (Fries et al. 2008; Melloni, Schwiedrzik, Wibral, et al. 2009; Yuval-Greenberg et al. 2009). Subsequently, the artefact has been characterised (Keren et al. 2010) and a few methods to suppress it have been proposed (Hassler et al. 2011; Keren et al. 2010; Plöchl et al. 2012). Importantly, the artefact is also thought to impair detection of sustained EEG gamma oscillations when microsaccades are concentrated in the baseline (Hipp & Siegel 2013), suggesting that it is important to determine the temporal distribution of microsaccades for each paradigm in order to predict the potential effect of the associated artefact. Although the artefact in MEG is thought not to affect parietal and occipital sensors (Carl et al. 2012), a direct test of whether the MEG visual gamma oscillations are affected is still lacking.

Microsaccades trigger increases in neural firing rates in the LGN (Martinez-Conde et al. 2002) , visual cortex (Bair & O'Keefe 1998; Kagan et al. 2008; Leopold & Logothetis 1998; Martinez-Conde et al. 2002), and potentially retinal photoreceptors (Donner & Hemilä 2007; Martinez-Conde et al. 2013). It has been suggested that this activity enhances spatial and temporal summation by synchronising neighbouring neurons (Martinez-Conde et al. 2000) or synchronising different regions of the visual cortex

(Leopold & Logothetis 1998). Recently, a few studies provided evidence for these suggestions. Bosman et al. (2009) indicated that gamma oscillations in the macaque visual cortex increase in amplitude before and after microsaccades. Regular saccades in humans (Nagasawa et al. 2011) and in monkeys (Rajkai et al. 2008) were suggested to increase visual gamma oscillations. It is not clear if the increased firing rates and gamma band oscillations reflect retinal motion induced by displacement of receptive fields or extra-retinal signals that enhance post-eye movement processing. Regardless of the origin of this activity, there is a possibility that visual gamma oscillations may reflect microsaccade-related neural activity.

In the present study, we detected and characterised microsaccades in a MEG paradigm optimised for sustained visual gamma oscillations to test if there is relationship between the occurrence of microsaccades and visual gamma oscillations. The results of this investigation will help to determine whether MEG visual gamma oscillations originate from the local cortical circuits in early visual cortex and reflect local inhibitory-excitatory interactions, or are partly or wholly generated by other possible sources such as muscle artefacts, retinal motion or extraretinal motor signals around eye movements.

3.3 Methods

3.3.1 Participants, stimuli, and task

Seventeen subjects participated in the experiment after giving informed consent, with all procedures approved by the Cardiff University School of Psychology Ethics Committee. Eye tracking data for three subjects were too noisy due to the challenging nature of recording eye movements in MEG environment, and hence were excluded from the analysis (see the specific criteria below). The remaining group of fourteen subjects consisted of an equal number of males and females and their average age was 24.86

years (SD = 1.7 years). Participants were screened for: personal histories of neurological and psychiatric disease; current recreational or prescription use of drugs that are known to affect central nervous system; eye disease and eye injury; eye movement disorders; ptosis ('drooping eyelid'). All participants reported normal or corrected to normal vision.

During the experiment, participants sat in a magnetically shielded room (MSR), 2.10 m in front of a Mitsubishi Diamond Pro 2070 monitor controlled by a Windows PC with MATLAB Psychtoolbox software. The screen resolution was 1024 by 768 pixels and the monitor frame rate was 100 Hz. The monitor was outside the MSR and was viewed through a cut-away portal. Stimuli consisted of vertical, stationary, maximum contrast, three cycles per degree, square-wave gratings presented centrally on a mean luminance background. The grating stimulus subtended 8 deg both horizontally and vertically. The duration of each stimulus was randomly varied between 1.5 – 2 s and preceded by 2 s of fixation spot only. Participants were instructed to fixate on a small red fixation spot in the centre of the screen for the entire experiment and they were instructed to 'press the response button as soon as the grating disappears'. The next trial started automatically 1 s after the grating disappeared, therefore in order for the response to be recorded participants had to press the button before the next trial had started. 200 stimuli were presented in a session and participants responded with the right hand by pressing a button on a response pad. The task took approximately 20 min.

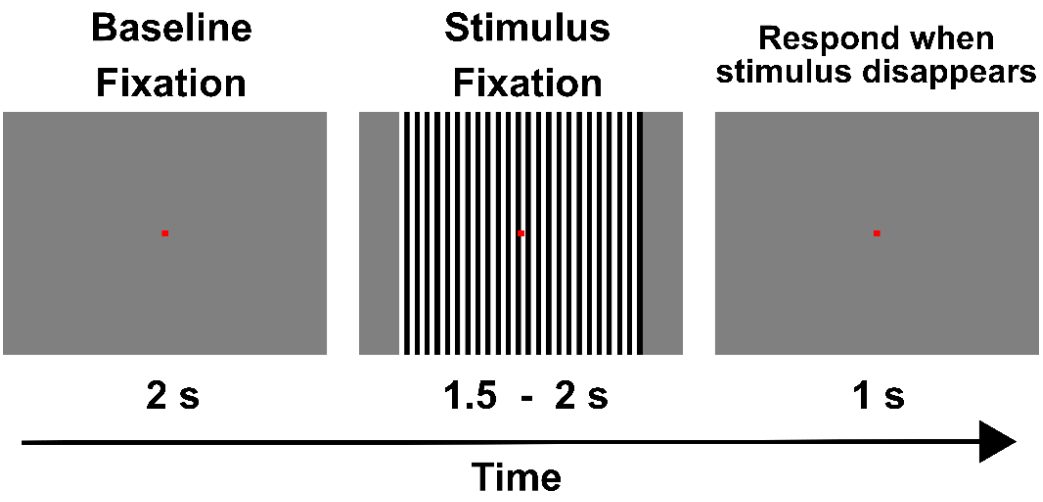

Figure 3-1. Experimental paradigm
Following an average luminance baseline, a 100% contrast grating was presented for a variable period of time. Participants were instructed to fixate on the central spot throughout the experiment and to respond with a button press within 1 s from grating offset

3.3.2 Eye tracking acquisition

Eye movements were recorded monocularly from the right eye with a MEG-compatible video-based remote eye tracker (iView X MEG, SMI GmbH). The eye tracker was positioned 120 cm in front of a participant below the monitor screen and data was acquired at a sampling rate of 250 Hz. After calibration (9 points) the system determined the gaze direction from the position of pupil only. Participants were asked to stay completely still during the recording and their head was immobilized in the MEG dewar with a head cuff and custom-built chin rest. Because head movements were almost completely absent using these procedures, we were able to collect/analyse eye movement data without using a corneal reflex – this resulted in substantially lower levels of noise in the estimation of gaze position (See previous Chapter). After every twenty-five trials, the system was recalibrated. Eye tracking recording was remotely controlled from the stimulus PC using iViewX functions within the MATLAB Psychtoolbox. The time of triggers sent from the visual stimulation computer were recorded alongside the eye position.

3.3.3 Microsaccade detection and characterisation

MSs were detected and characterised in 4 s intervals centred on the stimulus onset using custom MATLAB functions written by the PhD candidate and functions from the EYE-EEG plug-in for EEGLAB (Dimigen et al. 2011). Following (Engbert & Mergenthaler 2006), MSs were defined as outliers in 2D velocity space. First, eye position data were transformed to velocities using a moving average of velocities over 5 data samples in order to supress high-frequency noise. Then detection thresholds for each trial were computed by calculating median-based standard deviations of velocity (separately for vertical and horizontal movement components) and multiplying it by the factor of 6, resulting in an elliptic threshold in 2D velocity space. Additionally, MSs had to have a minimum duration of at least 3 data samples (12 ms) and amplitude between 0.1 and 2 deg. For each trial, performance of the detection algorithm was verified by offline visual inspection of position and velocity time courses and of eye image videos. This visual inspection procedure together with conservative detection thresholds resulted in good quality data, demonstrated by the identified microsaccades clearly conforming to the expected 'main sequence' distribution (Fig. 3-2 B; Zuber et al. 1965), confirming the validation work presented in Chapter 2.

Trials were excluded from analysis if any of following occurred: loss of pupil data (mostly due to blinks); median based standard deviation of velocity for either horizontal or vertical coordinate was higher than 2.5 (indicative of large noise); an eye movement larger than 2 deg; artefacts in the MEG signal (see below). Three subjects were completely excluded from the analysis because for each of them more than 50% of trials were excluded for the analysis. For the remaining fourteen subjects, on average 28% of trials were excluded from the analysis.

3.3.4 MEG acquisition and pre-processing

Whole head MEG recordings were made using a CTF-Omega 275-channel radial gradiometer system sampled at 1200 Hz (0–300 Hz band-pass). An additional 29 reference channels were recorded for noise cancellation purposes and the primary sensors were analysed as synthetic third-order gradiometers. Three of the 275 channels were turned off due to excessive sensor noise. At the commencement of each active period of stimulation a TTL pulse was sent to the MEG system. Each participant had a 1 mm isotropic FSPGR MRI scan available for source localisation analysis. To achieve MRI/MEG co-registration, the fiduciary markers were placed at fixed distances from anatomical landmarks identifiable in participants' anatomical MRIs (tragus, eye centre). Fiduciary locations were verified afterwards using digital photographs. Offline, recordings were downsampled to 600 Hz (0 – 150 Hz bandpass) and cardiac artefact was removed using independent component analysis based on time course and topography of the identified components. Trials contaminated with large muscle artefacts, signal jumps or distortions of the magnetic field were identified by visual inspection and removed.

3.3.5 Source localization of stimulus induced gamma oscillations

In order to obtain source localization maps of gamma oscillations induced by the stimulus we employed a commonly used variant of the beamformer approach; synthetic aperture magnetometry (SAM) (Vrba & Robinson 2001). For each participant a global covariance matrix was calculated for the gamma band (30 - 70 Hz). Based on this covariance matrix, a set of beamformer weights was computed for the entire brain at 4 mm isotropic voxel resolution. A multiple local-spheres volume conductor model was derived by fitting spheres to the brain surface extracted by FSL's Brain Extraction Tool. For gamma-band SAM image reconstruction, virtual sensors were constructed for each beamformer voxel and Student t images of band-limited (30–70 Hz) source power

changes computed using a baseline period of −1.5 to 0 s and an active period of 0 to 1.5 s. Peak locations of gamma band activity (max t-values) for each participant were found consistently in the visual cortex.

3.3.6 Induced gamma activity in the visual cortex source

Having defined a target location for each of the datasets, virtual sensors were generated for these locations using SAM beamformer coefficients obtained using covariance matrices bandpass filtered between 0 and 140 Hz. Time–frequency analysis of virtual sensors was conducted using the Hilbert transform between 1 and 140 Hz at 0.5 Hz frequency step intervals (filtering with an 8 Hz bandpass, 3rd order Butterworth filter). Time–frequency spectrograms were computed as a percentage change from the baseline energy for each frequency band.

3.4 Results

3.4.1 Microsaccades

Participants were instructed to maintain fixation throughout the experiment while they were repeatedly presented with a high-contrast grating and instructed to respond with a button press whenever the grating disappeared (Fig. 3-1). In total, 6178 microsaccades were detected during 7380 seconds of fixation in 14 subjects, which resulted in an average microsaccade frequency of 0.84 Hz. The somewhat low frequency of microsaccades is consistent with other reports when subjects received strong fixation instructions (Dimigen et al. 2009; Steinman RM, Cunitz RJ, Timberlake GT 1967). The median of microsaccade magnitude was 0.26°, median peak velocity was 22.26°/s, and median duration was 20 ms. In agreement with previous research, we observed a number of typical microsaccade characteristics. First, the vast majority (87%) of microsaccades were oriented horizontally

(Fig. 3-2 A; Dimigen et al. 2009; Rolfs 2009) despite the fact that in our task there were no horizontally displaced targets for covert attention. Second, microsaccade magnitude and peak velocity were highly correlated (r = 0.92, p < 0.01) and followed the 'main sequence' (Zuber et al. 1965) characteristic for saccadic eye movements (Fig. 3-2 B). Third, we observed the typical suppression - rebound sequence of microsaccade occurrences following stimulus presentation. Namely, the occurrence of microsaccades was lowest in the 110 - 190 ms and highest in the 220 - 300 ms time-window after stimulus onset (Fig. 3-2C). It is the latter effect that underlies the microsaccadic spike artefact being mistaken for cortical gamma in some EEG studies (Yuval-Greenberg et al. 2008). Fourth, the frequency distribution of the inter-microsaccade interval peaked ~ 200 ms and then decreased in an exponential fashion (Fig 3-2 D; Otero-Millan et al. 2008; Bosman et al. 2009). In summary, these characteristics mean that we can be confident that we have successfully measured microsaccades in the MEG environment using remote video based eye tracking.

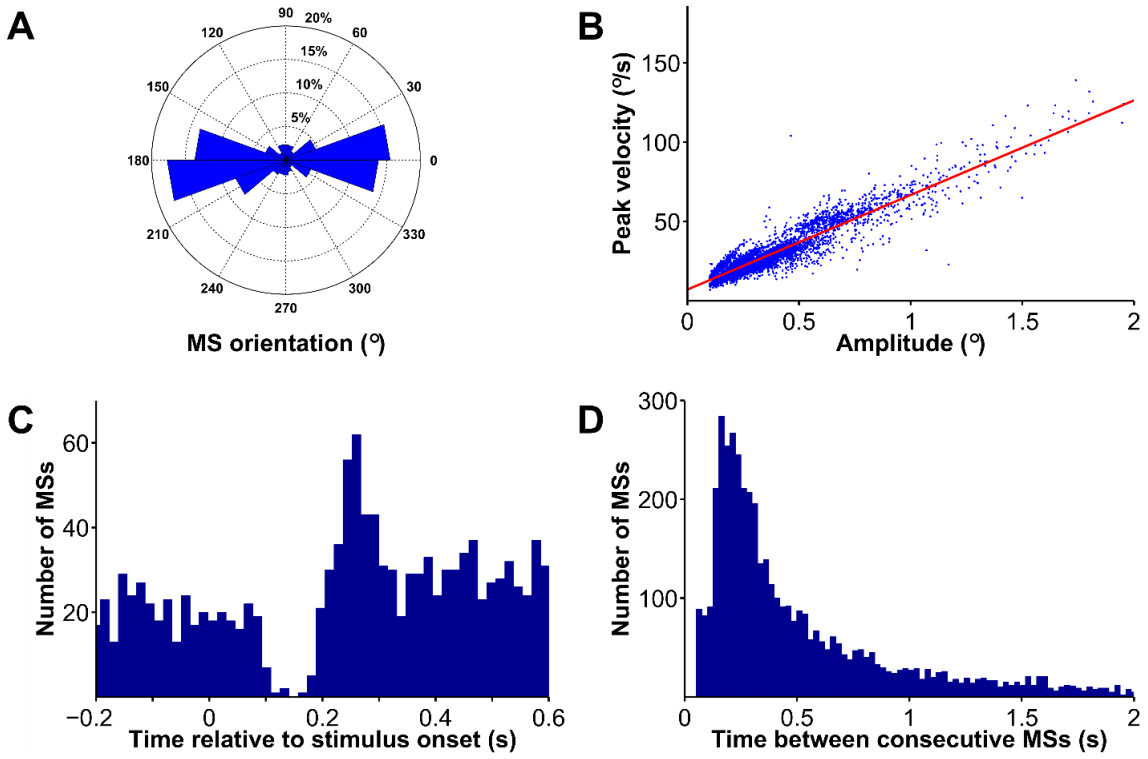

Figure 3-2. Microsaccade characteristics
A. Rose plot of orientations grouped in 18 bins (bin width: 20°). Length and width of each triangle represents the relative percentage of microsaccades in the corresponding orientation bin. Note a predominantly horizontal orientation. **B**. Scatterplot illustrating the typical 'main sequence' distribution i.e. a strong linear relationship between MS magnitude and peak velocity (with one dot per MS). **C**. Average temporal distribution of microsaccades around stimulus onset (bin width: 16 ms). Note the characteristic suppression - rebound sequence following stimulus onset. **D**. Frequency distribution of time since last MS (bin width: 25 ms). Note the peak ~ 200 ms and an exponential decrease.

3.4.2 No evidence for a relationship between microsaccades and visual gamma oscillations across subjects

To investigate if there is a between-subject relationship between microsaccades and visual gamma oscillations we source-localized stimulus-related gamma oscillations (30 – 70 Hz) to the early visual cortex (Fig. 3-3) and expressed gamma amplitude as a percent change from baseline for each participant. The group average time courses of the microsaccade occurrence and visual gamma amplitude did not show any apparent

relationship (Fig. 3-4 A). Average gamma amplitude in the baseline was, by definition, approximately 0 and rose sharply after stimulus onset, reaching a peak around 0.15 s, and then decreased until 0.3 s (transient gamma). Then between 0.3 and stimulus offset gamma amplitude was sustained at a relatively constant level (sustained gamma) – this is consistent with previous studies using a similar paradigm (e.g. (Swettenham et al. 2009; Muthukumaraswamy et al. 2010). In contrast, microsaccades were almost completely absent during the high-amplitude transient gamma window and their numbers peaked between 0.2 s and 0.3 s after stimulus onset - that is when gamma amplitude was decreasing. During the sustained gamma window microsaccade numbers briefly increased between 0.5 and 0.75 s. and steadily decreased between 1 and 1.5 s.

Both microsaccade rates and the amplitude of visual gamma oscillations varies markedly across individuals (Muthukumaraswamy et al. 2010; Otero-Millan et al. 2012) and here we investigated if the two variables were related. We did not find significant correlations (Fig. 3-4 B and C) between rates of microsaccades in the corresponding time-windows for transient gamma (0 – 0.3 s, 35 – 80 Hz) amplitude ($r = 0.09$, $p = 0.76$) or sustained gamma (0.3 – 1.5 s, 40 – 65 Hz) amplitude ($r = 0.15$, $p = 0.52$). These results do not provide evidence for the hypothesis that the properties of visual gamma oscillations are related to the occurrence of microsaccades, when assessed across subjects.

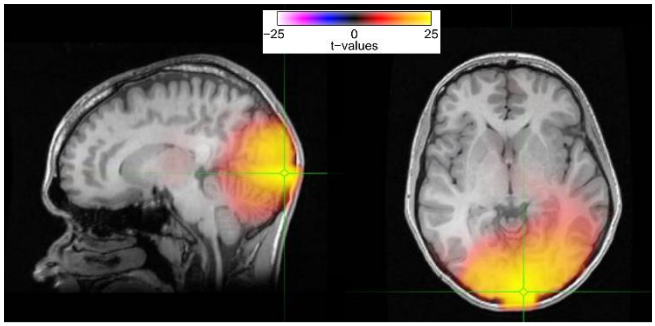

Figure 3-3. Beamformer source-localization of stimulus-related gamma oscillations (30 – 70 Hz) to the early visual cortex. Colour superimposed on an individuals MRI image indicates t-value from a students t-test between baseline and post-stimulus onset gamma amplitude. Peak t-value (location of the virtual electrode) is indicated with the green cross-hair.

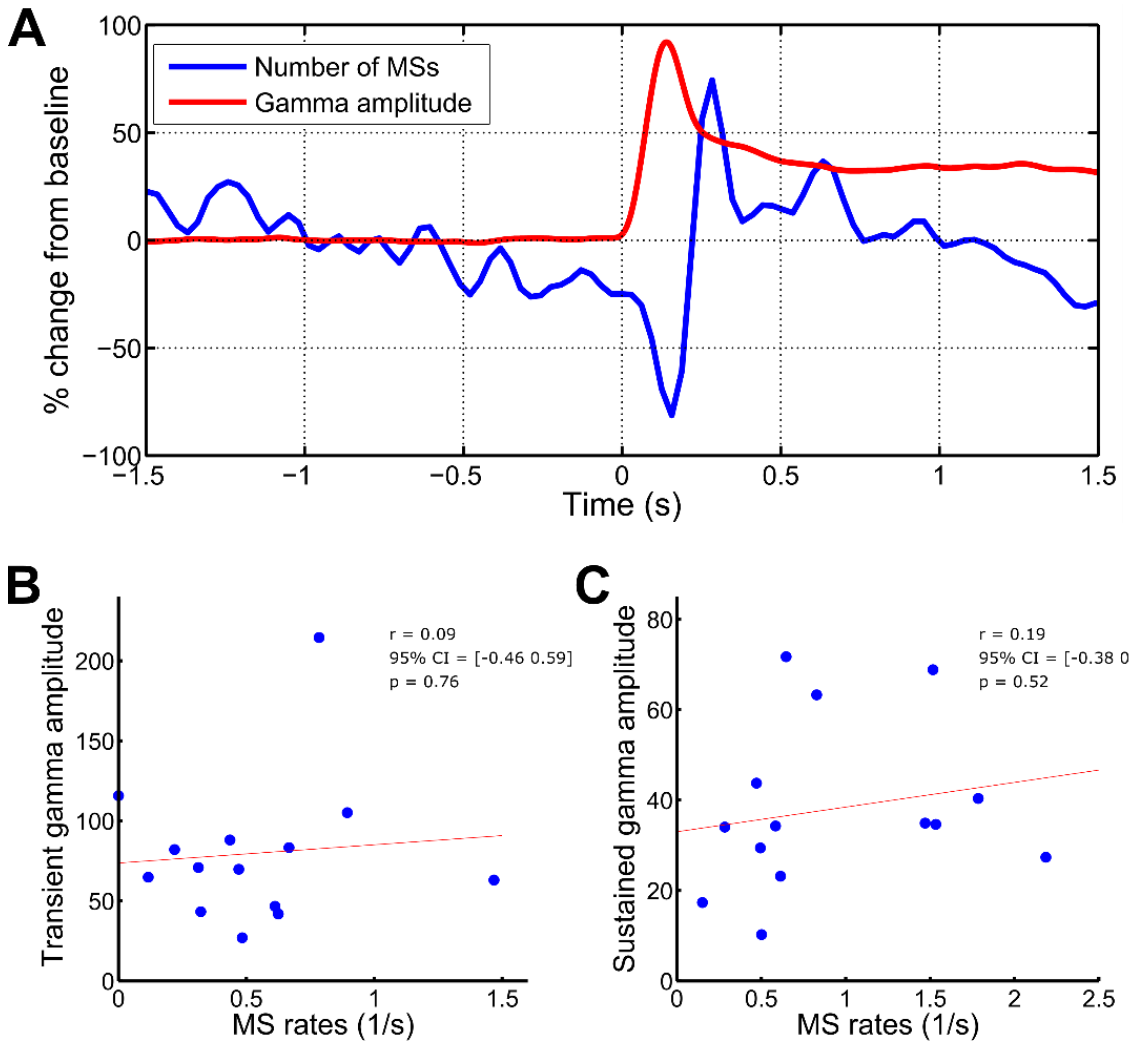

Figure 3-4. No relationship between occurance of microsaccades and gamma amplitude. A. Group average time-courses of microsaccade numbers (blue) and gamma (30 – 70 Hz) amplitude (red) expressed as % change from baseline . **B**. Scatterplot illustrating lack of significant relationship between transient gamma amplitude (0 – 0.3 s) and microsaccade rates in the corresponding time-window across individuals. **C.** Same as B but for sustained gamma amplitude (0.3 – 1.5 s).

3.4.3 Visual gamma oscillations with and without microsaccades

Similarly to Yuval-Greenberg et al. (2008) , we took advantage of the fact that a proportion of trials did not contain microsaccades in the stimulus time-window (0 – 1.5 s). Consequently, we grouped trials into two post-hoc conditions 'with microsaccades' and 'without microsaccades' for each participant. 10 out of 14 subjects had an approximately even number of trials in the two conditions (between 35% and 65% in each condition). For these 10 participants we calculated time-frequency plots for the two conditions based on the activity localized to the occipital cortex (Fig. 3-3) and averaged them within each condition. Figure 3-5 shows the average time-frequency plots with the corresponding distribution of microsaccades. Importantly, as shown in Figure 3-5 A & B, trials with microsaccades as well as without microsaccades produced the typical visual gamma response (Hoogenboom et al. 2006; Muthukumaraswamy et al. 2010). We did not find any increases in gamma amplitude associated with the presence of microsaccades. Interestingly, however, a cluster-based permutation test found a significant difference between the two conditions in the time-frequency window corresponding to the transient gamma response (Fig. 3-5 C). Namely, average transient gamma amplitude was lower on trials with microsaccades than on trials without microsaccades ($p < 0.01$).

These results were confirmed when average amplitudes and peak frequencies were compared between the two conditions (Fig. 3-6). Sustained gamma amplitude (0.3 – 1.5 s, 40 – 65 Hz) did not differ between the two conditions ($t(9) = 0.21$, $p = 0.84$) whereas average transient gamma amplitude (0.05 – 0.29 s, 35 – 80 Hz) was larger for trials with microsaccades ($t(9) = -6.22$, $p < 0.01$). Also, the peak gamma frequencies, important individual markers that were shown to predict performance and to be highly heritable (Edden et al. 2009; van Pelt et al. 2012), did not differ between the two

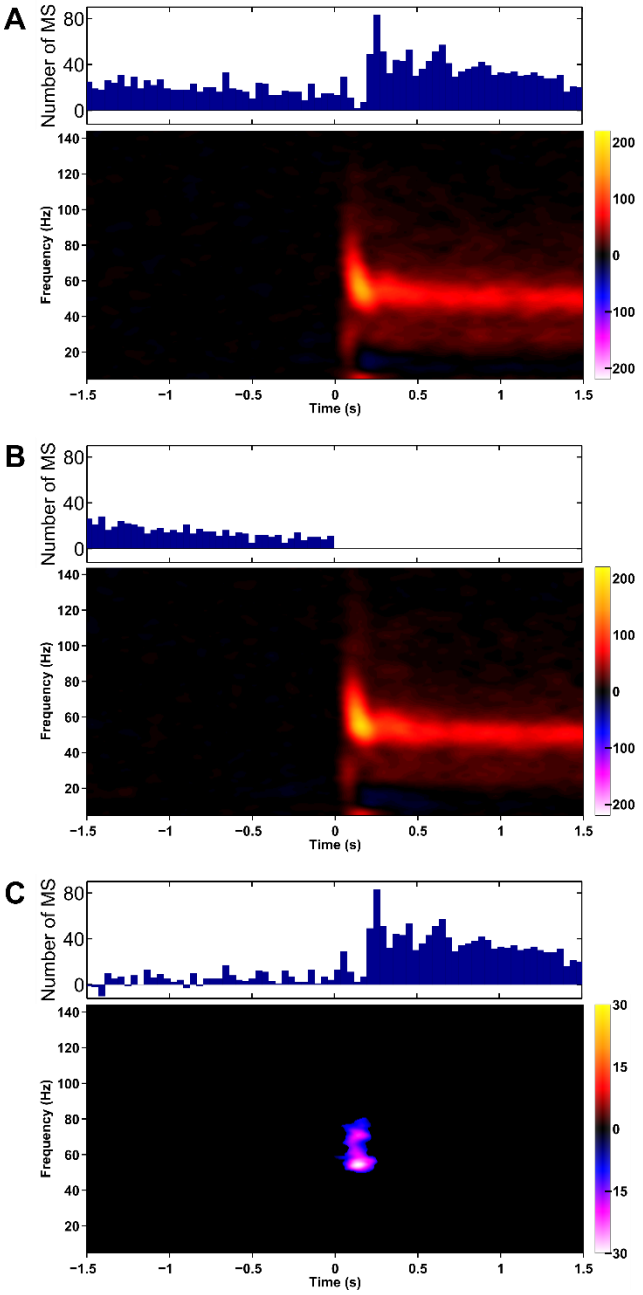

Figure 3-5. **Stimulus-induced gamma oscillations in the visual cortex and the corresponding distributions of microsaccades**. **A**. For trials with microsaccades after the stimulus onset. **B**. For trials without microsaccades after the stimulus onset. **C**. Difference between A and B with a significance mask ($p<0.01$) produced using a randomisation test with cluster correction for multiple comparisons.

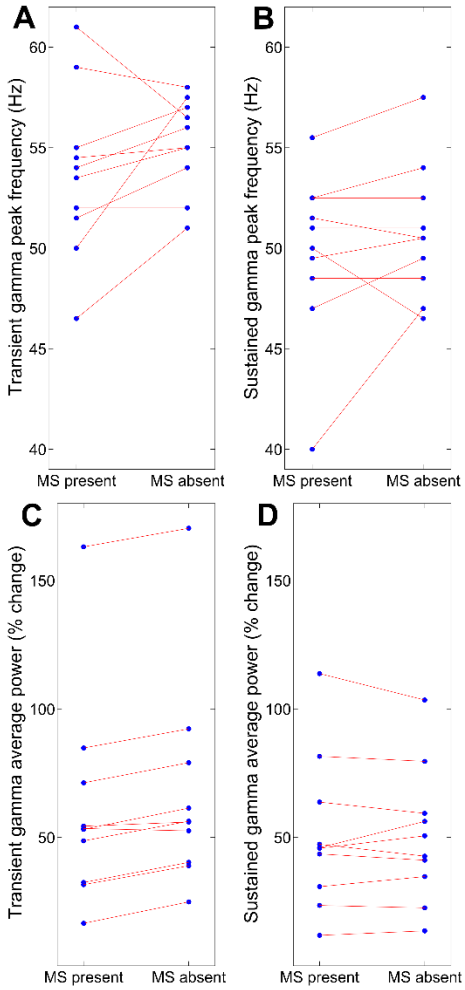

Figure 3-6. **Comparison of visual gamma characteristics between trials with and without microsaccades**. The only significant difference is a reduced transient gamma amplitude for trials with microsaccades (in C)

conditions neither for sustained gamma ($t(9) = -1.48$, $p = 0.17$) nor for transient gamma ($t(9) = 0.21$, $p = 0.83$). Furthermore, all the results described in this paragraph were not influenced by baseline gamma levels (Figure 7-2 Appendix) and the lower transient gamma for trials with microsaccades cannot be explained by attentional fluctuations between trials (as indexed by baseline alpha levels and baseline pupil size, Figure 7-2 in the Appendix).

3.4.4 No substantial evidence for a relationship between microsaccades and sustained visual gamma oscillations across trials

The remaining 4 subjects who were not included in the analysis described in the paragraph above had microsaccades present in the vast majority of trials and also had the highest microsaccadic frequencies of all participants (2.11, 1.91, 1.18 and 1.16 microsaccades/s). To test whether there is a relationship between microsaccades and sustained gamma oscillations in these subjects we carried out a single-trial analysis. For each subject, we correlated the number of microsaccades in each given trial with average sustained gamma power on that trial. This analysis is illustrated in Figure 3-7 with trials sorted from the lowest to the highest sustained gamma amplitude. From the figure it appears that there is no striking relationship between number of microsaccades and sustained gamma power on a trial basis. Indeed, we did not find any positive correlations between number of microsaccades and sustained gamma power. For three subjects we did not find significant correlations (Subjects 7: $r = -0.18$, $p = 0.07$; Subject 13: $r = -0.17$, $p = 0.06$; Subject 14: $r = -0.16$, $p = 0.11$) and for one subject we found a weak significant negative correlation (Subject 3: $r = -0.26$, $p < 0.01$). These results do not provide substantial evidence for the hypothesis that microsaccades are related to sustained gamma power on single-trial basis.

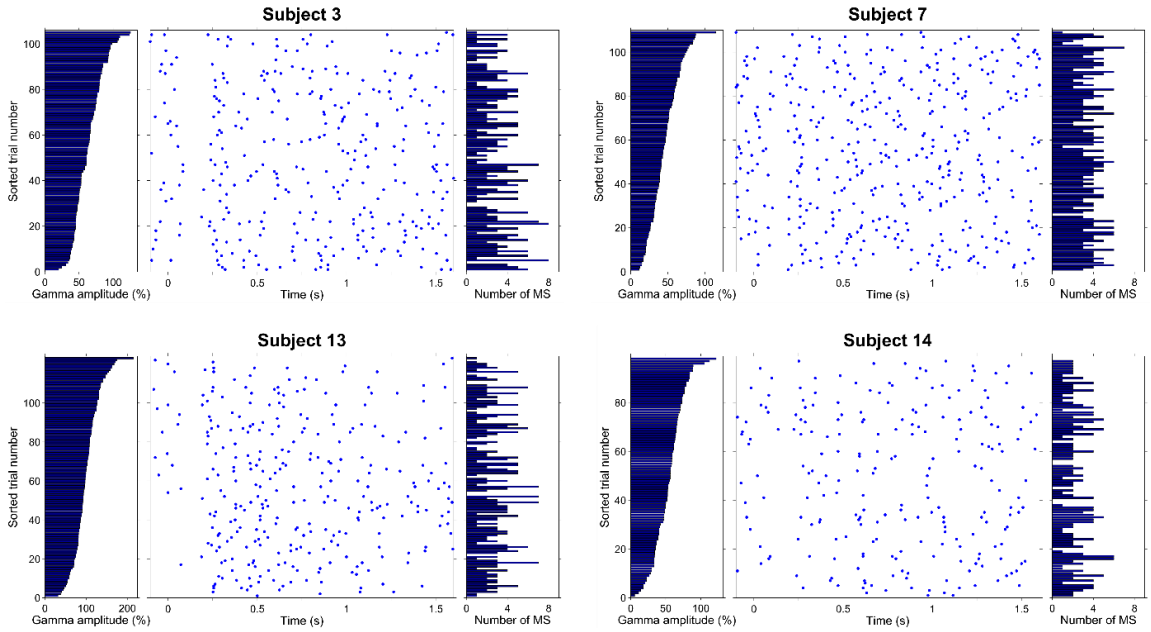

Figure 3-7. Comparison of sustained gamma amplitude (0.3 – 1.5 s) and number of microsaccades on a single trial basis for four subjects with highest microsaccade rates. For each subject, trials are sorted from the lowest to the highest average sustained gamma amplitude (left panels). Middle panels illustrate the temporal distribution of microsaccades on each trial and the right hand panels illustrate number of microsaccades on each trial.

3.5 Discussion

By detecting microsaccades in a paradigm commonly used in animal and human studies for inducing visual gamma oscillations we here provide the first direct evidence that sustained visual gamma oscillations recorded with MEG are unlikely to be related to microsaccades. We did not find evidence for a relationship between rates of microsaccades and the amplitudes of visual gamma oscillations across time, nor across participants. Furthermore, we observed typical gamma oscillations on trials with and without microsaccades. Whereas sustained gamma amplitude and frequency were not significantly different between the two types of trials, transient gamma amplitude was surprisingly found to be lower in trials with microsaccades. For subjects with highest

microsaccade rates, for whom grouping trials into with and without microsaccades conditions was not possible, correlations across trials did not find any positive relationship between number of microsaccades and sustained gamma amplitude. These results suggest that MEG sustained visual gamma oscillations are unlikely to be related to microsaccades and therefore reflect stimulus processing in local cortical circuits rather than muscle artefacts or peri-microsaccadic activity of retinal (motion on the receptors during eye movement) or extraretinal origin (motor corollary discharges).

These results are important because they provide validity to the studies that have used sustained gamma oscillations in humans to study a number of topics. In terms of links to human behaviour: they predicted the speed of change detection (Hoogenboom et al. 2010) and individual differences in orientation discrimination performance (Edden et al. 2009); they were also related to the allocation of attention (Koelewijn et al. 2013). MEG visual sustained gamma oscillations have been used to investigate the neuronal basis of the MRI BOLD signal (Muthukumaraswamy & Singh 2008; Zumer et al. 2010) and the relationship to the GABA neurotransmitter (Cousijn et al. 2014; Muthukumaraswamy et al. 2009). A number of drug studies shed light on the possible molecular mechanisms of these oscillations (Saxena et al. 2013; Shaw et al. 2015). Moreover, it has been shown that symptoms of schizophrenia are related to abnormal visual oscillations in the gamma band (Grützner et al. 2013; Uhlhaas & Singer 2010).

Although the transient gamma response characteristics (short-lived, broadband) resemble those of the saccadic spike artefact (Carl et al. 2012; Keren et al. 2010), here we showed that the transient gamma response is unlikely to berelated to the artefact for a number of reasons. First, saccadic spike artefact is known to occur at eye movement onset and the observed transient gamma's peak time-window (0.1 – 0.2 s) corresponds to the microsaccadic-inhibition period following stimulus presentation with very few microsaccades present. Second, transient gamma amplitude was lower on trials when

microsaccades were present. Third, a number of animal LFP studies reported the same transient broadband gamma response between 0.1 and 0.2 s from stimulus onset (e.g. Ray & Maunsell 2011; Xing et al. 2012). LFPs sample local populations of neurons (Buzsáki et al. 2012) , as these signals can be very different for electrodes separated by 1 mm (Destexhe et al. 1999), and it is highly unlikely that occipital electrodes would be affected by the artefact originating from the extraocular muscles. Therefore the transient and sustained gamma responses are both likely to be of neural origin.

The fact the transient gamma response was weaker on trials with microsaccades may suggest that we found first evidence for the so called 'microsaccadic suppression' phenomenon in the human visual cortex. Similar to perceptual suppression during saccades (called 'saccadic suppression'), an increase in visual thresholds for microsaccades, which might contribute to perceptual stability during fixation, was also observed (Beeler 1967; Zuber & Stark 1966). Recent neurophysiological findings have identified a possible neural basis of microsaccadic suppression. Namely, microsaccades near the onset of a test stimulus decreased detection and suppressed activity in middle temporal, lateral intraparietal and ventral intraparietal areas (Herrington et al. 2009). Moreover, another study found that stimulus onsets that were temporally close to microsaccades elicited visual bursts in the SC less effectively than stimuli that were presented in the absence of microsaccades (Hafed & Krauzlis 2010). Therefore it is possible that transient gamma difference between the two conditions in our experiment stems from suppression of stimulus processing by microsaccades occurring just after stimulus onset.

Although both transient and sustained gamma components become stronger with increasing stimulus size and contrast (Gieselmann & Thiele 2008; Perry 2015; Perry et al. 2013; Ray & Maunsell 2010; Ray & Maunsell 2011), there are marked differences between the two that can to some extent explain why only the transient component was affected

by the presence of microsaccades. Invasive recordings from primary visual cortex of primates demonstrated that a broadband gamma response is closely coupled to local firing rates and a narrowband response reflects a coherent oscillation in the LFP across an extended region of cortex which is tuned differently to local firing rates and may reflect the influence of fast-spiking interneurons on the membrane potentials of pyramidal cells (Cardin et al. 2009; Jia et al. 2011; Ray & Maunsell 2011). Moreover, laminar analysis of field and spiking activity in monkey V1 showed that the transient response in each layer reflects input to the layer where it is recorded and it is larger in output than input layers because the LGN input into layer 4C in amplified within the cortex. The sustained component, on the other hand, is likely to be generated by recurrent or feedback interactions that are layer-specific (Xing et al., 2012). The cortical origin of the sustained gamma oscillations is further supported by the observation that in alert macaques they were only found in V1 but not in LGN (Bastos et al. 2014), whereas transient gamma is found in the retina, LGN and V1 (Castelo-Branco et al. 1998).

Visual oscillations are not only related to low-level visual processing, they also play a role in cognitive processes such as visual selective attention. Covertly shifting attention produces retinotopically specific modulations of alpha (~ 10 Hz) power with a relative decrease contralateral to the attended hemifield and a relative increase ipsilateral to the attended hemifield (Händel et al. 2011; Siegel et al. 2008; Thut et al. 2006; Worden et al. 2000). Microsaccades also appear to play a role in covert attention (Engbert & Kliegl 2003). Directions of microsaccades are often biased towards the attended location (Laubrock et al. 2010) and in some circumstances this bias may account for the attention-related improvements in behavioural performance (Hafed 2013). In the next chapter, I will investigate whether the attentional processes mediated by microsaccades and alpha oscillations are related or independent.

Chapter 4:
Visual alpha oscillations and microsaccades in spatial attention

4.1 Abstract

Alpha oscillations are thought to play an important role in attention. In covert attention tasks, alpha amplitude shows relative decreases contralateral to the attended hemifield and relative increases ipsilateral to the attended hemifield, which are thought to represent the prioritisation of relevant information and inhibition of the processing of distracting/irrelevant information respectively. Counter to a common assumption that covert orienting occurs in the absence of oculomotor activity, microsaccades have been shown to also play a role in covert attention. Their directions are often biased towards the direction of attention, however the exact time-course and functional significance of this effect are not well-established. By recording MEG and high-speed video eye tracking simultaneously while participants completed a covert spatial attention task where they were instructed by a cue to attend to either left or right hemifield and after a delay period discriminate target orientation at the cued location, we aimed to investigate whether the attentional mechanisms represented by microsaccades and alpha oscillations are the same or independent of each other. We found that, in agreement with previous studies, all subjects showed stronger alpha oscillations in the sensors ipsilateral to the direction of cued attention – the so-called alpha lateralisation effect. Microsaccades directions were biased towards the target location only in a short interval after cue onset. We did not find evidence for a between-subject relationship between alpha lateralisation and microsaccade lateralisation. We conclude that microsaccades and alpha oscillations represent two independent attentional mechanisms - the former related to early attention shifting and the latter to maintaining sustained attention.

4.2 Introduction

In the previous chapter I recorded and characterised microsaccades in a paradigm commonly used to study visual gamma oscillations in animals and humans. I showed that visual gamma oscillations are not related to microsaccades and that they most likely reflect stimulus processing in local neural circuits. Another class of visual oscillations commonly recorded non-invasively in humans are alpha oscillations. Microsaccades and alpha oscillations are both thought to play important roles in spatial attention. In this chapter I investigate whether they are related or represent independent attentional mechanisms.

To make sense of the overwhelming, continuous flow of sensory information it is critical to actively select and prioritize information that is important for our behavioural goals. For instance, humans can select what part of the visual space they attend to by either overtly directing their attention to the location of interest with saccadic eye movements or by shifting their central processing resources covertly (without eye movements) to a selected location in the periphery of the visual field for preferential processing (Anton-Erxleben & Carrasco 2013; Posner 1980). The latter process is known as top-down covert spatial selective attention and research has shown that it facilitates many aspects of visual performance such as spatial resolution (Yeshurun & Carrasco 1998), contrast sensitivity (Herrmann et al. 2010) and grouping (Scholte et al. 2001). At the neural level, covert attention enhances processing of visual input from task-relevant locations and suppression of distracting input from task-irrelevant locations (Ungerleider 2000).

Many MEG and EEG studies suggest that alpha (~ 10 Hz) oscillations support covert attention. Covertly shifting attention produces retinotopically specific modulations of alpha power with a relative decrease contralateral to the attended hemifield and a relative increase ipsilateral to the attended hemifield (Händel et al. 2011; Siegel et al. 2008; Thut et al. 2006; Worden et al. 2000). This modulation is thought to prioritise the

processing of relevant information and inhibit the processing or irrelevant/distracting information. Pre-stimulus alpha lateralization predicts reaction time (Thut et al. 2006) and accuracy (Händel et al. 2011; Siegel et al. 2006) in attentional tasks. Moreover, the alpha modulation by covert spatial attention effect is very robust: four orientations of covert attention (25% chance level) were reliably classified on a single trial level with 69% correct (van Gerven & Jensen 2009). In general the link between alpha modulation and covert attention forms the bedrock of theories that propose that alpha oscillations plays an active role in controlling information flow in the brain (Klimesch et al. 2007; Jensen & Mazaheri 2010) rather than just a passive marker of a behavioural state.

Recently, however, it became apparent that the assumption that covert attention operates in the absence of oculomotor behaviour (Carrasco 2011) does not hold. With the use of high-speed video eye tracking it has been observed that covert attention shifts often correlate with the occurrence and direction of microsaccades (Engbert & Kliegl 2003; Hafed & Clark 2002; Hafed et al. 2013; Laubrock et al. 2010; Pastukhov & Braun 2010). However, the exact details of this effect appear to vary between studies. Laubrock et al. 2010 suggested that direction of microsaccades shortly after cue onset (during the microsaccade rebound interval that is between 0.2 and 0.3 s after cue onset) is consistent with the direction of cue, whereas directions of later microsaccades do not follow the direction of attention and instead may be determined by other factors such as compensation for not sufficient drift movements. Others have found that cue directions are correlated with microsaccade directions throughout sustained covert attention intervals of few seconds (Hafed et al. 2011) and immediately before anticipated target onset (Pastukhov & Braun 2010). Moreover, Hafed (2013) found that microsaccade directions fluctuated between cue-congruent and cue-incongruent after cue onset and suggested that behavioural performance improvement in covert attention tasks (a relatively small effect in the first place) can be explained to a large extent by a

microsaccadic compression of space phenomenon (similarly to regular saccades (Ross et al. 1997)) when microsaccades occur around ~50 ms before target onset.

Apart from the fact that both alpha oscillations and microsaccades are lateralised and related to performance in the pre-stimulus interval in covert-attention tasks, they also share other similarities. For instance, both the execution of microsaccades and lateralisation of alpha oscillations is thought to be controlled by frontal eye fields (Capotosto et al. 2009; Martinez-Conde et al. 2013). What is more, microsaccades have been shown to explain a link between behaviour and neural activity in a motion detection task (Herrington et al. 2009)

Here we investigated whether microsaccades and alpha oscillations represent independent or related mechanisms of covert attentional selection.

4.3 Methods

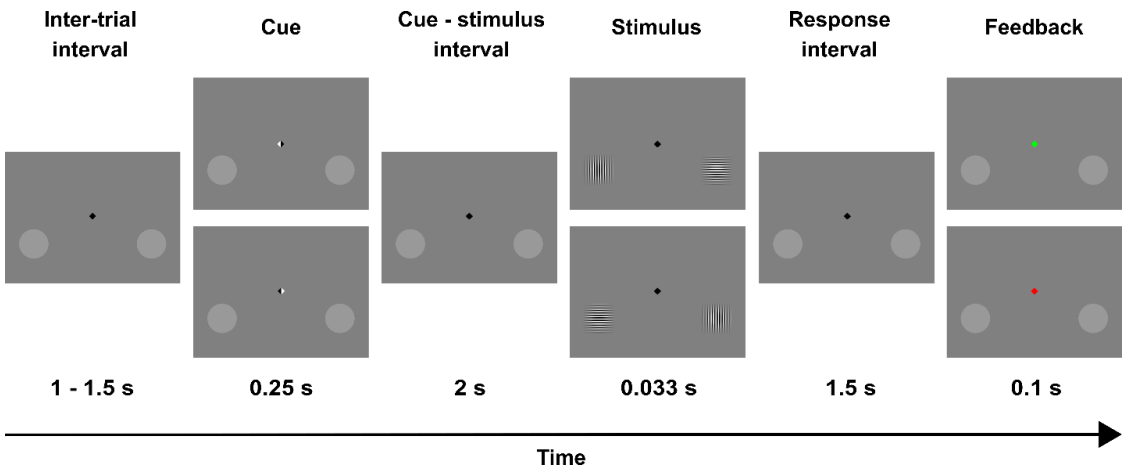

Figure 4-1. A schematic representation of the experimental paradigm for our cued spatial attention task. The participants' task was to covertly attend (without moving their eyes) to the cued luminance pedestal and to judge the orientation of a Gabor patch (clockwise or anticlockwise from vertical) that appeared on the cued pedestal after a 2 second delay (cue-target interval).

4.3.1 Participants, stimuli, and task

Sixteen volunteers participated in the experiment after giving informed consent, with all procedures approved by the Cardiff University School of Psychology Ethics Committee. Eye tracking data for four participants were too noisy due to the challenging nature of recording eye movements in the MEG environment, and hence were excluded from the analysis (see the specific criteria below). The remaining group of twelve participants consisted of an equal number of males and females and their average age was 26.58 years (SD = 1.44 years). Participants were screened for: personal histories of neurological and psychiatric disease; current recreational or prescription use of drugs that are known to affect central nervous system; eye disease and eye injury; eye movement disorders; ptosis ('drooping eyelid'). All participants reported normal or corrected to normal vision.

During the experiment participants sat upright in a magnetically shielded room (MSR), 0.8 m in front of a projector screen. The visual stimuli were rear projected onto the screen via a Sanyo PLC-XP41 DLP projector controlled by a Windows PC with MATLAB Psychtoolbox software (Brainard 1997). The display resolution was 1024 by 768 pixels and the projector frame rate was 60 Hz. Participants performed a cued spatial attention task. Participants were instructed to fixate their gaze on a central fixation spot throughout the experiment. The central fixation spot was a black square 0.4 deg in size and rotated by 45 deg. Each trial began with either the left or right part of the fixation spot briefly (0.25 s) turning white and therefore forming an arrowhead. This spatial cue instructed participants to covertly (without moving their eyes) attend to one of two luminance pedestals in the lower left and lower right quadrants of the screen. The pedestals were positioned on the screen so that their centres were 2.5 deg below the horizontal meridian, and 8 deg to the left and right of the vertical meridian. The pedestals themselves had a radius of 4 deg. The cues were 100% valid. After a cue-stimulus interval of 2 s a Gabor

patch (100 % contrast, 3 cycles/deg) was presented at each luminance pedestal. The cued patch (target) was tilted either clockwise or anticlockwise from the vertical. The non-cued patch (distractor) was either horizontal or vertical. Patches were displayed for ~ 0.033 s (two display frames) and the participant's task was to report the orientation of the target patch (clockwise or counter-clockwise) with a button press and to ignore the distractor patch. Participants were instructed to perform the task as quickly and as accurately as possible and to make their best guess when they could not clearly see the orientation of the target patch. Only responses made up to 1.5 s after stimulus offset were recorded. Subsequently the fixation spot changed colour to green (indicating a correct response) or red (indicating an incorrect or missed response) for 0.1 s. Trials were separated by an interval of variable duration between 1 and 1.5 s. Each combination of cue direction (left and right), target orientation (clockwise and counter clockwise) and distractor orientation (horizontal or vertical) was equally likely and the order of trials was randomised for each participant.

Each participant first completed a titration session with four blocks of 60 trials (240 trials in total) where 8 different levels of tilt were used (from 0.25 to 2 deg in steps of 0.25 deg). A psychometric function was fitted to each participant's behavioural data and the tilt level corresponding to 70% correct performance was obtained. The main experimental MEG session then took place no longer than a week after the titration session. In this experimental session each participant completed four blocks of 100 trials (400 trials in total) and the target patch was always tilted according to their 70% correct performance level from the titration session. The two sessions were otherwise identical. The total task duration in the experimental session was approximately 35 min. MEG and eye tracking were recorded only in the experimental session.

4.3.2 Eye tracking acquisition

Eye movements were recorded monocularly from the right eye with a MEG-compatible video-based remote eye tracker (iView X MEG, SMI GmbH). The eye tracker was positioned 120 cm in front of a participant below and behind the projector screen and data was acquired at a sampling rate of 250 Hz. After calibration (9 points) the system determined the gaze direction using the position of the pupil only. Participants were asked to stay completely still during the recording and their head was immobilized in the MEG dewar with a head cuff and custom-built chin rest. Because head movements were almost completely absent using these procedures, we were able to collect/analyse eye movement data without using a corneal reflex – this resulted in substantially lower levels of noise in the estimation of gaze position. The system was recalibrated immediately before the start of each block. Eye tracking recording was remotely controlled from the stimulus PC using iViewX functions within the MATLAB Psychtoolbox (Brainard 1997). The time of triggers sent from the visual stimulation computer were recorded alongside the eye position.

4.3.3 Microsaccade detection and characterisation

Microsaccades were detected and characterised using custom MATLAB functions written by the PhD candidate and functions from the EYE-EEG plug-in for EEGLAB (Dimigen et al. 2011). Following Engbert & Mergenthaler (2006), microsaccades were defined as outliers in 2D velocity space. First, eye position data were transformed to velocities using a moving average of velocities over 3 data samples in order to supress high-frequency noise. Then detection thresholds for each trial were computed by calculating median-based standard deviations of velocity (separately for vertical and horizontal movement components) and multiplying it by the factor of 6, resulting in an elliptic threshold in 2D velocity space. Additionally, microsaccades had to have a minimum duration of at least 3 data samples (12 ms) and an amplitude below 2 deg. For each trial,

performance of the detection algorithm was verified by offline visual inspection of position and velocity time courses and of eye image videos. This visual inspection procedure together with conservative detection thresholds resulted in good quality data, demonstrated by the identified microsaccades clearly conforming to the expected 'main sequence' distribution (Figure 4-2 A; Zuber et al. 1965).

Trials were excluded from analysis if any of following occurred: loss of pupil data (mostly due to blinks); the median-based standard deviation of velocity for either horizontal or vertical coordinate was higher than 2.5 (indicative of large noise); an eye movement larger than 2 deg; artefacts in the MEG signal (see below). Application of these criteria eliminated trials with noisy data and trials in which participants did not comply with the fixation instruction. Three subjects were completely excluded from the analysis because, for each of them, more than 50% of trials were excluded from the analysis. For the remaining fourteen subjects, on average 23% of trials were excluded from the analysis.

4.3.4 Microsaccadic lateralisation

We wanted to study the time-courses of microsaccade directions in relation to the spatial cue directions in order to determine when microsaccades followed the direction of attention. To this aim microsaccades whose directions were +/- 45 deg from horizontal (93% of all microsaccades) were divided into two groups: microsaccades whose directions were consistent with the cue (towards the target grating patch and therefore away from the distractor) and those whose directions were opposite to the cue (away from the target grating patch and therefore towards the distractor). For each participant separately, microsaccade onset times from each group were binned into 4 ms (sample duration) temporal bins and the number of microsaccades in each bin was divided by the number of good trials times sample duration (4 ms) to arrive at time courses of microsaccadic rates for each group. These time courses were subsequently smoothed with two passes of a

sliding average filter with a width of 9 bins (36 ms) that acted as a low-pass filter on the noisy microsaccade time-courses. Each of the two smoothed time courses of microsaccadic rates (one for microsaccades towards target and one for microsaccades away from target), separately for each individual, was then divided by the average microsaccade rate in the 0.25 – 2.25 time interval from cue onset. This way each of the time-courses was normalised in order to account for individual-differences in absolute microsaccade rates. Microsaccadic lateralisation indices for each participant were calculated separately for early (0.25 – 0.4 s) and late (0.4 – 2.25) time-windows (see the Results section for explanation) as the average difference between the normalised time-courses of microsaccade rates towards target and away from target in the respective time-windows.

4.3.5 MEG acquisition and pre-processing

Whole head MEG recordings were made using a CTF-Omega 275-channel axial gradiometer system sampled at 600 Hz (0–150 Hz band-pass). An additional 29 reference channels were recorded for noise cancellation purposes and the primary sensors were analysed as synthetic third-order gradiometers. Three of the 275 channels were turned off due to excessive sensor noise. At cue onset and stimulus onset a TTL pulse was sent to the MEG system. Data analysis was carried out using the fieldtrip MATLAB toolbox (Oostenveld et al. 2011) and custom MATLAB functions written by the PhD candidate. Continuous data was epoched from - 0.5 s to 2.5 s relative to cue onset and demeaned. Trials contaminated with large muscle artefacts, signal jumps or distortions of the magnetic field were identified by visual inspection and removed. Subsequently, a cardiac artefact was also removed using independent component analysis (Jung et al. 2000) based on the time course and topography of the identified components. Trials were separated into ‘Attend Left’ and ‘Attend Right’ conditions and all subsequent analyses were carried out

separately for the two conditions. In order to simplify the interpretation of sensor level analyses we computed and carried out all subsequent analysis on planar gradients because the strongest field of the planar gradient signal usually is situated above the neural sources. The horizontal and vertical components of the planar gradients were estimated at each sensor location using the fields from the sensor and its neighbouring sensors (Bastiaansen & Knösche 2000). Importantly, the power values for the horizontal and vertical components were summed for each sensor location after the time-frequency analysis. Time–frequency analysis was conducted using the Hilbert transform between 1 and 40 Hz at 0.5 Hz frequency step intervals (filtering with a 6 Hz bandpass, 3rd order Butterworth filter).

4.3.6 Cluster test

We hypothesised, based on previous EEG/MEG studies, that there would be an lateralised difference in Alpha amplitude between the two conditions ('Attend Left' and 'Attend Right') and this was investigated using a nonparametric randomization method identifying clusters of sensors with significant differences in the 7 - 14 Hz frequency and 0.25 – 2.25 time- window. This method corrects for multiple comparisons over sensors in-within subject comparisons (Maris & Oostenveld 2007; Nichols & Holmes 2002). Clusters were defined as spatially adjacent sensors where the t statistics from testing the difference between the two conditions exceeded the $p > 0.05$ threshold. The cluster-level test statistic was defined as the sum of the t statistics of the sensors in a cluster. The type-I error rate for the 272 sensors was controlled by evaluating the cluster-level test statistic under the randomization null distribution of the maximum cluster-level test statistic. This was obtained by randomly permuting the data between the two experimental conditions within every participant. A reference distribution from 1000 random sets of permutations allowed

the p value to be estimated as the proportion of the elements in the randomization null distribution exceeding the observed maximum cluster-level test statistic.

4.3.7 Alpha amplitude lateralisation

For each subject, Ipsilateral and Contralateral time-frequency spectra were divided by the average of the two in the 0.25 – 2.25 time window, separately for each frequency band. This normalised the time-frequency spectra to correct for individual variability in the absolute amplitude. Alpha lateralisation for each subject was calculated as the average difference between the Ipsilateral and Contralateral spectra in the 0.25 – 2.25 s time and 7-14 Hz frequency window.

4.4 Results

4.4.1 Microsaccade characteristics

For testing the relationship between alpha oscillations and microsaccades in selective attention we chose the time interval from 0.25 s after cue onset to target onset (at 2.25 s after cue onset). This way we avoid the influence of cue onset-related responses on alpha oscillations while including most of the cue-target interval where attentional mechanisms operate and the relationship between alpha oscillations and microsaccades is hypothesised to exist. In the 0.25 – 2.25 s time-window from cue onset 12 subjects made 8392 microsaccades in 7068 second of fixation. Median microsaccade rate (across subjects) was 1.3 microsaccades/second, median amplitude was 0.34 deg and median peak velocity was 28.31 deg/s. In agreement with previous research, we observed a number of typical microsaccade characteristics. First, microsaccade amplitude and peak velocity were highly correlated ($r = 0.92$, $p < 0.01$) and followed the 'main sequence' (Zuber et al. 1965) characteristic for saccadic eye movements (Fig. 4-2 A). Second, the large

majority of microsaccades (93%) had directions in the +/- 45 deg range from horizontal (Fig. 4-2 B; Dimigen et al. 2009; Rolfs 2009).

All horizontal microsaccades were divided into two groups, depending on whether their direction was towards the cued target location or toward the distractor location. Time courses of microsaccadic rates for the two groups of microsaccades are plotted in Figure 4-3 A and B. The time courses showed the typical inhibition of microsaccade rates from 0.125 to 0.225 s and a rebound from 0.25 to 0.4 s after cue onset. Interestingly a similar pattern of suppression and rebound was observed at the same latencies after cue offset. From around 0.5 s microsaccade rates were steadily decreasing.

The direction of microsaccades initiated during the first rebound interval (0.25 to 0.4 s) was systematically biased (Fig. 4-3C), with a higher rate of microsaccades towards the cued target location (mean = 0.96 microsaccades/s, SD = 0.68) than towards the distractor location (mean = 0.53 microsaccades/s, SD = 0.43) as revealed by a paired t test ($t(11) = 3.42$, $p < 0.01$). Thus, in line with previous studies (Engbert & Kliegl 2003; Laubrock et al. 2007), microsaccades in the rebound period tended to follow the direction indicated by the cue. This bias was not present during the rest of the cue-target interval (0.45 - 2.25 s; Fig. 4-3 D), where we did not find any evidence for a difference in microsaccadic rates between microsaccades towards the cued target location (mean = 0.59, std = 0.39) and microsaccades towards the distractor location (mean = 0.6, std = 0.41) when investigated with a paired t test ($t(11) = - 0.18$, $p = 0.86$). Because of the possibility that these results may be influenced by the large inter-individual variability in absolute microsaccade rates, we also calculated microsaccade time courses for the two groups, each normalised at a single subject level by each individual's mean microsaccade rate in the two conditions. Fig. 4-3 B shows microsaccade time courses expressed as a fraction of the mean microsaccade rate in the 0.25 – 2.25 time-window. The time courses

look very similar and therefore we conclude that they were not markedly affected by the large inter-individual variability.

The normalised time-courses of microsaccadic rates (Fig 4-3 B) were used to calculate 'microsaccade lateralisation indices' for each subject and separately for the early (0.25 -0.4) and late (0.4 – 2.25 s) time-windows. The microsaccade lateralisation indices were calculated as the difference between the normalised rate of microsaccades towards the cued target location and away from the target location separately for each time-window. The microsaccade lateralisation indices are used in the final analysis where it is investigated whether they are related to alpha lateralisation indices.

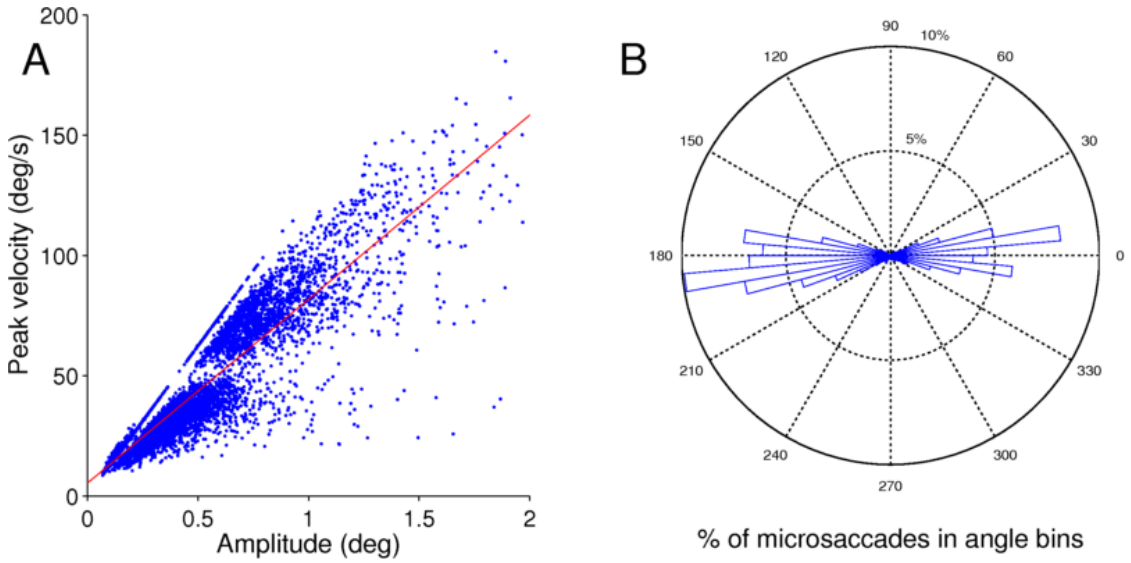

Figure 4-2. Group level microsaccade characteristics in the 0.25 – 2.25 time-window from cue onset. **A**. Scatterplot illustrating the typical 'main sequence' distribution i.e. a strong linear relationship between microsaccade amplitude and peak velocity (with one dot per microsaccade). **B.** Polar percentage histogram of directions grouped in 72 bins (bin width: 5 deg). Length and width of each triangle represents the relative percentage of microsaccades in the corresponding orientation bin. Note a predominantly horizontal orientation.

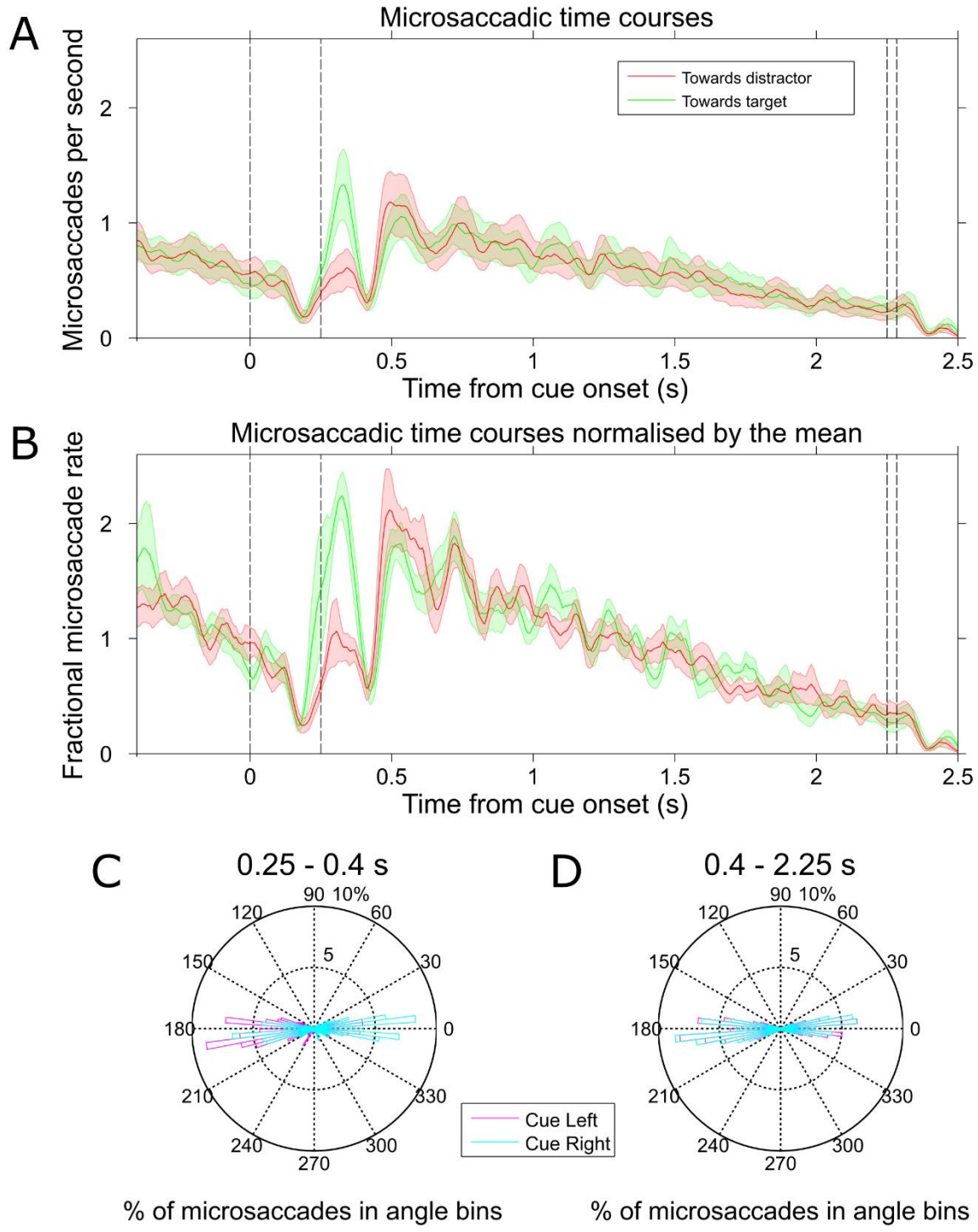

Figure 4-3. Microsaccadic time courses and lateralisation. **A**. Average time courses of microsaccade rates plotted separately for microsaccades towards cued target location

(green) and towards distractor location (red). Vertical dashed lines mark (starting from left): cue onset, cue-offset, target onset, target offset. The shaded regions mark standard error of the mean. **B**. Same as in A except the time courses were normalised by the common mean for each subject separately before calculating the average time-courses. **C**. Polar percentage histogram of microsaccade directions in the 0.25 – 4 s time-window after cue onset (microsaccade rebound) for Attend Left (cyan) and Attend Right (magenta) conditions. Note the directional bias towards cued target location. **D**. Same as C for the 0.4 -2.25 s time-window. Note the absence of the directional bias.

4.4.2 Alpha lateralisation at the group level

Previous studies have shown a relative decrease of alpha power contralateral to the attended hemifield and a relative increase ipsilateral to the attended hemifield in covert attention tasks (Händel et al. 2011; Marshall et al. 2015; Siegel et al. 2008; Thut et al. 2012; Worden et al. 2000). To investigate the same effect in our data, the difference in alpha amplitude (7 - 14 Hz) in the cue-stimulus interval (0.25 – 2.25 s after cue onset) between the Attend Left and Attend Right conditions was calculated for each subject. Then, the difference was normalised by the mean of the two conditions for each subject separately to account for inter-subject differences in absolute alpha amplitude. Topographies of this normalised difference for each subject are illustrated in Figure 7-4 in the Appendix. A group-level cluster-based permutation test revealed two significant clusters of sensors where the difference between the two conditions was significant: one cluster of left posterior sensors with positive values ($p = 0.021$) and one cluster of right posterior sensors with negative values ($p = 0.008$) were identified (Figure 4-4 A). These results are consistent with previous studies that observed this alpha lateralisation, namely: following a spatial cue onset, alpha power was higher in areas ipsilateral to the direction of cue than in contralateral areas.

4.4.3 Alpha lateralisation for single subjects

To quantify the extent to which each subject modulated their alpha amplitude according to attentional demands, alpha lateralisation indices were calculated. To obtain alpha lateralisation indices for single subjects, average time-frequency representations were calculated for each subject using sensors from clusters identified in the analysis described in the previous section for Ipsilateral (right sensors in the Attend Right condition and left sensors in the Attend Left condition) and for Contralateral (right sensors in the Attend Left Condition and left sensors in the Attend Right condition) sensors. These group-averaged spectra are shown in Figure 4-4 B and C. Next, the spectra were normalised by the average amplitude from Ipsilateral and Contralateral in each frequency band separately and for each subject separately. This way we controlled for the fact that absolute amplitude varied to a great extent between individual subjects. Then, for each participant we calculated a difference between the Ipsilateral and Contralateral normalised spectra and the average difference within the time-frequency window of interest (7-14 Hz, 0.25 – 2.25 s) determined the lateralisation index for each subject. Spectra of the difference for each subject with the corresponding lateralisation indices are illustrated in Figure 4-5. Each subject showed a positive lateralisation index meaning that for each subject alpha amplitude was stronger in the sensors ipsilateral to the direction of the spatial cue. However, as shown in Figure 4-5, the size of this effect varied greatly between participants. The group average of the normalised difference spectra (lateralisation) can be seen in Figure 4-4 D. Figure 4-4 E illustrates the alpha amplitude time-courses for Ipsilateral and Contralateral sensors. The difference emerges around 0.4 s, is present for the rest of the cue-stimulus interval and is of highest magnitude between 1.5 s and target onset.

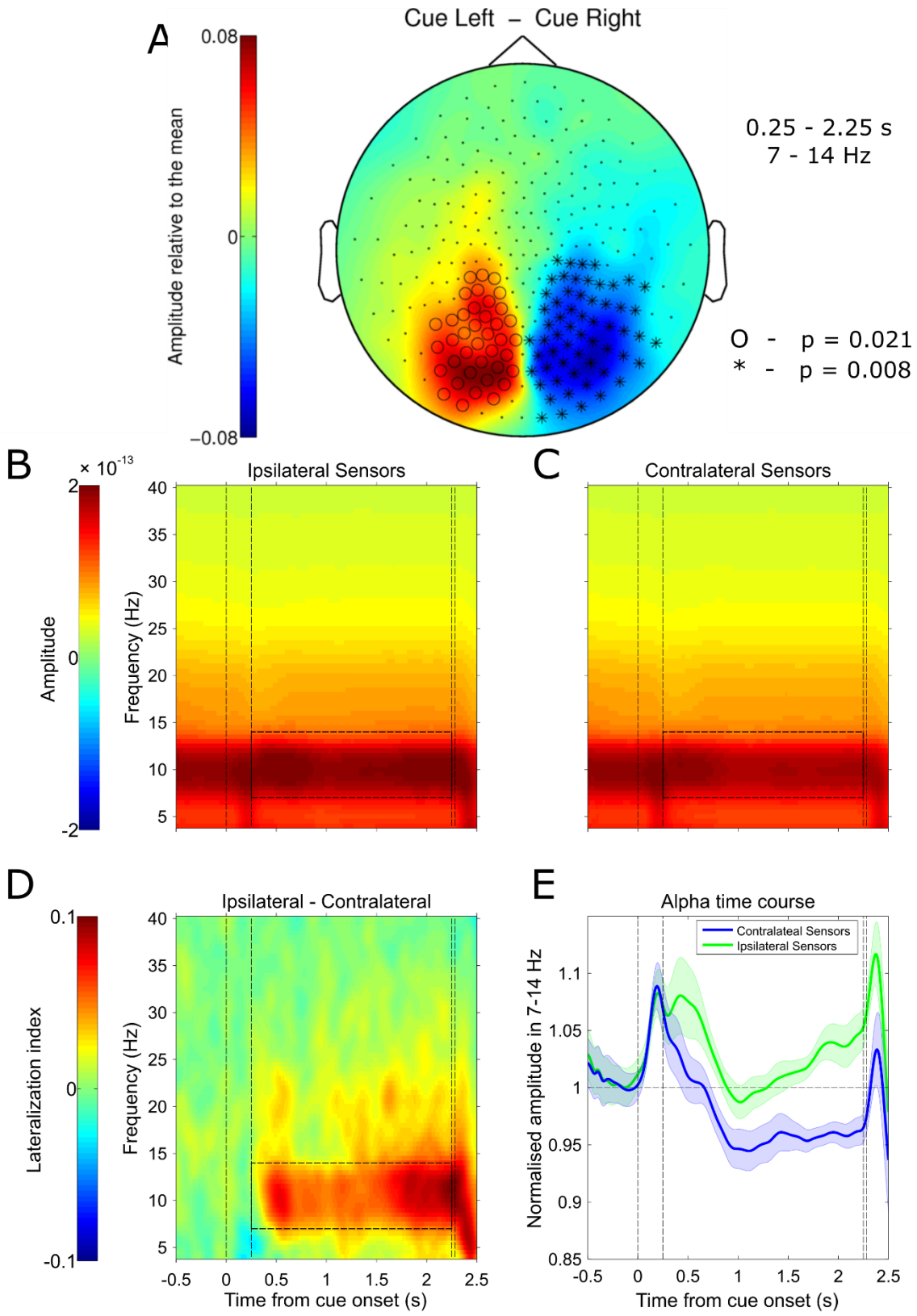
A
Cue Left – Cue Right
0.08
0
−0.08
Amplitude relative to the mean
0.25 - 2.25 s
7 - 14 Hz
O - p = 0.021
* - p = 0.008
B
× 10^-13
2
0
-2
Amplitude
Ipsilateral Sensors
Frequency (Hz)
40
35
30
25
20
15
10
5
C
Contralateral Sensors
D
Ipsilateral - Contralateral
0.1
0
-0.1
Lateralization index
-0.5
0
0.5
1
1.5
2
2.5
Time from cue onset (s)
E
Alpha time course
Contralateal Sensors
Ipsilateral Sensors
Normalised amplitude in 7-14 Hz
1.1
1.05
1
0.95
0.9
0.85

Figure 4-4. Group level characteristics of the alpha lateralisation effect in the Cue-Target interval. **A**. Topographical representation of the difference between Cue Left and Cue Right conditions. Note the two significant clusters of sensors. **B**. Time-freqency spectra for sensors Ipsilateral to the direction of the Cue. Vertical dashed lines mark (starting from left): cue onset, cue-offset, target onset, target offset. **C**. Time-freqency spectra for sensors Contralateral to the direction of the Cue. **D**. Diffrence beweeen normalised Ipsilateal and Contralateral spectral. **E**. Time-courses of normalised alpha power for sensors Contralteal and Ipsilateral to the direction of the Cue. Shaded regions illustrate the standard error on the mean.

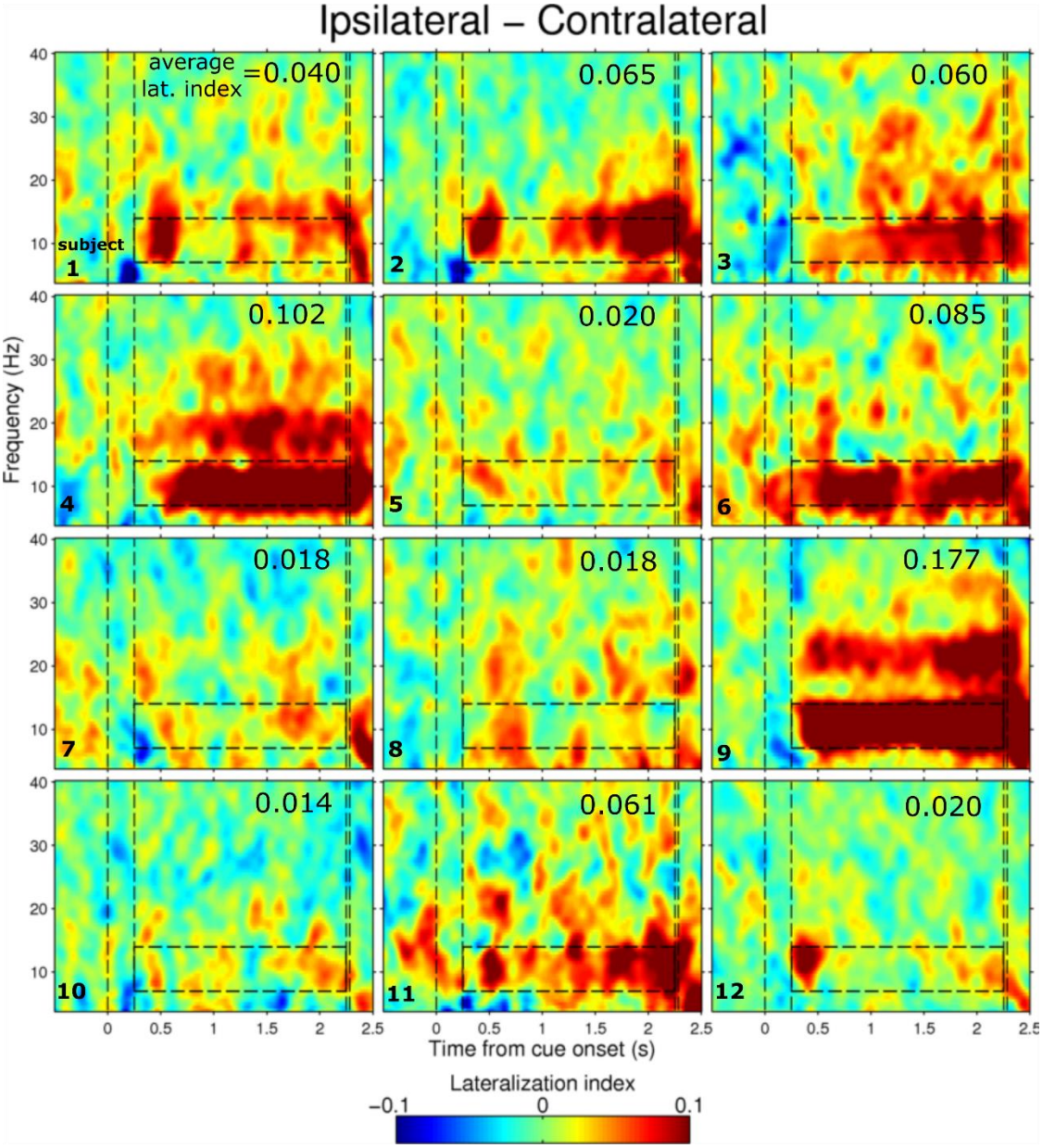

Figure 4-5. Difference between time-frequency spectra from sensors ipsilateral and Contralateal to the direction of the spatial cue. Vertical dashed lines mark (starting from left): cue onset, cue-offset, target onset, target offset. Average laralisation index for each subject (averaged over the time-frequency window indicated by the horizontal rectangle formed from dashed-lines) is stated in the top-right corners. Subject numbers are stated in the bottom left corners.

4.4.4 Relationship between alpha oscillations and microsaccades.

To investigate any relationship between alpha oscillations and microsaccades in covert spatial attention, we compared previously calculated lateralsation indices of alpha amplitude and microsaccade directions. If microsaccades play a direct role in mediating covert spatial attention, via active neural facilitation and inhibition represented by alpha suppresion and enhancement, those subjects who show the highest alpha lateralisations should also show the greatest microsaccade directional biases.

In this analysis, positive values of lateralation indices for alpha amplitude reflect a relatively higher amplitude in sensors ipsilateral to the direction of the spatial cue. Positive values of lateralisation indices for microsaccadic lateralisation relfect a relatively higher number of microsaccade directions towards the cued target location while negative values reflect relatively higher number of microsaccade directions away from the cued target location (and therefore towards the distractor location).

Because we only observed significant attentional biasing of microsaccade directions towards the target location in the early time-window of the cue target interval (0.25 – 0.4 s after cue onset; Figure 4-3 A,B and C) we hypothesised that this early microsaccadic lateralisation effect is related to the alpha lateralisation in the entire cue-target interval (0.25 – 2.25 s after cue onset) after cue onset and was present during the remaining part of the cue-target interval. However, in contradiction to this hypothesis, we did not find any evidence that early microsaccadic lateralsation was related to alpha lateralisation between-subjects ($r = 0.33$, $p = 0.31$). The scatterplot illustrating this analysis is shown in the left panel of Figure 4-6.

Although we did not observe a signifcant attentional biasing of microsaccade directions in the late time-window of the cue target interval on a group-level (0.4 – 2.25 s after cue onset; Figure 4-3 A,B and D) most subjects showed positive values of lateralisation indices and we further hypothesised that the between-subject variability in

the late microsaccadic lateralisation may be related to the between-subject variability in the alpha amplitude lateralisation. We did not find evidence for the hypothesized relationship (r = -0.19, p = 0.56). The scatterplot illustrating this analysis is shown in the right panel of Figure 4-6.

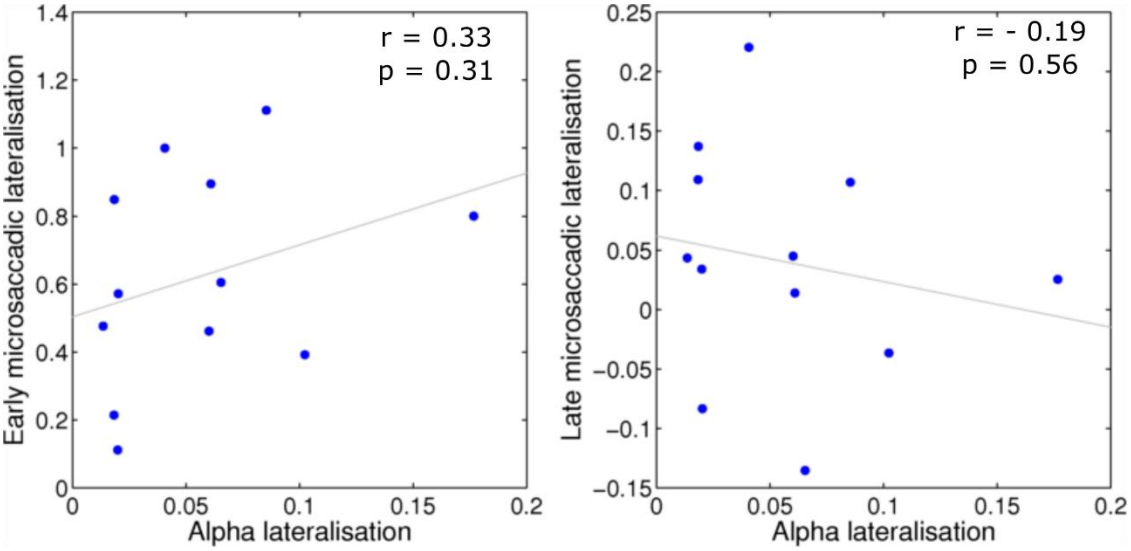

Figure 4-6. Scatterplots illustrating the lack of significant relationship between alpha lateralisation (Ipsilateral minus Contralateral) and microsaccadic lateralisation (Towards Target minus Towards Distractor), across subjects. Each dot represents one subject. **Left.** Alpha lateralisation and early (0.25 – 0.4 s after cue onset) microsaccadic lateralisation and. **Right**. Alpha lateralisation and late (0.4 – 2.25 s after cue onset) microsaccadic lateralisation.

4.5 Discussion

The aim of this study was to investigate whether alpha oscillations and microsaccades represent related or independent attentional mechanisms. To this end, we recorded MEG and high-speed video eye tracking simultaneously while human subjects performed a spatial cueing task that involved allocation of covert attention to the cued hemifield before target onset. We observed the typical inhibition and subsequent rebound of microsaccadic rates following cue onset. What is more, we observed, for the first time, that cue-offsets were also followed by an inhibition and a rebound of microsaccade rates.

After the second rebound, microsaccade rates declined steadily. During the first rebound, microsaccade directions were biased towards the cue direction – an effect well established in the literature (Engbert & Kliegl 2003; Laubrock et al. 2010). We did not find the same effect in the later, longer, time window (1.85 s) between the first rebound and the target onset. Alpha oscillation amplitude in the cue-target interval was higher for the occipital sensors ipsilateral to the direction of attention than for the sensors contralateral to the direction of attention – an effect well established in the literature (Worden et al. 2000; Siegel et al. 2008; Händel et al. 2011; Marshall et al. 2015). This alpha lateralisation on a group-level started around 0.4 s after cue onset, was sustained for rest of the cue target interval and was the strongest from ~ 1.5 s after cue onset until target onset. In order to test whether alpha oscillations represent related or independent mechanisms, we correlated early and late microsaccade lateralisation with alpha lateralisation across subjects. We did not find any evidence for either late or early microsaccade lateralisation being related to alpha lateralisation.

Based on these observations, we suggest that the lateralisation of microsaccade directions and the lateralisation of occipital alpha oscillation amplitude reflect two different aspects of attention. The lateralisation of microsaccade directions was only significant early in a trial and therefore appears to be mainly representing the initial shifting of attention after cue presentation (Laubrock et al. 2010). This attentional shifting process may stem from a cue-related imbalance (Engbert 2012) within the activation map of the superior colliculus (SC) - a key neural structure in microsaccade generation (Hafed et al. 2009). Microsaccades during the later windows of the cue-target interval would be largely independent of this shifting process, and instead play a more mundane role in restoring central fixation (Engbert & Kliegl 2004). Another possibility is that the early microsaccade lateralisation reflects a reflexive, default orienting response that is later actively suppressed by the instruction to fixate (Hafed 2013). This possibility is supported by the

observation that SC activity is highly sensitive to cue onsets (Boehnke & Munoz 2008), and the close proximity of the SC to the motor output (Gandhi & Katnani 2011) creates an efficient circuit for fast orienting reflexes. In any case, it is important to stress that it is not clear whether attention plays a causal role in microsaccade lateralisation. On the one hand, instructed shifts of attention can cause momentary imbalance in the superior colliculus' activation maps (Hafed et al. 2013) a state that plays causal role in microsaccade generation (Hafed et al. 2009). On the other hand, microsaccades were shown to induce the performance enhancements we call "covert attention" (Hafed 2013). Another possibility is that both attention and microsaccades reflect a third, more general process. All these explanations are compatible with the novel finding that spontanous microsaccades (no cueing present) are associated with shifts of attention (Yuval-Greenberg et al. 2014).

Attention-related lateralisation of alpha oscillations, on the other hand may reflect the process of maintenance of sustained spatial attention. In our study, alpha-lateralisation was present from ~ 0.4 s after cue onset until target onset and became stronger in the later parts of the cue-target interval possibly reflecting the build-up of sustained attention. Because the cue-target interval had a fixed duration, participants could predict when the target and distractor appear and therefore lateralise their alpha amplitudes most effectively before target appearance. The observed alpha lateralisation from ~ 1 s after cue onset was driven by absolute increases in alpha amplitude in the ipsilateral sites (Figure 4-4 E). This pattern of lateralisation was also observed by Rihs et al. (2009) and they speculated that the late alpha increases are related to the phenomenon of inhibition of return (Klein 2000). Inhibition of return encourages orienting towards novel locations after attention is removed from a peripheral location. Late alpha increases may therefore stem from an elevated need for suppressing input from to-be-ignored locations by endogenous control, in order to prevent reflexive orienting to this novel position after

the initial orienting to the cued hemifield, as reflected in biased early microsaccade directions. This provides further support for the notion that alpha plays a role in inhibiting task-irrelevant regions (Klimesch et al. 2007) and potentially routes information to task relevant regions (Jensen & Mazaheri 2010). Here too it has to be stressed that the nature of the relationship between attention and alpha oscillations is not clear. On the one hand, multiple studies that manipulated alpha amplitude in the visual cortex using TMS point to a causal role of alpha oscillations in attention (Romei et al. 2010; Herring et al. 2015; Thut et al. 2012). On the other hand, only few studies from a vast literature observed a relationship between alpha ampliude and attention-related performance enhancement (Händel et al. 2011; Thut et al. 2006). Therefore it is impossibe to unequivocally state whether alpha oscillations moderate or cause attentional processes.

One weakness of our analysis is that it only looked at between-subject correlations in a very few number of subjects. A future analysis should look at trial-to-trial variance in numbers of microsaccades and related to trial-to-trial variance in alpha lateralisation, similar to the analysis performed in Chapter 3.

Our observation that microsaccade rates in the late part of the cue-target interval were steadily decreasing and reached its lowest point before target onset is consistent with and can be explained by similar observations in other covert attention studies. Hafed et al. (2011) reported that when monkeys anticipated occurrence of brief stimulus probes, microsaccade rates decreased even seconds before the actual target onset. This phenomenon was explained by the fact that microsaccades occurring at the same time as the stimulus probes were associated with reduced perceptual performance. Pastukhov & Braun (2010) obtained similar results in human subjects and concluded that their participants learned to voluntarily suppress microsaccades in anticipation of target onset because microsaccades coinciding with target presentation significantly decreased performance and increased reaction time. Additionally they reported that microsaccade

rates were even lower in a 'high attentional load' condition which is consistent with our study where microsaccade rates decreased and our task was of high attentional demand because the targets were titrated to yield ~ 70% correct performance.

Our results also provide strong evidence for the role of alpha oscillations in covert attention despite the recently established observation that eye movements are in fact present during covert attentional orienting (Hafed & Clark 2002; Engbert & Kliegl 2003). The previously reported dependence of successful behavioural performance in attentional tasks on alpha lateralisation (Thut et al. 2006; Siegel et al. 2008; Händel et al. 2011) is unlikely to be explained by the recently reported microsaccade-related improvements in performance due to the pre-microsaccadic compression of space mechanism (Hafed 2013). This is because, microsaccade-related improvements in performance are only present in trials where microsaccades directed towards the target occurred up to ~75 ms after target onset. Our data shows strong alpha lateralisation before target onset when microsaccade were rare and in the absence of significant microsaccade lateralisation.

In the current and in the previous chapter we investigated the relationship between microsaccades and two classes of oscillations in the visual cortex: gamma oscillations during low-level stimulus processing and to alpha oscillations during top-down covert attention. In both of these chapters we adopted a correlational approach to understand the relationship between microsaccades and specific oscillations associated with specific aspects of visual and attentional processing. In the next chapter, we adopt a more hypothesis-free approach and we will investigate spectral responses that are time-locked (but not necessarily phase-locked) to and therefore induced by microsaccades to fully understand the relationship between microsaccades and oscillations in the visual system.

Chapter 5: Microsaccade-related spectral responses

5.1 Abstract

Microsaccades are thought to play a number of important roles in vision such as counteracting visual adaptation, optimal sampling of the environment and enhancing signal-noise-ratio in visual processing. To understand how these functions of microsaccades may be implemented at the neural level it is important to study peri-microsaccadic modulations of neural activity in the visual cortex. Neural oscillations constitute a good candidate for mediating the role of microsaccades in visual processing because they provide a rich coding space for the complicated dynamics of interaction between eye movements and vision. In order to characterise spectral responses to microsaccades noninvasively in the human cortex we recorded MEG and high-speed video eye tracking while participants fixated on small central spot, both in the baseline period and when one of three different stimulus types was present. Our paradigm consisted of long stimulus durations and enabled us to study responses to microsaccades as function of stimulus type while it also allowed us to isolate microsaccade-related responses from those related to stimulus onsets and offsets. We identified three microsaccade-related responses that had an occipital topography. Frist, in all three stimulus conditions (vertical grating, horizontal grating, and gray uniform image) we observed a transient increase in theta amplitude (3-9 Hz) that peaked ~ 0.125 s after microsaccade onset. This effect was stronger for microsaccades that occurred during the vertical grating presentation than during the gray image. Second, a transient increase in broadband beta amplitude (13 – 40 Hz) immediately after microsaccade onset was present only in the vertical grating condition. Third, a decrease in alpha (9 – 14) amplitude between 0.25 and 0.5 s was present in all conditions, with no significant difference found between conditions. The putative functions of these spectral components are discussed.

5.2 Introduction

In the previous chapter, we found that visual alpha oscillations and microsaccades represent independent attentional mechanisms. Microsaccades were biased towards the direction of covert attention immediately after spatial cue onset and this effect may represent shifting of spatial attention. Alpha oscillations, on the other hand, showed amplitude lateralisation (higher amplitude in sensors ipsilateral to the direction of attention) that started ~ 0.4 s after spatial cue onset and continued until target onset. We did not find evidence that the early biasing of microsaccade directions was related to the sustained alpha lateralisation.

Human eyes are never still. Even when we attempt to fix our gaze, small ocular movements involuntarily shift our eye position. Despite their relatively small size, these fixational eye movements shift the projection of the stimulus over many receptors on the retina and they yield motion signals that would be immediately visible had they originated from the stimulus (Kowler 2011). Among the three distinct types of fixational eye movements (drift, tremor, and microsaccades), microsaccades represent the fastest component with the largest amplitude and occur at an average rate of 1 to 2 per second (Martinez-Conde et al. 2013; Rolfs 2009). Although microsaccades were once thought to merely represent oculomotor noise and not to serve any useful purpose, evidence amassed in the past two decades showed that microsaccades aid vision in many ways, such as through control of fixation position (Engbert & Kliegl 2004), scanning of small regions of space (Otero-Millan et al. 2008), and during spatial attention (Engbert & Kliegl 2003; Hafed & Clark 2002; Hafed 2013).

Most importantly, however, microsaccades are thought to have a fundamental impact on visual processing. First, microsaccades were shown to counteract foveal and peripheral visual fading during fixation (Martinez-Conde et al. 2006; McCamy et al. 2012) and are dynamically triggered immediately after periods of low retinal image slip (Engbert

& Mergenthaler 2006). Given that striking visual fading is observed in the laboratory due to adaptation when eye movements are completely suppressed (for instance, with retinal stabilization techniques: DITCHBURN & GINSBORG (1952)) it may be that, without microsaccades, our vision would be substantially compromised. Second, microsaccades may enhance the signal-to-noise ratio of the visual input. This proposal is supported by the fact that moving a stimulus with a frequency and amplitude that resembles microsaccades increases the signal-to-noise ratio of a threshold-level stimulus in cat visual cortex (Funke et al. 2007). Also psychophysical results from human subjects showed that microsaccades improve discrimination of high spatial frequency stimuli that are masked by noise through enhancement of the signal-to-noise ratio (Rucci et al. 2007). Third, microsaccades were proposed to constitute a discrete temporal sampling method of the visual system based on the observations that transient firing patterns in visual neurons are similar following microsaccades and stimulus onsets (Martinez-Conde et al. 2002; Martinez-Conde et al. 2004). Others have proposed that the discrete sampling function of microsaccades is mediated by the fact that visual processing after microsaccades is enhanced due to corollary activity from the motor system (Melloni, Schwiedrzik, Rodriguez, et al. 2009).

In order to understand the neural mechanisms of the impact of microsaccades on visual processing one has to study activity in the visual system around microsaccades onsets. Most studies that investigated peri-microsaccadic activity in the visual system used invasive single-neuron recordings in monkeys and the following general pattern emerged from these studies. First, microsaccade-related spiking activity is present at many stages of visual processing from the LGN (Martinez-Conde et al. 2002; Reppas et al. 2002) through primary visual cortex (Kagan et al. 2008; Leopold & Logothetis 1998; Martinez-Conde et al. 2002) and visual association areas (Bair & O'Keefe 1998; Herrington et al. 2009; Leopold & Logothetis 1998) to the end points of the ventral (Leopold

& Logothetis 1998) and dorsal (Herrington et al. 2009) pathways in temporal and parietal lobes respectively. Second, peri-microsaccadic activity often takes the form of burst spiking (Martinez-Conde et al. 2002; Martinez-Conde et al. 2000), and (3) microsaccades modulate neural activity in the V1 primarily through early increases in spike rates due to retinal motion and decreases in spike rates due to extraretinal responses that are generally smaller and occur with higher latency (Martinez-Conde et al. 2013; Troncoso et al. 2013).

Some researchers have suggested that microsaccades might enhance spatial and temporal summation by generating bursts of spikes and by synchronizing the activity of visual neurons with neighbouring receptive fields (Martinez-Conde et al. 2004; Martinez-Conde et al. 2000). However, only recently, research has begun to tackle the physiological effects of microsaccades on populations of visual neurons. One of the most salient characteristics of population activity are synchronous neural oscillations. Neural oscillations play a role in integration of information and could constitute a mechanism through which visual processing and eye movements signals are integrated. Recently, Melloni et al. (2009) suggested that corollary activity related to saccades and microsaccades interacts with the ongoing oscillations in the visual cortex to enhance the processing of visual signals immediately after eye movements. A recent study observed microsaccade-related modulations of visually induced gamma oscillations in areas V1 and V4 of alert monkeys and that these modulations were correlated with variability in behavioural response speed suggesting that microsaccades structure the sampling of environment through transient gamma-band synchronisation of visual neuronal ensembles (Bosman et al. 2009).

Moreover, most studies of neurophysiological responses to microsaccades in the visual system are conducted on primates. It is important to study these mechanisms in humans to gain insights into the mechanisms of interaction between microsaccades and

human vision. So far, only two human studies identified microsaccade-related visual responses. Firstly, an fMRI study found BOLD modulations that diminished in strength from V1 to V3 that were similar for microsaccades at attempted fixation and small voluntary saccades (P. U. Tse et al. 2010). Secondly, microsaccade-related evoked potentials that contain similar components to stimulus-evoked potentials were observed in scalp-EEG studies (Dimigen et al. 2009).

In the present study we aimed, for the first time, to describe oscillatory responses to microsaccades in human visual cortex. We used a paradigm with long stimulus durations to avoid influence of stimulus events (onsets and offsets) on the oscillatory activity. To distinguish between spectral responses sensitive to retinal stimulation and those independent of retinal stimulation we used three stimulus conditions: a vertical grating, a horizontal grating and a uniform gray image of mean luminance.

5.3 Methods

5.3.1 Participants, stimuli, and task

Twenty three subjects participated in the experiment after giving informed consent, with all procedures approved by the Cardiff University School of Psychology Ethics Committee. Eye tracking data for two subjects were too noisy due to the challenging nature of recording eye movements in the MEG environment, and hence were excluded from the analysis (see the specific criteria below). Additionally three other subjects did not make enough microsaccades in each condition to obtain robust MEG responses (see the specific criteria below). The remaining group consisted of eighteen subjects (ten females) and their average age was 25.36 years (SD = 2.1 years). Participants were screened for: personal histories of neurological and psychiatric disease; current recreational or prescription use of drugs that are known to affect central nervous system; eye disease

and eye injury; eye movement disorders; ptosis ('drooping eyelid'). All participants reported normal or corrected to normal vision.

During the experiment participants sat in a magnetically shielded room (MSR), 2.10 m in front of a Mitsubishi Diamond Pro 2070 monitor controlled by a Windows PC with MATLAB Psychtoolbox software (Brainard 1997). The screen resolution was 1024 by 768 pixels and the monitor frame rate was 100 Hz. The monitor was outside the MSR and was viewed through a cut-away portal. On each trial, participants were instructed to fixate on a small red fixation spot in the centre of the screen and try not to blink. Subjects were consecutively presented with three stimuli: a vertical grating, a horizontal grating and a uniform gray image (mean luminance). The gratings were stationary, maximum contrast, three cycles per degree, square-wave and presented centrally on a mean luminance background. The monitor image had previously been gamma-corrected for luminance using a photometer. The gratings subtended 8 deg both horizontally and vertically. Each of the three stimuli was presented for 6.5 s (total trial length = 3 x 6.5 s = 19.5 s). After each trial, participants had an 8 s rest period during which they could blink and move their eyes before the next trial started. The order of stimuli presentation within a trial was balanced across trials and the trial order was random. Each participant completed 60 trials (180 presentations of each of the three stimuli) separated into three blocks of 20 trials. Between the blocks there were self-paced rest breaks. The task took approximately 35 minutes.

5.3.2 Eye tracking acquisition

Eye movements were recorded monocularly from the right eye with a MEG-compatible video-based remote eye tracker (iView X MEG, SMI GmbH). The eye tracker was positioned 120 cm in front of a participant below the monitor screen and data was acquired at a sampling rate of 250 Hz. After calibration (6 points) the system determined

the gaze direction from the position of pupil only. Participants were asked to stay completely still during the recording and their head was immobilized in the MEG dewar with a head cuff and custom-built chin rest. Because head movements were almost completely absent using these procedures, we were able to collect/analyse eye movement data without using a corneal reflex – this resulted in substantially lower levels of noise in the estimation of gaze position. Before the start of every new block, the system was recalibrated. Eye tracking recording was remotely controlled from the stimulus PC using iViewX functions within the MATLAB Psychtoolbox. The time of triggers sent from the visual stimulation computer were recorded alongside the eye position.

5.3.3 Microsaccade detection and characterisation

Microsaccades were detected and characterised using custom MATLAB functions written by the PhD candidate and functions from the EYE-EEG plug-in for EEGLAB (Dimigen et al. 2011). Following Engbert & Mergenthaler 2006, microsaccades were defined as outliers in 2D velocity space. First, eye position data were transformed to velocities using a moving average of velocities over 3 data samples in order to suppress high-frequency noise. Then detection thresholds for each trial were computed by calculating median-based standard deviations of velocity (separately for vertical and horizontal movement components) and multiplying it by a factor of 6, resulting in an elliptic threshold in 2D velocity space. Additionally, microsaccades had to have a minimum duration of at least 3 data samples (12 ms) and amplitude below 2 deg. For each trial, performance of the detection algorithm was verified by offline visual inspection of position and velocity time courses and of eye image videos. This visual inspection procedure, together with conservative detection thresholds, resulted in good quality data, demonstrated by the identified microsaccades clearly conforming to the expected ‘main sequence’ distribution (Fig. 5-1; Zuber et al. 1965). Only microsaccades that occurred at

least 0.9 s after stimulus onset and at most 0.9 s before new stimulus onset were included in the analysis. Only microsaccades that occurred at least 0.9 s before or after a blink were included in the analysis. This way we avoided including neural responses to stimulus onsets, offsets and blinks in the MEG data epochs centred on microsaccade onsets and could study neural activity related exclusively to microsaccades as a change from baseline. Only microsaccades with horizontal directions (+/- 45 deg from horizontal) were included in the analysis. This way we assured that vast majority of the recorded microsaccades displaced the retinal receptive fields across the contrast of the vertical grating and along the contrast of the horizontal grating. A single cycle of the gratings subtended 0.33 deg i.e. the spatial frequency was 3 cycles/degree.

Trials were excluded from analysis if any of following occurred: median based standard deviation of velocity for either horizontal or vertical coordinate was higher than 2.5 (indicative of large noise); an eye movement larger than 2 deg; artefacts in the MEG signal (see below). Application of these criteria eliminated trials with noisy data and trials in which participants did not comply with the fixation instruction. Two subjects were completely excluded from the analysis because, for each of them, more than 50% of trials were excluded for the analysis based on the above-mentioned criteria. Three other subjects made less than 100 microsaccades in at least one of the three stimulus presentations conditions. With this small number of trials we could not ensure robust MEG responses to microsaccades and therefore these participants were also excluded from the analysis. For the remaining eighteen subjects on average 14% of trials were excluded from the analysis.

5.3.4 MEG acquisition and pre-processing

Whole head MEG recordings were made using a CTF-Omega 275-channel axial gradiometer system sampled at 600 Hz (0–150 Hz band-pass). An additional 29 reference

channels were recorded for noise cancellation purposes and the primary sensors were analysed as synthetic third-order gradiometers. Four of the 275 channels were turned off due to excessive sensor noise. Data analysis was carried out using the fieldtrip MATLAB toolbox (Oostenveld et al. 2011) and custom MATLAB functions written by the PhD candidate. Triggers marking microsaccade onsets were added to the continuous MEG data based on the eye tracking analysis. Continuous MEG data was epoched from - 0.8 s to 0.8 s relative to microsaccade onset and then the data was demeaned. Trials contaminated with large muscle artefacts, signal jumps or distortions of the magnetic field were identified by visual inspection and removed. Subsequently, cardiac artefact was removed using independent component analysis (Jung et al. 2000) based on the time course and topography of the identified components. Epochs centred around microsaccades that occurred during the same visual stimulus (vertical grating, horizontal grating and uniform gray screen) were grouped together and all subsequent analyses were carried out separately for the three conditions. In order to simplify the interpretation of the sensor level analyses we computed and carried out all subsequent analysis on planar gradients because the strongest field of the planar gradient signal usually is situated above the neural sources. The horizontal and vertical components of the planar gradients were estimated at each sensor location using the fields from the sensor and its neighbouring sensors (Bastiaansen & Knösche 2000). Importantly, the power values for the horizontal and vertical components were summed for each sensor after the time-frequency analysis but before baselining. Time–frequency analysis was conducted using the Hilbert transform between 1 and 100 Hz at 1 Hz frequency step intervals (filtering with a 6 Hz wide bandpass, 3rd order Butterworth filter). Time–frequency spectrograms were computed as a percentage change from the baseline energy (-0.6 to -0.15 s relative to microsaccade onset) for each frequency band and hence will reveal responses that are

either evoked (phase-locked to micro-saccadic onset) or induced (time- but not phase-locked).

5.3.5 Cluster test

Differences in amplitude for the three identified time-frequency windows of interest between the three conditions (9 tests in total) were investigated using nonparametric randomization method identifying clusters of sensors with significant differences. This method corrects for multiple comparisons over sensors, in within subject comparisons (Maris & Oostenveld 2007; Nichols & Holmes 2002). Clusters were defined as spatially adjacent sensors where the t statistics from testing difference between two conditions exceeded the $p > 0.05$ threshold. The cluster-level test statistic was defined as the sum of the t statistics of the sensors in a cluster. The type-I error rate for the 271 sensors was controlled by evaluating the cluster-level test statistic under the randomization null distribution of the maximum cluster-level test statistic. This was obtained by randomly permuting the data between two experimental conditions within every participant. A reference distribution from 1000 random sets of permutations allowed the p value to be estimated as the proportion of the elements in the randomization null distribution exceeding the observed maximum cluster-level test statistic.

5.4 Results

5.4.1 Microsaccades

Only horizontal microsaccades that occurred at least 0.9 before or after stimulus transition or blinks were included in the analysis (see the methods section for more details). Subjects made on average 0.99 (SD = 0.49) microsaccade per second during the vertical grating presentation, 1.03 (SD = 0.54) microsaccades per second during the

horizontal grating stimulus, and 1.11 (SD = 0.58) microsaccade per second during the uniform gray image presentation. A one-way repeated measures ANOVA determined that the mean microsaccade rate differed significantly between the three stimulus conditions ($F(2, 17) = 5.441$, $p = 0.009$). Post-hoc paired t-tests revealed the microsaccade rate was significantly higher during the gray image then during vertical grating ($t(17) = 2.764$, $p = 0.039$) or during the horizontal grating ($t(17) = 2.717$, $p = 0.045$). The difference between vertical and horizontal grating was not significant ($t(17) = 1.117$, $p = 0.850$). P-values for post-hoc tests were corrected for multiple comparisons using the Bonferroni method. The average microsaccade amplitude was 0.339 deg (SD = 0.157 deg) for the vertical grating, 0.351 deg (SD = 0.169 deg) for the horizontal grating and 0.363 (SD = 0.172 deg) for the uniform gray image. The distribution of amplitudes for each condition is illustrated in Fig. 5-1 B. Using one-way repeated measures ANOVA we did not find evidence for a significant difference in average microsaccade amplitude between the three stimulus conditions ($F(2, 17) = 3.014$, $p = 0.061$).

Microsaccade amplitude and peak velocity were highly correlated in all three conditions (horizontal grating: $r = 0.95$, $p < 0.001$; vertical grating: $r = 0.94$, $p < 0.001$; uniform gray: $r = 0.95$, $p < 0.001$) and therefore followed the expected 'main sequence' (Zuber et al. 1965) characteristic for saccadic eye movements (Fig. 5-1 A)

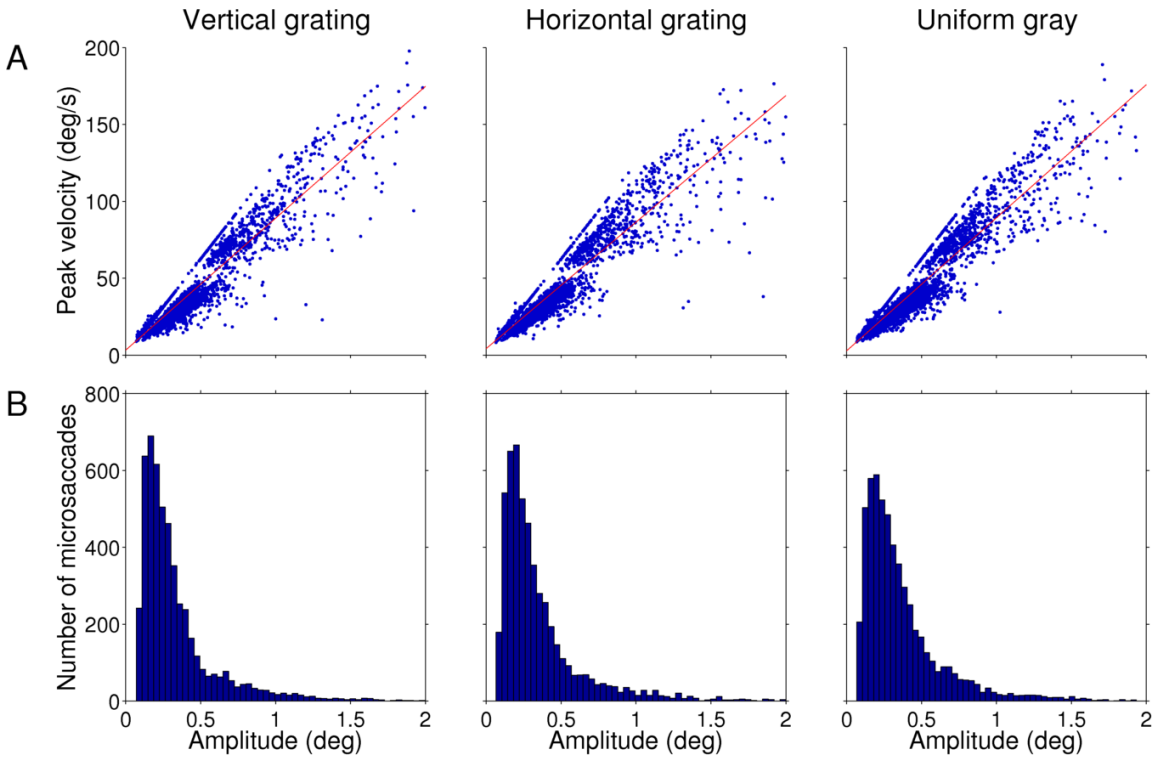

Figure 5-1. Characteristics of microsaccades for the three stimulus conditions. **A**. Strong relationship between microsaccade peak velocity and amplitude, the so called 'main sequence'. Each microsaccade is represented by one dot in these scatterplots. **B**. Distribution of microsaccade amplitudes.

5.4.2 Microsaccade-related MEG responses

To study spectral dynamics related to microsaccades, for each subject and each channel we calculated trial-averaged time-frequency representations of the MEG signal epochs centred on microsaccade onsets separately for each condition. The time-frequency data was expressed as amplitude % change from the pre-microsaccadic baseline between – 0.6 and - 0.15 relative to microsaccade onset. We did not include the time-interval immediately preceding a microsaccade as it is possible that some peri-microsaccadic neural responses occur before or at microsaccade onset. By visual inspection of group-average data for each condition we determined that the strongest responses were in the central occipital sensors. We specifically identified three strongest

responses: a theta band (3 – 9 Hz) increase in amplitude from 0.05 to 0.25 s from microsaccade onset; a beta band (13 – 40 Hz) increase in amplitude from 0.025 to 0.15 s; an alpha (9 – 14 Hz) decrease in amplitude from 0.25 to 0.5 s. The beta response appeared to be present only in the vertical grating condition whereas other two responses appeared to present in all three conditions. Figure 5-2 illustrates these group-average responses for five central occipital sensors and Figure 5-3 illustrates the topography of each response. All the effects have an occipital topography and therefore they most probably reflect peri-microsaccadic induced activity in the visual cortex.

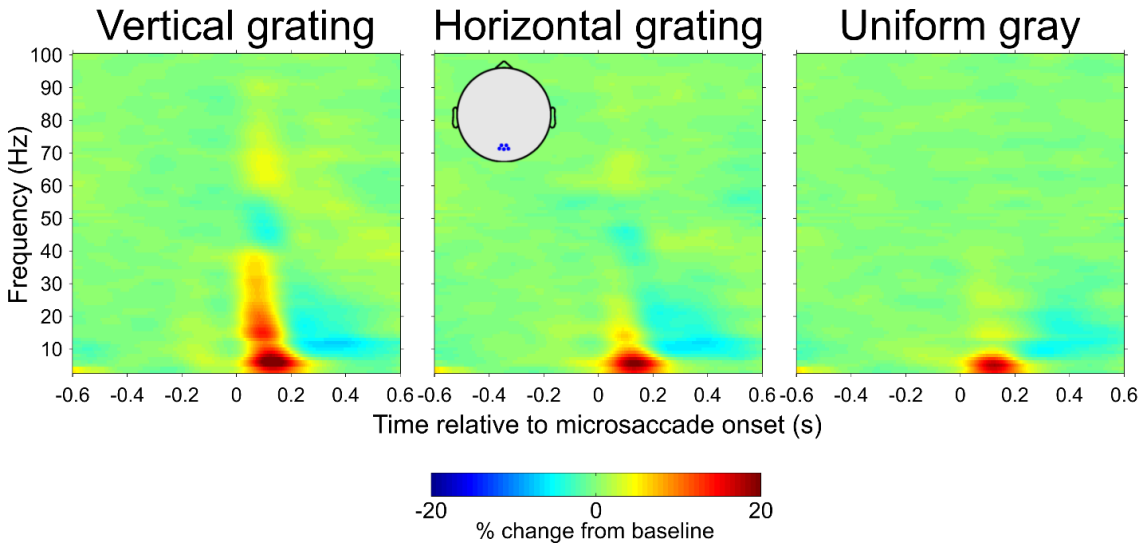

Figure 5-2 Group-average microsaccade-related changes in amplitude from baseline (-0.6 to -0.15) for the three stimulus conditions. The time-frequency representations are averages from 5 occipital sensors (location of sensors illustrated in the inset in the middle panel) where the effects appeared to be the strongest.

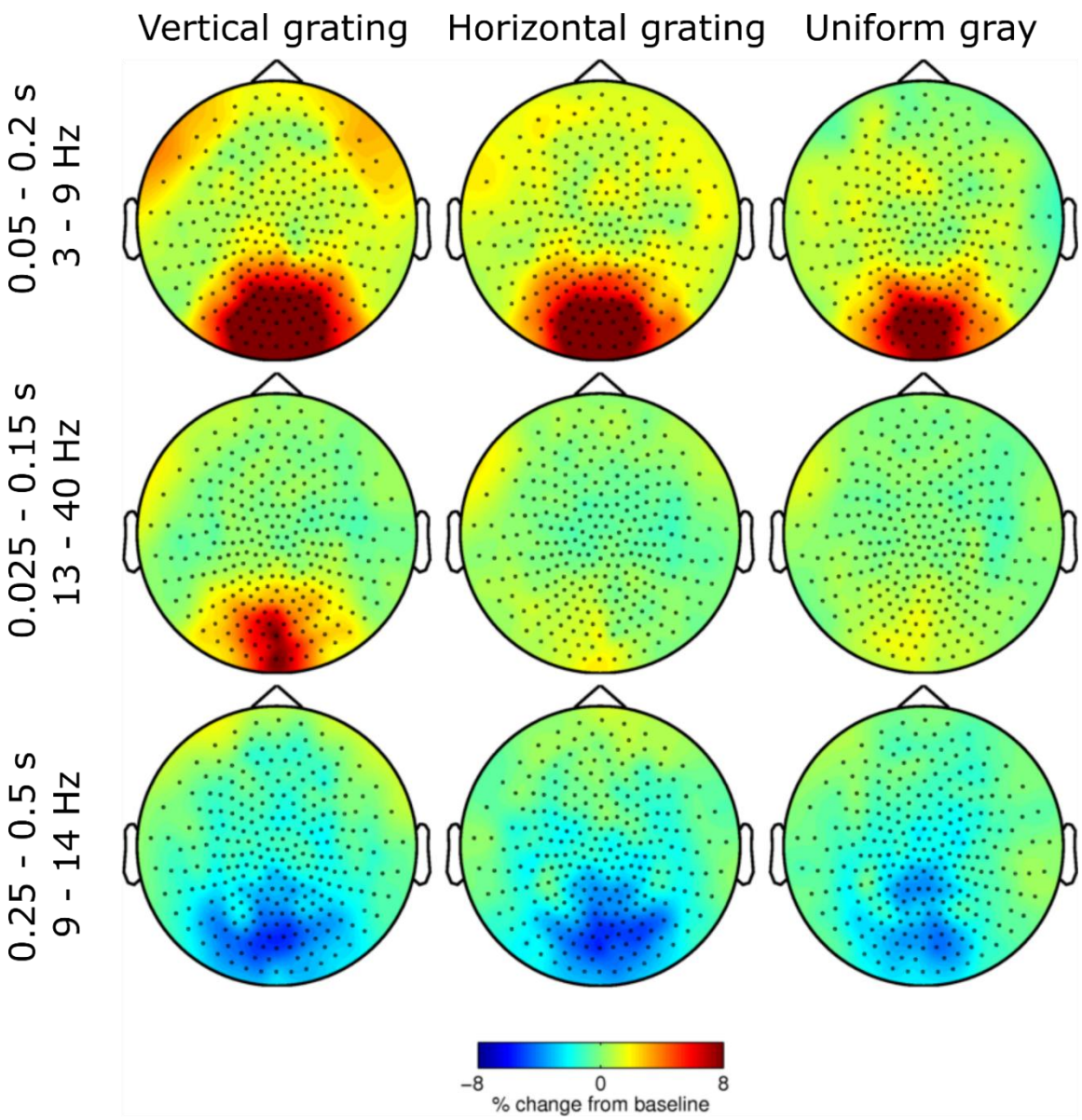

Figure 5-3 Group-average topographies of the three identified microsaccade-related effects (rows) for the three stimulus conditions (columns).

To investigate whether there were any effects of the stimulus condition on each of the three identified microsaccade-related responses we conducted cluster-based permutation tests between each pair of the three stimuli for each of the three identified responses (9 tests in total, see the methods section for details). For the theta response (3 – 9 Hz) we found a posterior cluster of sensors where the amplitude change from baseline was significantly higher for the vertical grating than for the uniform gray screen ($p = 0.010$).

For the beta response (13 – 40 Hz) we found a posterior cluster of sensors where the amplitude change from baseline was significantly higher for the vertical grating than for the horizontal grating (p=0.001) and another posterior cluster of sensors where the amplitude change from baseline was significantly higher for the vertical grating than for the uniform gray screen (p=0.005). We did not find any evidence for other significant differences between the stimulus conditions.

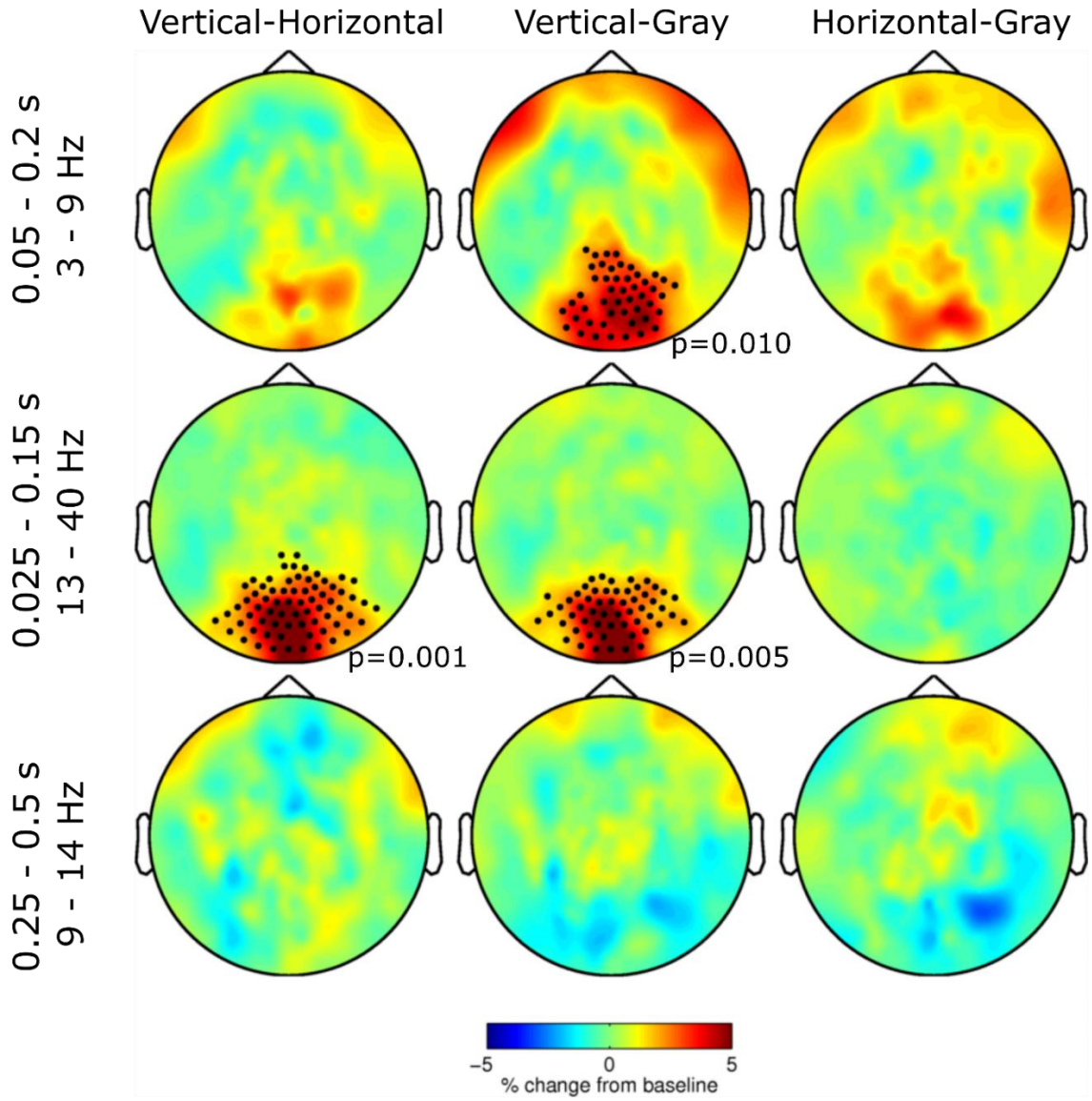

Figure 5-4 Topographies of the differences between each pair of the three stimulus conditions (columns) for the three identified microsaccade-related effects (rows). The black dots indicate clusters of sensors where a difference between conditions was significant according to cluster-based permutation tests.

5.5 Discussion

Using simultaneous recordings of eye movements with high-speed video eye tracking and brain activity with MEG in human subjects fixating a small spot, we investigated microsaccade-related changes in spectral power of visual cortex activity. Our paradigm consisted of long stimulus durations and enabled us to study responses to microsaccades as function of stimulus type while it also allowed us to isolate microsaccade-related responses from those related to stimulus onsets and offsets. We identified three microsaccade-related responses that had an occipital topography. First, in all three stimulus conditions (vertical grating, horizontal grating, and gray uniform image) we observed a transient increase in theta amplitude (3-9 Hz) that peaked ~ 0.125 s after microsaccade onset. This effect was stronger for microsaccades that occurred during the vertical grating presentation than during the gray image. Second, a transient increase in broadband beta amplitude (13 – 40 Hz) immediately after microsaccade onset was present only in the vertical grating condition. Third, a decrease in alpha (9 – 14) amplitude between 0.25 and 0.5 s was present in all conditions and we did not find any differences between conditions.

The theta response appears to be sensitive to stimulus type and as such it may reflect retinal motion. However, it does not critically depend on the presence of strong contrast because it was also observed in the uniform gray image condition. Our observation of microsaccade-related theta responses is supported by other findings in the literature. Theta increases in amplitude with a similar latency were also observed in macaque visual cortex following regular saccades during a pattern recognition task (Purpura 2003) and regular saccades made in complete darkness (Rajkai et al. 2008). The latter result may indicate that visual stimulation is not critical for the theta response but that the response is enhanced by receptive field displacement along contrast bars. What is a more, a number of studies have reported relevant results related to theta-phase

locking. Bosman et al. (2009) found that LFPs (in areas V1 and V4 of macaque monkey) in the same frequency were phase-locked to the onset of microsaccades and this phase-locking effect peaked around the same time as the theta response observed in our study. What is more Rajkai et al. (2008) suggested that theta oscillations phased-locked to fixation-onset enable post-fixational enhancement in visual processing because this phase resetting of an ongoing theta oscillation placed new retinal input in an optimal excitability phase. This phase locking of theta oscillations around 0.125 s after saccades is not specific to visual cortex but was also found in the hippocampus and may reflect a more general mechanism that spans multiple levels of neural processing (Hoffman et al. 2013). Although, we did not evaluate whether the theta component in our study was phase-locked to microsaccades, it is very likely that such transient, low frequency, early latency components reflect evoked activity phase-locked to the event of interest. In summary, although the early theta response is sensitive to stimulus type it may also represent a non-visual mechanism for structuring visual input for whom the presence of contrast or event luminance is not critical.

The fact that the beta response was higher in the vertical grating condition than in the other two conditions and also its early latency suggests that it reflects retinal stimulus motion. Receptive fields of most ganglion cells in the retina and of most neurons in the LGN have a simple centre-surround structure (Kuffler 1953) and respond either to the presentation of a light spot on a dark background (on-center) or to the presentation of a dark spot on a light background (off-center). Receptive fields in early stages of processing are also substantially smaller than in later stages. During vertical grating presentation horizontal microsaccades will displace the centre-surround receptive fields across the edges of the grating modulating activity of their respective neurons. During the horizontal grating presentation most of the microsaccades will displace the centre-surround receptive fields along the edges of the grating, and therefore not trigger a higher response than from

a uniform luminance screen. In summary, the beta response is likely to represents a purely bottom-up effect from early stages of visual processing.

Unlike the two responses described above, we did not find evidence that the microsaccade-related decrease in alpha amplitude was different in the three stimulus conditions. This may indicate that the alpha response reflects an extraretinal corollary signal. A number of authors have hypothesized about the existence of such a saccade and microsaccade-related corollary signal (Martinez-Conde et al. 2013; Rajkai et al. 2008; Melloni, Schwiedrzik, Rodriguez, et al. 2009). Low alpha amplitude was linked to improved visual processing such as in threshold level target detection (van Dijk et al. 2008). Enhanced excitability in the visual system has also been associated with reduced alpha amplitude (Lange et al. 2013). Therefore the alpha response observed in our study could potentially account for some of the functions of microsaccades in restoring vision, counteracting visual adaptation (Martinez-Conde et al. 2006; McCamy et al. 2012) and responding to low retinal image slip (Engbert & Mergenthaler 2006). However, we did not collect behavioural responses about the subjective stimulus visibility nor did we adjust our stimuli at threshold-level to induce visual fading. Therefore future studies will have to address the direct link between microsaccade-related reductions in alpha amplitude and stimulus visibility. Moreover, reductions in alpha amplitude are observed in covert attention tasks, however, we did not find any evidence for a relationship to microsaccades in Chapter 4.

In summary we succeeded, for the first time, to record non-invasively in humans visual spectral responses to very small, involuntary microsaccadic eye movements. A number of identified time-frequency components are likely to reflect retinal motion and extraretinal corollary signals.

Chapter 6:
General Discussion

6.1 Overview

The experiments reported in this thesis were designed to investigate the interplay between oscillations in the human visual cortex and microsaccades. Both neural oscillations and microsaccades serve important functions in visual processing and attention and therefore I hypothesized that they may be related. In the first section of this chapter, I show that characteristics of microsaccades in all experiments reported in this thesis matched those observed in other studies. It shows that we reliably detected and characterised microsaccades. In the second section, for each chapter separately, I present the implications of our findings and point to some future directions to further improve of our understanding of the relationship between oscillations and microsaccades. In the last section I present some general implications of our findings.

6.2 Microsaccade characteristics

To my knowledge, the experiments described in this thesis are the first reported experiments that succeeded in detecting microsaccades during MEG recordings. This was possible thanks to MEG-compatible video-based eye tracking. Estimating gaze from pupil position only, as opposed to using pupil position corrected by corneal reflection, resulted in substantially higher precision and enabled us to study even smaller microsaccades. An inflatable head-cuff and a chinrest were used to support the head and this way we avoided artefacts due to head movement. These methodological improvements can be applied to most video-based eye trackers and show that, even with equipment that is relatively cheap and no longer considered as state-of-the art, one can study microsaccades during brain activity recordings. We hope that our results will encourage more researchers to look at eye movement patterns during visual neuroscience experiments.

Additionally, a good validation for the eye tracking method used in our experiments is the fact that we observed all the microsaccade characteristics commonly reported in published articles. First, we observed that human subjects made on average ~ 1 microsaccade per second. Although the rate is slightly lower than in the majority of studies (Martinez-Conde et al. 2009) it is consistent with the fact that experience with fixating small spots (most our participants were very familiar with visual psychophysical tasks) and strong fixational instructions results in lower microsaccade rates (Steinman RM, Cunitz RJ, Timberlake GT 1967; Dimigen et al. 2009; Cherici et al. 2012). Moreover, microsaccade rates appeared to steadily decrease as participants anticipated an event (stimulus offset and target onset) that they were required to perform a behavioural task on (Hafed et al. 2011; Pastukhov & Braun 2010). Second, there was a strong linear relationship between microsaccade amplitude and peak velocity, the so called 'main sequence', due to the ballistic nature of microsaccades (Zuber et al. 1965; Bahill et al. 1975). Third, the vast majority of recorded microsaccades (> 90%) had horizontal directions (Rolfs 2009; Martinez-Conde et al. 2009). Fourth, the amplitude distribution peaked ~ 0.25 deg and tended to asymptote as it approached 1 deg (Martinez-Conde et al. 2009). Fifth, the distribution of inter-microsaccadic intervals peaked ~ 0.2 s and then decreased in an approximately exponential fashion, suggesting a possible rhythmic pattern of microsaccades (Otero-Millan et al. 2008; Bosman et al. 2009). Last, but not least, microsaccade characteristics were strongly modulated by cue and stimulus onsets (Engbert & Kliegl 2003; Laubrock et al. 2010; Rolfs et al. 2008). Both spatial cues and contrast stimuli first triggered a drop in microsaccade rate to a minimum shortly after stimulus onset (at ~ 0.15 s, 'microsaccadic inhibition') and then an increase to a higher rate (at ~0.25 s, 'microsaccadic rebound'). Finally, following spatial cues, microsaccade directions were biased towards the cue direction during the rebound interval. These results

suggest that microsaccades can be reliably detected in MEG and their relationship to visual oscillations can be effectively studied.

6.3 Implications and future directions

Having the means to carry high-precision eye tracking during MEG recordings opens up opportunities for conducting novel studies on the relationship between oscillations in the visual cortex and microsaccades.

In Chapter 3, we provided the first direct evidence that induced sustained visual gamma oscillations are not related to microsaccades. Therefore, the results support the view that these oscillations reflect a stimulus-driven, emergent cortical state that is generated within local cortical columns of primary visual cortex, via coupled populations of inhibitory interneurons and pyramidal cells (for a review see Fries et al. (2007)). Our results suggest that it does not reflect the eye muscle artefact concomitant with microsaccades or genuine cortical activity (retinal and extraretinal) evoked by microsaccades. This finding provides validity for the past and future studies of visual gamma oscillations and shows that human MEG studies, using source localization techniques, can probe similar mechanisms of high-frequency oscillations as invasive animal studies. It is still possible, however, that other MEG-measured gamma oscillations, especially those recorded at temporal and frontal sites, may be influenced by the microsaccadic muscle artefact. Future studies will have to determine whether these oscillations are related to microsaccades. It is also still possible that oscillations in other frequency bands (see Chapter 5) may reflect microsaccade-related cortical activity rather than task or stimulus related effects.

In the same experiment, we stumbled upon an interesting finding. Trials that contained microsaccades in the stimulus time-window showed reduced amplitude of the early transient broadband gamma response. While the cause of this effect cannot be

conclusively determined in our study because the of small number of trials, two interesting explanations can be proposed, based on the fact that trials with weak transient gamma amplitude appeared to have higher microsaccade rates around stimulus onset and during the rebound period (See Figure 7.3 in the Appendix). First, it may stem from the fact that microsaccades around stimulus onsets suppress the processing of the stimulus in line with the microsaccadic suppression phenomenon (Zuber et al. 1965). If this is really the case, it would be the first demonstration of microsaccadic suppression at a neural level reported in human studies. Second, it may be that weak transient gamma leads to a less efficient inhibition of microsaccades following stimulus onset, in which case it would provide the first mechanistic evidence for the possible determinants of the inhibition-rebound pattern of microsaccade rates after stimulus onset. The two explanations are not mutually exclusive. Future studies should employ designs with a larger number of trials to precisely map microsaccade dynamics associated with high and low amplitudes of oscillatory activity related to early visual processing.

In Chapter 4, we investigated the relationship between anticipatory alpha oscillations and microsaccades in covert spatial attention. We found that the pre-target lateralisation of alpha oscillation amplitude at occipital and parietal sites and microsaccade direction lateralisation were not related. We conclude that microsaccades and alpha oscillations play different roles in covert attention. The former may be important for initial shifting of attention and the latter may serve the function of maintaining sustained attention by inhibiting the processing of task-irrelevant information. Moreover, considering the rather recent discovery that eye movements are present during and are even modulated by covert attention (Engbert & Kliegl 2003; Hafed & Clark 2002), our results show that the alpha amplitude lateralisation is a robust phenomenon that cannot be explained by these eye movements. Future studies should try to determine the experimental conditions under

which sustained biasing of microsaccade directions towards cue direction occurs and test if the relationship to alpha oscillations is present in such tasks.

In Chapter 5 we recorded, for the first time, spectral responses time-locked (but not necessarily phase locked) to microsaccades at occipital sites in humans. Long stimulus presentations enabled us to study these responses as a function of stimulus type while making sure that the microsaccade-related activity is not confounded with activity related to stimulus onsets and offsets. Studying these responses should enable us to understand what impact microsaccades have on visual processing and disentangle retinal and extraretinal responses. We found microsaccade-related amplitude modulations in theta, alpha and beta frequency bands. The responses may reflect the structuring of visual input, a corollary mechanism that may potentially play a role enhancing visual performance, and processing of microsaccade-triggered retinal motion respectively. To conclusively test which spectral components are retinal and which are extraretinal, future studies could measure responses to microsaccades in complete darkness (excluding any influence of retinal motion), and measure responses to image movement that resembles retinal motion after microsaccades in the absence of actual eye movements (excluding any influence of extraretinal corollary signals). Moreover, microsaccade-related spectral responses should be studied during specific visual tasks together with behavioural performance so that they can be linked to specific visual functions.

6.4 General implications for the effect of microsaccades on visual oscillations

Although we showed that sustained visual gamma oscillations are not related to microsaccades, we cannot exclude the possibility that other central oscillatory activities are contaminated by, or even generated by, microsaccades. First, the possibility that microsaccades occurring at stimulus onset may supress the neural activity related to early

stimulus processing, 'microsaccadic suppression' as suggested in Chapter 3, can have important implications. In certain paradigms stimuli are presented with high temporal frequency, such as, for instance, in rapid serial visual presentation (RSVP) and in steady state visually evoked potentials (SSVEP) studies. If the frequency is ~ 4 Hz, every stimulus change will trigger the microsaccadic rebound effect (elevated microsaccade rates), that will peak approximately at the next change of the stimulus (after 0.25 s) and potentially suppress neural activity related to this change. Future studies should address this effect and it could be that stimulus presentation/change frequencies ~ 4 Hz should be avoided. Second, because as we showed, microsaccades modulate amplitude in a number of frequency bands, we propose that some stimulus/task effects observed in these frequency bands should be re-evaluated. To illustrate this I will provide a specific example. We showed that microsaccades reduce alpha amplitude, and other studies showed that microsaccades are related to target visibility (Martinez-Conde 2006; Costela et al. 2013) and visual excitability (Martinez-Conde et al. 2000). Reduced alpha amplitude, in turn, was also associated with target visibility (van Dijk et al. 2008) and enhanced visual system excitability (Lange et al. 2013). Therefore it is important to investigate whether microsaccades can account for these behavioural effects that are currently attributed to spontaneous fluctuations in alpha amplitude. Moreover, one can imagine how this logic can be applied to many other situations. To illustrate I will provide a hypothetical example. Imagine that some study found stronger beta amplitude after presentations of stimulus A than after presentation of stimulus B. If stimulus A contains more vertical contrast structure than stimulus B, these results could be explained by the microsaccade-related increases in beta amplitude during presentation of a vertical grating but not during a horizontal grating. Research grade, high-speed eye trackers are now widely available and all vision studies should use them to take into consideration patterns of fixational eye movements in their paradigms when interpreting their results. Future studies should also characterise

the temporal distribution of microsaccades and their amplitudes in non-standard paradigms, that is, other than those involving brief presentations of static stimuli (e.g. sustained motion presentation) to serve as a reference function for similar vision studies that could not detect microsaccades in their experiments.

Appendix

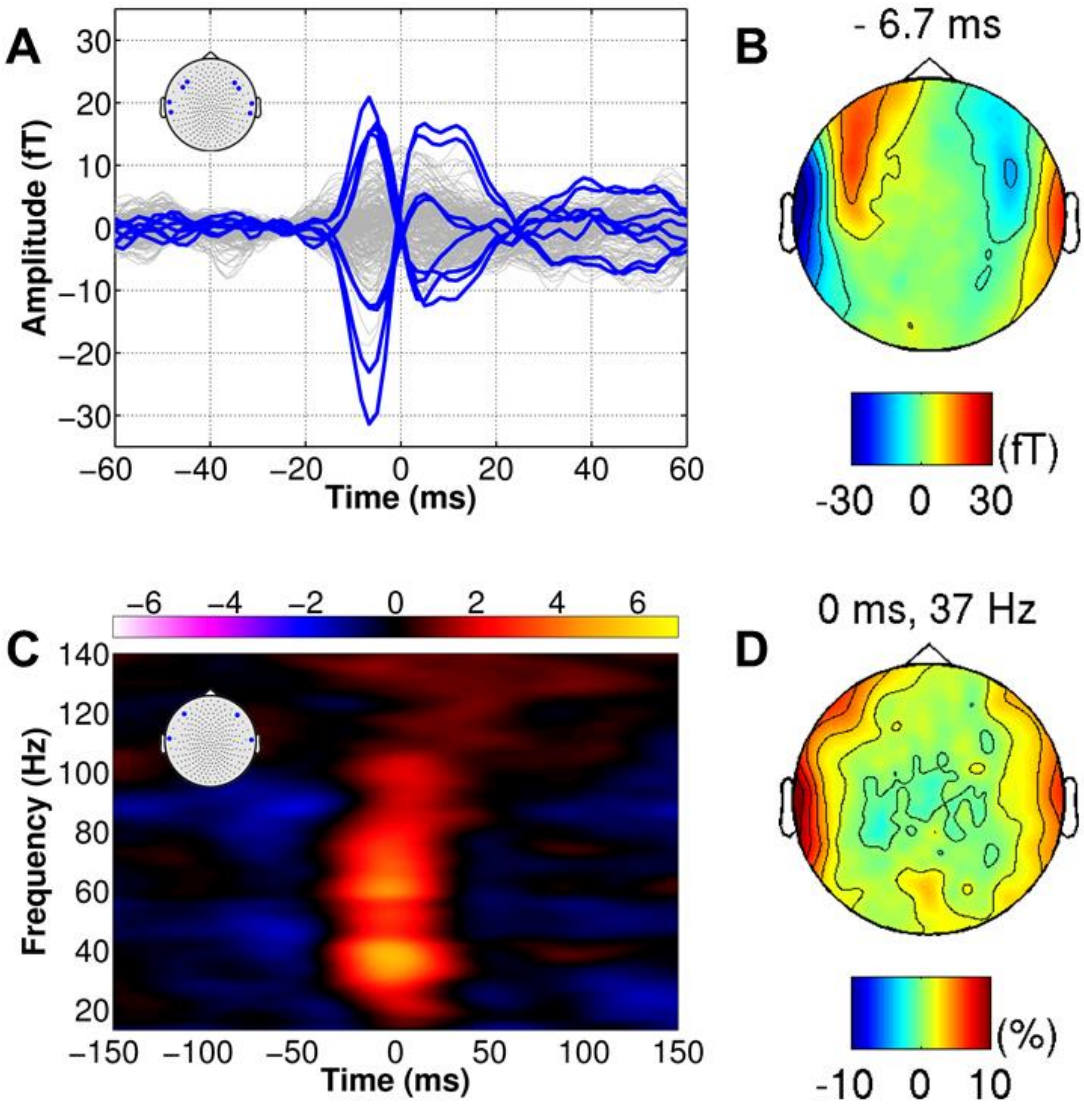

Figure. 7-1 (Chapter 3). Spike artefact characteristics. A. Grand average time courses aligned to microsaccade onsets. All sensors shown in gray and eight sensors with high amplitude (four temporal and four frontal, illustrated in the inset) highlighted in blue. **B**. Topography of the saccadic spike field from A at its first peak. **C**. Grand average power change around the onset of microsaccades across four selected sensors (two temporal and two frontal, illustrated in the inset). **D**. Topography of the relative power changes from C at 37 Hz. Relatively low values for 40 - 60 Hz are due to a notch filter used in order to remove the 50Hz line noise.

Microsaccadic spike artefact

Microsaccades, just like any other saccadic eye movements, are executed by extra ocular muscles and the contraction of these muscles is believed to produce the associated myographic artefact (Yuval-Greenberg et al. 2008; Keren et al. 2010; Carl et al. 2012). In MEG, this spike artefact has previously been thoroughly characterised for instructed large saccades and involuntary microsaccades (Carl et al. 2012). Here, we are showing artefact characteristics consistent with the previous report but based on microsaccades detected independently of the artefact using high-speed video eye tracking and during a condition of prolonged fixation. Average time courses (ERFs - event-related fields) of sensor data aligned to microsaccade onsets showed a transient bi-phasic field deflection that peaked 6.7 ms before microsaccade onset (Fig. 7-1 A). A second peak after microsaccade onset was probably distorted by the concurrent corneo-retinal artefact reflecting the rotation of the corneo-retinal dipole (Keren et al. 2010) and therefore had lower amplitude. Topography of the saccadic spike, estimated from the first peak, was characterized by increases and decreases at frontal and temporal sensors for our axial gradiometer MEG system (Fig. 7-1B). The average absolute amplitudes across subjects were highest at temporal and frontal sensors reaching 32 fT. Parietal and occipital sensors were relatively unaffected by the artefact. Time-frequency analysis of sensor data aligned to microsaccade onsets showed that the bi phasic deflection evident in ERFs, translated into a transient broadband increase in gamma amplitude (25 - 105 Hz) around microsaccade onset that peaked at 37 Hz (Fig.7-1 C) and had similar fronto-temporal topography (Fig. 7-1 D).

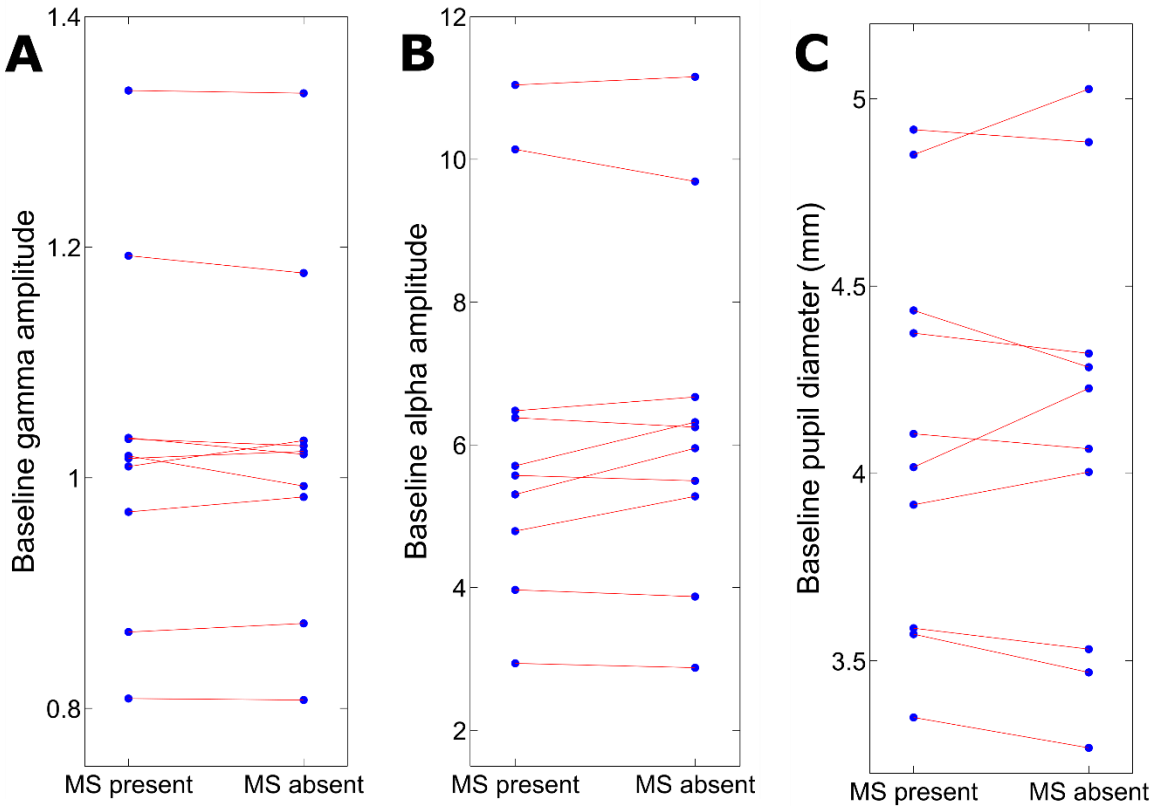

Figure 7-2 (Chapter 3). Control analysis for trials sorted into two groups (MS present and MS absent) based on whether at least one microsaccade occurred during stimulus presentation. Each pair of dots connected with a red line represents one subject. **A**. Baseline gamma amplitude. **B**. Baseline alpha amplitude. **C**. Baseline pupil diameter.

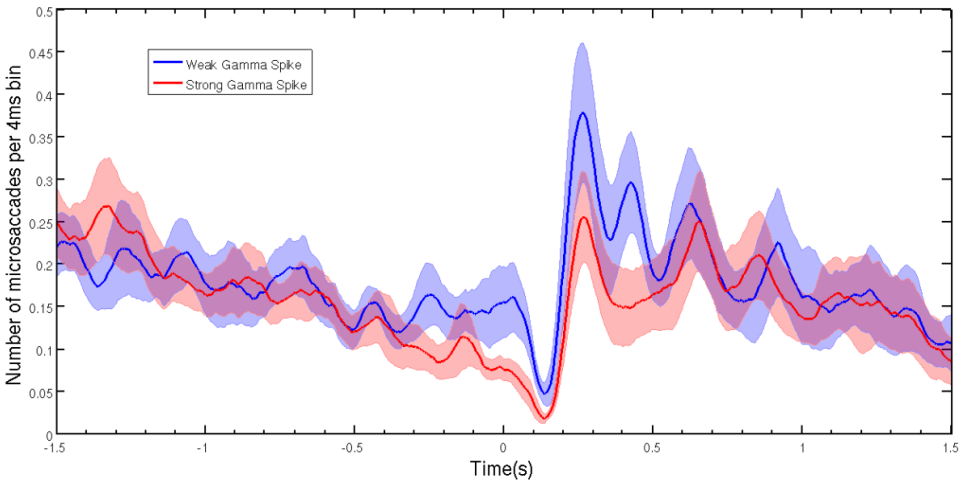

Figure 7-3. (Chapter 3). Time-courses of microsaccade rates plotted separately for trials with weak transient gamma (blue) and strong transient gamma (red) amplitudes (median split). The shaded regions indicate standard error of the mean. Time = 0 is stimulus onset.

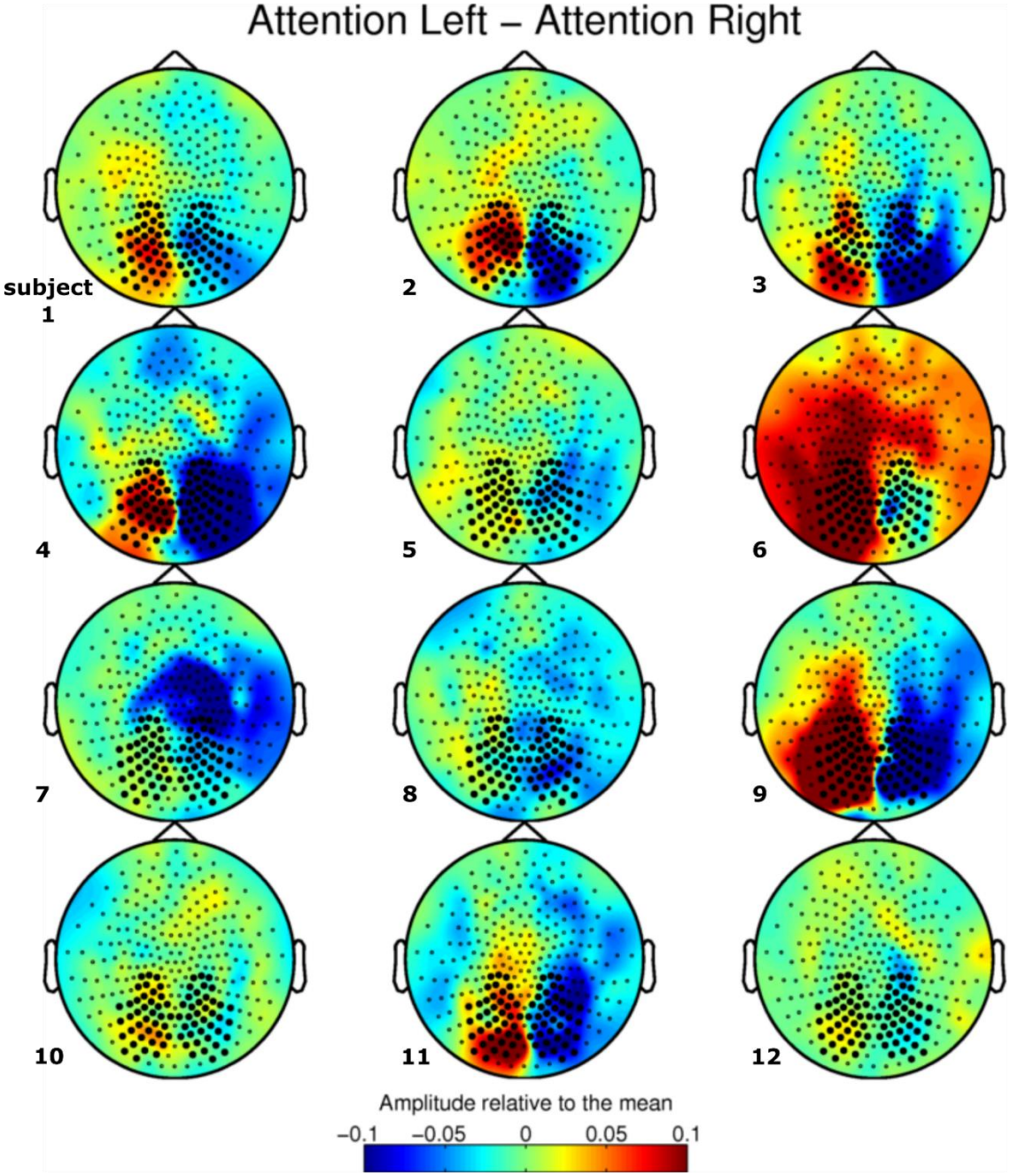

Figure 7-4. (Chapter 4). Topographical plots illustrating difference between Attention Left and Attention Right conditions for each subject separately. The difference is in mean-normalised amplitude of alpha frequency band (7-14 Hz) in the 0.25 – 2.25 time-window after cue onset. Subject numbers are shown in the bottom left corner of each plot.

References

Adjamian, P. et al., 2004. Induced visual illusions and gamma oscillations in human primary visual cortex. *European Journal of Neuroscience*, 20(2), pp.587–592.

Adrian, E.D. & Matthews, B.H., 1934. The interpretation of potential waves in the cortex. *Journal of Physiology*, 81(4), pp.440–471.

Aissani, C. et al., 2014. Beta, but not gamma, band oscillations index visual form-motion integration. *PloS one*, 9(4), pp.1 –11.

Amit, R. & Greenberg, S., 2015. Inter-dependency of microsaccades and its modulation by visual context. *Journal of Vision*, 15(12), p.1276.

Anton-Erxleben, K. & Carrasco, M., 2013. Attentional enhancement of spatial resolution: linking behavioural and neurophysiological evidence. *Nature Reviews Neuroscience*, 14(3), pp.188–200.

Aytekin, M., Victor, J.D. & Rucci, M., 2014. The Visual Input to the Retina during Natural Head-Free Fixation. *Journal of Neuroscience*, 34(38), pp.12701–12715.

Bahill, A.T., Clark, M.R. & Stark, L., 1975. The main sequence, a tool for studying human eye movements. *Mathematical Biosciences*, 24(3-4), pp.191–204.

Bair, W. et al., 1994. Power spectrum analysis of bursting cells in area MT in the behaving monkey. *Journal of Neuroscience*, 14(5), pp.2870–2892.

Bair, W. & O'Keefe, L.P., 1998. The influence of fixational eye movements on the response of neurons in area MT of the macaque. *Visual Neuroscience*, 15(4), pp.779–786.

Bastiaansen, M.C.M. & Knösche, T.R., 2000. Tangential derivative mapping of axial MEG applied to event-related desynchronization research. *Clinical Neurophysiology*, 111(7), pp.1300–1305.

Bastos, A.M. et al., 2014. Simultaneous Recordings from the Primary Visual Cortex and Lateral Geniculate Nucleus Reveal Rhythmic Interactions and a Cortical Source for Gamma-Band Oscillations. *Journal of Neuroscience*, 34(22), pp.7639–7644.

Beeler, G.W., 1967. Visual threshold changes resulting from spontaneous saccadic eye movements. *Vision Research*, 7(9-10), pp.769–775.

Boehnke, S.E. & Munoz, D.P., 2008. On the importance of the transient visual response in the superior colliculus. *Current Opinion in Neurobiology*, 18(6), pp.544–551.

Bonneh, Y.S., Adini, Y. & Polat, U., 2015. Contrast sensitivity revealed by microsaccades. *Journal of Vision*, 15(9), pp.1–12.

Bosman, C.A. et al., 2009. A Microsaccadic Rhythm Modulates Gamma-Band Synchronization and Behavior. *Journal of Neuroscience*, 29(30), pp.9471–9480.

Brainard, D.H., 1997. The Psychophysics Toolbox. *Spatial vision*, 10(4), pp.433–436.

Buzsáki, G., 2006. *Rhythms of the Brain*, USA: Oxford University Press.

Buzsáki, G., Anastassiou, C. a & Koch, C., 2012. The origin of extracellular fields and currents — EEG, ECoG, LFP and spikes. *Nature Reviews Neuroscience*, 13(6), pp.407–420.

Buzsáki, G. & Draguhn, A., 2004. Neuronal oscillations in cortical networks. *Science*, 304(5679), pp.1926–9.

Buzsáki, G. & Wang, X.-J., 2012. Mechanisms of Gamma Oscillations. *Annual Review of Neuroscience*, 35(1), pp.203–225.

Capotosto, P. et al., 2009. Frontoparietal cortex controls spatial attention through modulation of anticipatory alpha rhythms. *Journal of Neuroscience*, 29(18), pp.5863–5872.

Cardin, J.A. et al., 2009. Driving fast-spiking cells induces gamma rhythm and controls sensory responses. *Nature*, 459(7247), pp.663–667.

Carl, C. et al., 2012. The saccadic spike artifact in MEG. *NeuroImage*, 59(2), pp.1657–1667.

Carrasco, M., 2011. Visual attention: The past 25 years. *Vision Research*, 51(13), pp.1484–1525.

Castelo-Branco, M., Neuenschwander, S. & Singer, W., 1998. Synchronization of visual responses between the cortex, lateral geniculate nucleus, and retina in the anesthetized cat. *Journal of Neuroscience*, 18(16), pp.6395–6410.

Cherici, C. et al., 2012. Precision of sustained fixation in trained and untrained observers. *Journal of Vision*, 12(6), pp.1–16.

Cohen, M.X., 2011. It's about Time. *Frontiers in Human Neuroscience*, 5(January), p.2.

Collewijn, H. & Kowler, E., 2008. The significance of microsaccades for vision and oculomotor control. *Journal of Vision*, 8(14), pp.1–21.

Costela, F.M. et al., 2013. Microsaccades restore the visibility of minute foveal targets. *PeerJ*, 1, p.e119.

Cousijn, H. et al., 2014. Resting GABA and glutamate concentrations do not predict visual gamma frequency or amplitude. *Proceedings of the National Academy of Sciences of the United States of America*, 111(25), pp.9301–9306.

Crane, H.D. & Steele, C.M., 1985. Generation-V dual-Purkinje-image eyetracker. *Applied Optics*, 24(4), pp.527 – 537.

Croft, R.J. & Barry, R.J., 2000. Removal of ocular artifact from the EEG: a review. *Neurophysiologie Clinique/Clinical Neurophysiology*, 30(1), pp.5–19.

Crunelli, V. & Hughes, S.W., 2010. The slow (<1 Hz) rhythm of non-REM sleep: a dialogue between three cardinal oscillators. *Nature Neuroscience*, 13(1), pp.9–17.

Dehghani, N. et al., 2010. Comparative power spectral analysis of simultaneous elecroencephalographic and magnetoencephalographic recordings in humans suggests non-resistive extracellular media. *Journal of Computational Neuroscience*, 29(3), pp.405–421.

Destexhe, a, Contreras, D. & Steriade, M., 1999. Spatiotemporal analysis of local field potentials and unit discharges in cat cerebral cortex during …. *Journal of Neuroscience*, 19(11), pp.4595–4608.

van Dijk, H. et al., 2008. Prestimulus Oscillatory Activity in the Alpha Band Predicts Visual Discrimination Ability. *Journal of Neuroscience*, 28(8), pp.1816–1823.

Dimigen, O. et al., 2011. Coregistration of eye movements and EEG in natural reading: Analyses and review. *Journal of Experimental Psychology: General*, 140(4), pp.552–572.

Dimigen, O. et al., 2009. Human Microsaccade-Related Visual Brain Responses. *Journal of Neuroscience*, 29(39), pp.12321–12331.

Ditchburn, R.W. & Ginsborg, B.L., 1952. Vision with a stabilized retinal image. *Nature*, 170(4314), pp.36–37.

Donner, K. & Hemilä, S., 2007. Modelling the effect of microsaccades on retinal responses to stationary contrast patterns. *Vision Research*, 47(9), pp.1166–1177.

Donner, T.H. et al., 2007. Population Activity in the Human Dorsal Pathway Predicts the Accuracy of Visual Motion Detection. *Journal of Neurophysiology*, 98(1), pp.345–359.

Donner, T.H. & Siegel, M., 2011. A framework for local cortical oscillation patterns. *Trends in Cognitive Sciences*, 15(5), pp.191–199.

Duncan, K.K. et al., 2010. Identifying spatially overlapping local cortical networks with MEG. *Human Brain Mapping*, 31(7), pp.1003–1016.

Edden, R. a E. et al., 2009. Orientation Discrimination Performance Is Predicted by GABA Concentration and Gamma Oscillation Frequency in Human Primary Visual Cortex. *Journal of Neuroscience*, 29(50), pp.15721–15726.

Engbert, R., 2012. Computational Modeling of Collicular Integration of Perceptual Responses and Attention in Microsaccades. *Journal of Neuroscience*, 32(23),

pp.8035–8039.

Engbert, R., 2006. Microsaccades: a microcosm for research on oculomotor control, attention, and visual perception. In *Progress in Brain Research*. pp. 177–192.

Engbert, R. & Kliegl, R., 2004. Microsaccades keep the eyes' balance during fixation. *Psychological Science*, 15(6), pp.431–436.

Engbert, R. & Kliegl, R., 2003. Microsaccades uncover the orientation of covert attention. *Vision Research*, 43(9), pp.1035–1045.

Engbert, R. & Mergenthaler, K., 2006. Microsaccades are triggered by low retinal image slip. *Proceedings of the National Academy of Sciences of the United States of America*, 103(18), pp.7192–71977.

Engel, A.K. & Fries, P., 2010. Beta-band oscillations—signalling the status quo? *Current Opinion in Neurobiology*, 20(2), pp.156–165.

Engel, A.K., Fries, P. & Singer, W., 2001. Dynamic predictions: Oscillations and synchrony in top–down processing. *Nature Reviews Neuroscience*, 2(10), pp.704–716.

Frens, M. a, 2002. Scleral Search Coils Influence Saccade Dynamics. *Journal of Neurophysiology*, 88(2), pp.692–698.

Friedman-Hill, S., 2000. Dynamics of Striate Cortical Activity in the Alert Macaque: I. Incidence and Stimulus-dependence of Gamma-band Neuronal Oscillations. *Cerebral Cortex*, 10(11), pp.1105–1116.

Frien, A. et al., 2000. Fast oscillations display sharper orientation tuning than slower components of the same recordings in striate cortex of the awake monkey. *European Journal of Neuroscience*, 12(4), pp.1453–1465.

Fries, P., 2001. Modulation of Oscillatory Neuronal Synchronization by Selective Visual Attention. *Science*, 291(5508), pp.1560–1563.

Fries, P., 2009. Neuronal Gamma-Band Synchronization as a Fundamental Process in Cortical Computation. *Annual Review of Neuroscience*, 32(1), pp.209–224.

Fries, P., Nikolić, D. & Singer, W., 2007. The gamma cycle. *Trends in Neurosciences*, 30(7), pp.309–316.

Fries, P., Scheeringa, R. & Oostenveld, R., 2008. Finding Gamma. *Neuron*, 58(3), pp.303–305.

Funke, K., Kerscher, N.J. & Wörgötter, F., 2007. Noise-improved signal detection in cat primary visual cortex via a well-balanced stochastic resonance-like procedure. *European Journal of Neuroscience*, 26(5), pp.1322–1332.

Gandhi, N.J. & Katnani, H.A., 2011. Motor Functions of the Superior Colliculus. *Annual Review of Neuroscience*, 34(1), pp.205–231.

van Gerven, M. & Jensen, O., 2009. Attention modulations of posterior alpha as a control signal for two-dimensional brain-computer interfaces. *Journal of Neuroscience Methods*, 179(1), pp.78–84.

Gieselmann, M. a. & Thiele, a., 2008. Comparison of spatial integration and surround suppression characteristics in spiking activity and the local field potential in macaque V1. *European Journal of Neuroscience*, 28(3), pp.447–459.

Gray, C.M. & Singer, W., 1989. Stimulus-specific neuronal oscillations in orientation columns of cat visual cortex. *Proceedings of the National Academy of Sciences of the United States of America*, 86(5), pp.1698–1702.

Grützner, C. et al., 2013. Deficits in high- (>60 Hz) gamma-band oscillations during visual processing in schizophrenia. *Frontiers in Human Neuroscience*, 7(March), pp.1–11.

Guestrin, E.D. & Eizenman, M., 2006. General Theory of Remote Gaze Estimation Using the Pupil Center and Corneal Reflections. *IEEE Transactions on Biomedical Engineering*, 53(6), pp.1124–1133.

Hafed, Z.M., 2013. Alteration of Visual Perception prior to Microsaccades. *Neuron*, 77(4), pp.775–786.

Hafed, Z.M., 2011. Mechanisms for generating and compensating for the smallest possible saccades. *European Journal of Neuroscience*, 33(11), pp.2101–2113.

Hafed, Z.M. & Clark, J.J., 2002. Microsaccades as an overt measure of covert attention shifts. *Vision research*, 42(22), pp.2533–45.

Hafed, Z.M., Goffart, L. & Krauzlis, R.J., 2009. A Neural Mechanism for Microsaccade Generation in the Primate Superior Colliculus. *Science*, 323(5916), pp.940–943.

Hafed, Z.M. & Ignashchenkova, A., 2013. On the Dissociation between Microsaccade Rate and Direction after Peripheral Cues: Microsaccadic Inhibition Revisited. *Journal of Neuroscience*, 33(41), pp.16220–16235.

Hafed, Z.M. & Krauzlis, R.J., 2010. Microsaccadic Suppression of Visual Bursts in the Primate Superior Colliculus. *Journal of Neuroscience*, 30(28), pp.9542–9547.

Hafed, Z.M., Lovejoy, L.P. & Krauzlis, R.J., 2011. Modulation of Microsaccades in Monkey during a Covert Visual Attention Task. *Journal of Neuroscience*, 31(43), pp.15219–15230.

Hafed, Z.M., Lovejoy, L.P. & Krauzlis, R.J., 2013. Superior colliculus inactivation alters the relationship between covert visual attention and microsaccades. *European Journal of Neuroscience*, 37(7), pp.1169–1181.

Hall, S.D. et al., 2005. The missing link: analogous human and primate cortical gamma oscillations. *NeuroImage*, 26(1), pp.13–17.

Hämäläinen, M. et al., 1993. Magnetoencephalography—theory, instrumentation, and applications to noninvasive studies of the working human brain. *Reviews of Modern Physics*, 65(2), pp.413–497.

Händel, B.F., Haarmeier, T. & Jensen, O., 2011. Alpha Oscillations Correlate with the Successful Inhibition of Unattended Stimuli. *Journal of Cognitive Neuroscience*, 23(9), pp.2494–2502.

Hansen, D.W. & Ji, Q., 2010. In the eye of the beholder: a survey of models for eyes and gaze. *IEEE transactions on pattern analysis and machine intelligence*, 32(3), pp.478–500.

Hassler, U., Trujillo Barreto, N. & Gruber, T., 2011. Induced gamma band responses in human EEG after the control of miniature saccadic artifacts. *NeuroImage*, 57(4), pp.1411–1421.

Henrie, J.A. & Shapley, R., 2005. LFP Power Spectra in V1 Cortex: The Graded Effect of Stimulus Contrast. *Journal of Neurophysiology*, 94(1), pp.479–490.

Hermens, F., 2015. Dummy eye measurements of microsaccades : Testing the influence of system noise and head movements on microsaccade detection in a popular video-based eye tracker. *Journal of Eye Movements Research*, 8(1), pp.1–17.

Herring, J.D. et al., 2015. Attention Modulates TMS-Locked Alpha Oscillations in the Visual Cortex. *Journal of Neuroscience*, 35(43), pp.14435–14447.

Herrington, T.M. et al., 2009. The Effect of Microsaccades on the Correlation between Neural Activity and Behavior in Middle Temporal, Ventral Intraparietal, and Lateral Intraparietal Areas. *Journal of Neuroscience*, 29(18), pp.5793–5805.

Herrmann, K. et al., 2010. When size matters: attention affects performance by contrast or response gain. *Nature Neuroscience*, 13(12), pp.1554–1559.

Hipp, J.F. & Siegel, M., 2013. Dissociating neuronal gamma-band activity from cranial and ocular muscle activity in EEG. *Frontiers in Human Neuroscience*, 7(July), p.338.

Hoffman, K.L. et al., 2013. Saccades during visual exploration align hippocampal 3–8 Hz rhythms in human and non-human primates. *Frontiers in Systems Neuroscience*, 7(August), p.43.

Holmqvist, K. et al., 2011. *Eye Tracking: A comprehensive guide to methods and measures.* 1st ed., Oxford: Oxford University Press.

Holmqvist, K., Nyström, M. & Mulvey, F., 2012. Eye tracker data quality: what it is and how to measure it. *Eye Tracking Research and Applications*, 1(212), pp.45–52.

Hoogenboom, N. et al., 2006. Localizing human visual gamma-band activity in frequency, time and space. *NeuroImage*, 29(3), pp.764–773.

Hoogenboom, N. et al., 2010. Visually induced gamma-band activity predicts speed of change detection in humans. *NeuroImage*, 51(3), pp.1162–1167.

Jensen, O. et al., 2015. Oscillatory mechanisms of feedforward and feedback visual processing. *Trends in Neurosciences*, 38(4), pp.192–194.

Jensen, O. et al., 2014. Temporal coding organized by coupled alpha and gamma oscillations prioritize visual processing. *Trends in Neurosciences*, 37(7), pp.357–369.

Jensen, O. & Mazaheri, A., 2010. Shaping Functional Architecture by Oscillatory Alpha Activity: Gating by Inhibition. *Frontiers in Human Neuroscience*, 4(November), p.186.

Jia, X., Smith, M. a & Kohn, A., 2011. Stimulus Selectivity and Spatial Coherence of Gamma Components of the Local Field Potential. *Journal of Neuroscience*, 31(25), pp.9390–9403.

Jung, T.P. et al., 2000. Removing electroencephalographic artifacts by blind source separation. *Psychophysiology*, 37(2), pp.163–178.

Kagan, I., Gur, M. & Snodderly, D.M., 2008. Saccades and drifts differentially modulate neuronal activity in V1: Effects of retinal image motion, position, and extraretinal influences. *Journal of Vision*, 8(14), pp.19–19.

Kapoula, Z. et al., 2014. Distinctive features of microsaccades in Alzheimer's disease and in mild cognitive impairment. *Age*, 36(2), pp.535–543.

Keil, J. et al., 2014. Prestimulus Beta Power and Phase Synchrony Influence the Sound-Induced Flash Illusion. *Cerebral Cortex*, 24(5), pp.1278–1288.

Keren, A.S., Yuval-Greenberg, S. & Deouell, L.Y., 2010. Saccadic spike potentials in gamma-band EEG: characterization, detection and suppression. *NeuroImage*, 49(3), pp.2248–63.

Khalilov, I. et al., 1997. A novel in vitro preparation: The intact hippocampal formation. *Neuron*, 19(4), pp.743–749.

Kimmel, D.L., Mammo, D. & Newsome, W.T., 2012. Tracking the eye non-invasively: simultaneous comparison of the scleral search coil and optical tracking techniques in the macaque monkey. *Frontiers in Behavioral Neuroscience*, 6(August), p.49.

Klein, R.M., 2000. Inhibition of return. *Trends in Cognitive Sciences*, 4(4), pp.138–147.

Klimesch, W., 2012. Alpha-band oscillations, attention, and controlled access to stored information. *Trends in Cognitive Sciences*, 16(12), pp.606–617.

Klimesch, W., 1996. Memory processes, brain oscillations and EEG synchronization. *International Journal of Psychophysiology*, 24(1-2), pp.61–100.

Klimesch, W., Sauseng, P. & Hanslmayr, S., 2007. EEG alpha oscillations: The inhibition-timing hypothesis. *Brain Research Reviews*, 53(1), pp.63–88.

Ko, H.-K., Poletti, M. & Rucci, M., 2010. Microsaccades precisely relocate gaze in a high visual acuity task. *Nature Neuroscience*, 13(12), pp.1549–1553.

Koelewijn, L. et al., 2013. Spatial attention increases high-frequency gamma synchronisation in human medial visual cortex. *NeuroImage*, 79, pp.295–303.

Kolakowski, S.M. & Pelz, J.B., 2006. Compensating for eye tracker camera movement. In *Proceedings of the 2006 symposium on Eye tracking research applications ETRA 06*. p. 79.

Kowler, E., 2011. Eye movements: The past 25years. *Vision Research*, 51(13), pp.1457–1483.

Kuffler, S.W., 1953. Dischard patterns and functional organisation of mammalian retina. *Journal of Neurophysiology*, 16(1), pp.37–68.

Lange, J., Oostenveld, R. & Fries, P., 2013. Reduced Occipital Alpha Power Indexes Enhanced Excitability Rather than Improved Visual Perception. *Journal of Neuroscience*, 33(7), pp.3212–3220.

Laubrock, J. et al., 2007. Microsaccades Are an Index of Covert Attention: Commentary on Horowitz, Fine, Fencsik, Yurgenson, and Wolfe (2007). *Psychological Science*, 18(4), pp.364–366.

Laubrock, J. et al., 2010. When do microsaccades follow spatial attention? *Attention, Perception, & Psychophysics*, 72(3), pp.683–694.

Leopold, D. a. & Logothetis, N.K., 1998. Microsaccades differentially modulate neural activity in the striate and extrastriate visual cortex. *Experimental Brain Research*, 123(3), pp.341–345.

Logothetis, N.K. et al., 2001. Neurophysiological investigation of the basis of the fMRI signal. *Nature*, 412(6843), pp.150–157.

Lopes da Silva, F., 2013. EEG and MEG: Relevance to Neuroscience. *Neuron*, 80(5), pp.1112–1128.

Lutzenberger, W. et al., 1995. Visual stimulation alters local 40-Hz responses in humans: An EEG-study. *Neuroscience Letters*, 183(1-2), pp.39–42.

Maier, A. et al., 2008. Divergence of fMRI and neural signals in V1 during perceptual suppression in the awake monkey. *Nature Neuroscience*, 11(10), pp.1193–1200.

Makeig, S. et al., 2004. Mining event-related brain dynamics. *Trends in Cognitive Sciences*, 8(5), pp.204–210.

Maris, E. & Oostenveld, R., 2007. Nonparametric statistical testing of EEG- and MEG-data. *Journal of Neuroscience Methods*, 164(1), pp.177–190.

Marshall, T.R. et al., 2015. Frontal Eye Fields Control Attentional Modulation of Alpha and

Gamma Oscillations in Contralateral Occipitoparietal Cortex. *Journal of Neuroscience*, 35(4), pp.1638–1647.

Martinez-Conde, S., 2006. Fixational eye movements in normal and pathological vision. In *Progres in Brain Research*. pp. 151–176.

Martinez-Conde, S. et al., 2006. Microsaccades counteract visual fading during fixation. *Neuron*, 49(2), pp.297–305.

Martinez-Conde, S. et al., 2009. Microsaccades: a neurophysiological analysis. *Trends in Neurosciences*, 32(9), pp.463–475.

Martinez-Conde, S., Macknik, S.L. & Hubel, D.H., 2000. Microsaccadic eye movements and firing of single cells in the striate cortex of macaque monkeys. *Nature Neuroscience*, 3(3), pp.251–258.

Martinez-Conde, S., Macknik, S.L. & Hubel, D.H., 2002. The function of bursts of spikes during visual fixation in the awake primate lateral geniculate nucleus and primary visual cortex. *Proceedings of the National Academy of Sciences*, 99(21), pp.13920–13925.

Martinez-Conde, S., Macknik, S.L. & Hubel, D.H., 2004. The role of fixational eye movements in visual perception. *Nature Reviews Neuroscience*, 5(3), pp.229–240.

Martinez-Conde, S., Otero-Millan, J. & Macknik, S.L., 2013. The impact of microsaccades on vision: towards a unified theory of saccadic function. *Nature Reviews Neuroscience*, 14(2), pp.83–96.

McCamy, M.B. et al., 2014. Highly Informative Natural Scene Regions Increase Microsaccade Production during Visual Scanning. *Journal of Neuroscience*, 34(8), pp.2956–2966.

McCamy, M.B. et al., 2012. Microsaccadic Efficacy and Contribution to Foveal and Peripheral Vision. *Journal of Neuroscience*, 32(27), pp.9194–9204.

McCamy, M.B., Najafian Jazi, A., et al., 2013. The effects of fixation target size and luminance on microsaccades and square-wave jerks. *PeerJ*, 1, p.e9.

McCamy, M.B., Macknik, S.L. & Martinez-Conde, S., 2014. Different fixational eye movements mediate the prevention and the reversal of visual fading. *The Journal of Physiology*, 592(19), pp.4381–4394.

McCamy, M.B., Macknik, S.L. & Martinez-Conde, S., 2013. Natural Eye Movements and Vision. In J. S. Werner & L. M. Chalupa, eds. *The New Visual Neurosciences*. Camridge: MIT Press, pp. 849–863.

Melloni, L., Schwiedrzik, C.M., Rodriguez, E., et al., 2009. (Micro)Saccades, corollary activity and cortical oscillations. *Trends in Cognitive Sciences*, 13(6), pp.239–245.

Melloni, L., Schwiedrzik, C.M., Wibral, M., et al., 2009. Response to: Yuval-Greenberg et al., “Transient Induced Gamma-Band Response in EEG as a Manifestation of Miniature Saccades.” Neuron 58, 429-441. *Neuron*, 62(1), pp.8–10; author reply 10–12.

Merchant, J., Morrissette, R. & Porterfield, J.L., 1974. Remote Measurement of Eye Direction Allowing Subject Motion Over One Cubic Foot of Space. *IEEE Transactions on Biomedical Engineering*, BME-21(4), pp.309–317.

Montgomery, S.M. & Buzsáki, G., 2007. Gamma oscillations dynamically couple hippocampal CA3 and CA1 regions during memory task performance. *Proceedings of the National Academy of Sciences of the United States of America*, 104(36), pp.14495–14500.

Morimoto, C.H. & Mimica, M.R.M., 2005. Eye gaze tracking techniques for interactive applications. *Computer Vision and Image Understanding*, 98(1), pp.4–24.

Muller, M. et al., 1996. Visually induced gamma-band responses in human electroencephalographic activity ? a link to animal studies. *Experimental Brain Research*, 112(1), pp.96–102.

Muthukumaraswamy, S.D., 2013. High-frequency brain activity and muscle artifacts in MEG/EEG: a review and recommendations. *Frontiers in Human Neuroscience*, 7(April), p.138.

Muthukumaraswamy, S.D. et al., 2009. Resting GABA concentration predicts peak gamma frequency and fMRI amplitude in response to visual stimulation in humans. *Proceedings of the National Academy of Sciences of the United States of America*, 106(20), pp.8356–8361.

Muthukumaraswamy, S.D. et al., 2010. Visual gamma oscillations and evoked responses: variability, repeatability and structural MRI correlates. *NeuroImage*, 49(4), pp.3349–3357.

Muthukumaraswamy, S.D. & Singh, K.D., 2008. Spatiotemporal frequency tuning of BOLD and gamma band MEG responses compared in primary visual cortex. *NeuroImage*, 40(4), pp.1552–1560.

Muthukumaraswamy, S.D. & Singh, K.D., 2013. Visual gamma oscillations: The effects of stimulus type, visual field coverage and stimulus motion on MEG and EEG recordings. *NeuroImage*, 69, pp.223–230.

Nagasawa, T. et al., 2011. Occipital gamma-oscillations modulated during eye movement tasks: Simultaneous eye tracking and electrocorticography recording in epileptic patients. *NeuroImage*, 58(4), pp.1101–1109.

Nichols, T.E. & Holmes, A.P., 2002. Nonparametric permutation tests for functional neuroimaging: a primer with examples. *Human brain mapping*, 15(1), pp.1–25.

Nyström, M., Hooge, I. & Holmqvist, K., 2013. Post-saccadic oscillations in eye movement data recorded with pupil-based eye trackers reflect motion of the pupil inside the iris. *Vision Research*, 92, pp.59–66.

Oeltermann, A., Ku, S.-P. & Logothetis, N.K., 2007. A novel functional magnetic resonance imaging compatible search-coil eye-tracking system. *Magnetic Resonance Imaging*, 25(6), pp.913–922.

Okazaki, M. et al., 2008. Perceptual change in response to a bistable picture increases neuromagnetic beta-band activities. *Neuroscience Research*, 61(3), pp.319–328.

Oostendorp, T.F., Delbeke, J. & Stegeman, D.F., 2000. The conductivity of the human skull: Results of in vivo and in vitro measurements. *IEEE Transactions on Biomedical Engineering*, 47(11), pp.1487–1492.

Oostenveld, R. et al., 2011. FieldTrip: Open Source Software for Advanced Analysis of MEG, EEG, and Invasive Electrophysiological Data. *Computational Intelligence and Neuroscience*, 2011, pp.1–9.

Ossandon, J.P. et al., 2010. Superposition Model Predicts EEG Occipital Activity during Free Viewing of Natural Scenes. *Journal of Neuroscience*, 30(13), pp.4787–4795.

Otero-Millan, J. et al., 2011. Distinctive Features of Saccadic Intrusions and Microsaccades in Progressive Supranuclear Palsy. *Journal of Neuroscience*, 31(12), pp.4379–4387.

Otero-Millan, J. et al., 2008. Saccades and microsaccades during visual fixation, exploration, and search: foundations for a common saccadic generator. *Journal of Vision*, 8(14), pp.21.1–18.

Otero-Millan, J., Macknik, S.L. & Martinez-Conde, S., 2014. Fixational eye movements and binocular vision. *Frontiers in Integrative Neuroscience*, 8(July), pp.1–10.

Otero-Millan, J., Macknik, S.L. & Martinez-Conde, S., 2012. Microsaccades and Blinks Trigger Illusory Rotation in the “Rotating Snakes” Illusion. *Journal of Neuroscience*, 32(17), pp.6043–6051.

Palva, S. & Palva, J.M., 2007. New vistas for ??-frequency band oscillations. *Trends in Neurosciences*, 30(4), pp.150–158.

Pastukhov, A. & Braun, J., 2010. Rare but precious: Microsaccades are highly informative about attentional allocation. *Vision Research*, 50(12), pp.1173–1184.

van Pelt, S., Boomsma, D.I. & Fries, P., 2012. Magnetoencephalography in Twins Reveals a Strong Genetic Determination of the Peak Frequency of Visually Induced Gamma-

Band Synchronization. *Journal of Neuroscience*, 32(10), pp.3388–3392.

Perry, G., 2015. The effects of cross-orientation masking on the visual gamma response in humans. *European Journal of Neuroscience*, 41(11), pp.1484–1495.

Perry, G. et al., 2013. The properties of induced gamma oscillations in human visual cortex show individual variability in their dependence on stimulus size. *NeuroImage*, 68, pp.83–92.

Pesaran, B. et al., 2002. Temporal structure in neuronal activity during working memory in macaque parietal cortex. *Nature Neuroscience*, 5(8), pp.805–811.

Pfurtscheller, G., 2001. Functional brain imaging based on ERD/ERS. *Vision Research*, 41(10-11), pp.1257–1260.

Piantoni, G., Kline, K.A. & Eagleman, D.M., 2010. Beta oscillations correlate with the probability of perceiving rivalrous visual stimuli. *Journal of Vision*, 10(13), pp.18–27.

Plöchl, M., Ossandón, J.P. & König, P., 2012. Combining EEG and eye tracking: identification, characterization, and correction of eye movement artifacts in electroencephalographic data. *Frontiers in Human Neuroscience*, 6(October), p.278.

Poletti, M. & Rucci, M., 2015. A compact field guide to the study of microsaccades: Challenges and functions. *Vision Research*, pp.1–15.

Poletti, M. & Rucci, M., 2010. Eye movements under various conditions of image fading. *Journal of Vision*, 10(3), pp.1–18.

Posner, M.I., 1980. Orienting of attention. *Quarterly Journal of Experimental Psychology*, 32(1), pp.3–25.

Purpura, K.P., 2003. Analysis of Perisaccadic Field Potentials in the Occipitotemporal Pathway During Active Vision. *Journal of Neurophysiology*, 90(5), pp.3455–3478.

Rajkai, C. et al., 2008. Transient Cortical Excitation at the Onset of Visual Fixation. *Cerebral Cortex*, 18(1), pp.200–209.

Ray, S. & Maunsell, J.H.R., 2010. Differences in Gamma Frequencies across Visual Cortex Restrict Their Possible Use in Computation. *Neuron*, 67(5), pp.885–896.

Ray, S. & Maunsell, J.H.R., 2011. Different Origins of Gamma Rhythm and High-Gamma Activity in Macaque Visual Cortex L. Ungerleider, ed. *PLoS Biology*, 9(4), p.e1000610.

Ray, W. & Cole, H., 1985. EEG alpha activity reflects attentional demands, and beta activity reflects emotional and cognitive processes. *Science*, 228(4700), pp.750–752.

Reppas, J.B., Usrey, W.M. & Reid, R.C., 2002. Saccadic Eye Movements Modulate Visual Responses in the Lateral Geniculate Nucleus. *Neuron*, 35(5), pp.961–974.

Riggs, L. & Ratliff, F., 1952. The effects of counteracting the normal movements of the

eye. *Journal of the Optical Society of America*, 42, pp.872 – 873.

Rihs, T. a., Michel, C.M. & Thut, G., 2009. A bias for posterior ??-band power suppression versus enhancement during shifting versus maintenance of spatial attention. *NeuroImage*, 44(1), pp.190–199.

Rolfs, M., 2009. Microsaccades: Small steps on a long way. *Vision Research*, 49(20), pp.2415–2441.

Rolfs, M., Kliegl, R. & Engbert, R., 2008. Toward a model of microsaccade generation: the case of microsaccadic inhibition. *Journal of vision*, 8(11), pp.1–23.

Rols, G. et al., 2001. Cortical mapping of gamma oscillations in areas V1 and V4 of the macaque monkey. *Visual Neuroscience*, 18(4), pp.527–540.

Romei, V., Gross, J. & Thut, G., 2010. On the Role of Prestimulus Alpha Rhythms over Occipito-Parietal Areas in Visual Input Regulation: Correlation or Causation? *Journal of Neuroscience*, 30(25), pp.8692–8697.

Ross, J., Morrone, M.C. & Burr, D.C., 1997. Compression of visual space before saccades. *Nature*, 386(6625), pp.598–601.

Rucci, M. et al., 2007. Miniature eye movements enhance fine spatial detail. *Nature*, 447(7146), pp.851–854.

Saxena, N. et al., 2013. Enhanced Stimulus-Induced Gamma Activity in Humans during Propofol-Induced Sedation. *PLoS ONE*, 8(3), pp.1–7.

Schmiedt, J.T. et al., 2014. Beta Oscillation Dynamics in Extrastriate Cortex after Removal of Primary Visual Cortex. *Journal of Neuroscience*, 34(35), pp.11857–11864.

Scholte, H.S., Spekreijse, H. & Roelfsema, P.R., 2001. The spatial profile of visual attention in mental curve tracing. *Vision Research*, 41(20), pp.2569–2580.

Shaw, A.D. et al., 2015. Ketamine amplifies induced gamma frequency oscillations in the human cerebral cortex. *European Neuropsychopharmacology*, 25(8), pp.1136–1146.

Siegel, M. et al., 2006. High-Frequency Activity in Human Visual Cortex Is Modulated by Visual Motion Strength. *Cerebral Cortex*, 17(3), pp.732–741.

Siegel, M. et al., 2008. Neuronal Synchronization along the Dorsal Visual Pathway Reflects the Focus of Spatial Attention. *Neuron*, 60(4), pp.709–719.

Singer, W., 1999. Neuronal Synchrony: A Versatile Code Review for the Definition of Relations? *Neuron*, 24, pp.49–65.

Singer, W. & Gray, C.M., 1995. Visual feature integration and the temporal correlation hypothesis. *Annual review of neuroscience*, 18, pp.555–586.

Singh, K.D., 2006. Magnetoencephalography. In C. Senior, T. Russell, & M. S. Gazzaniga, eds. *Methods in Mind*. Hong Kong: MIT Press, pp. 291 – 326.

Sinn, P. & Engbert, R., 2015. Small saccades versus microsaccades: Experimental distinction and model-based unification. *Vision Research*.

Sohal, V.S., 2012. Insights into cortical oscillations arising from optogenetic studies. *Biological Psychiatry*, 71(12), pp.1039–1045.

Stampe, D.M., 1993. Heuristic filtering and reliable calibration methods for video-based pupil-tracking systems. *Behavior Research Methods, Instruments, & Computers*, 25(2), pp.137–142.

Steinman RM, Cunitz RJ, Timberlake GT, H.M., 1967. Voluntary control of microsaccades during maintained monocular fixation. *Science*, 155, pp.1577–1579.

Steriade, M., 2001. Impact of network activities on neuronal properties in corticothalamic systems. *Journal of Neurophysiology*, 86(1), pp.1–39.

Steriade, M., McCormick, D. & Sejnowski, T., 1993. Thalamocortical oscillations in the sleeping and aroused brain. *Science*, 262(5134), pp.679–685.

Swettenham, J.B., Muthukumaraswamy, S.D. & Singh, K.D., 2009. Spectral Properties of Induced and Evoked Gamma Oscillations in Human Early Visual Cortex to Moving and Stationary Stimuli. *Journal of Neurophysiology*, 102(2), pp.1241–1253.

Tallon-Baudry, C. et al., 1996. Stimulus specificity of phase-locked and non-phase-locked 40 Hz visual responses in human. *Journal of Neuroscience*, 16(13), pp.4240–4249.

Thaler, L. et al., 2013. What is the best fixation target? The effect of target shape on stability of fixational eye movements. *Vision Research*, 76, pp.31–42.

Thickbroom, G. & Mastaglia, F., 1985. Presaccadic “spike”potential: investigation of topography and source. *Brain Rsearch*, 339, pp.271–280.

Thut, G. et al., 2006. Alpha-Band Electroencephalographic Activity over Occipital Cortex Indexes Visuospatial Attention Bias and Predicts Visual Target Detection. *Journal of Neuroscience*, 26(37), pp.9494–9502.

Thut, G., Miniussi, C. & Gross, J., 2012. The functional importance of rhythmic activity in the brain. *Current Biology*, 22(16), pp.R658–R663.

Troncoso, X.G. et al., 2013. V1 neurons can distinguish between motion in the world and visual displacements due to eye movements: a microsaccade study. *BMC Neuroscience*, 14(Suppl 1), p.P262.

Tse, P., Baumgartner, F. & Greenlee, M., 2010. fMRI BOLD signal reveals neural correlates of microsaccades. *Journal of Vision*, 7(9), pp.318–318.

Tse, P.U., Baumgartner, F.J. & Greenlee, M.W., 2010. Event-related functional MRI of cortical activity evoked by microsaccades, small visually-guided saccades, and eyeblinks in human visual cortex. *NeuroImage*, 49(1), pp.805–816.

Uhlhaas, P.J. & Singer, W., 2010. Abnormal neural oscillations and synchrony in schizophrenia. *Nature Reviews Neuroscience*, 11(2), pp.100–113.

Ungerleider, S.K. and L.G., 2000. Mechanisms of Visual Attention in the Human Cortex. *Annual Review of Neuroscience*, 23(1), pp.315–341.

Valsecchi, M., Betta, E. & Turatto, M., 2007. Visual oddballs induce prolonged microsaccadic inhibition. *Experimental Brain Research*, 177(2), pp.196–208.

Le Van Quyen, M. & Bragin, A., 2007. Analysis of dynamic brain oscillations: methodological advances. *Trends in Neurosciences*, 30(7), pp.365–373.

Wang, X.-J., 2006. *Encyclopedia of Cognitive Science* L. Nadel, ed., Chichester: John Wiley & Sons, Ltd.

Wehner, D.T. et al., 2008. Head movements of children in MEG: Quantification, effects on source estimation, and compensation. *NeuroImage*, 40(2), pp.541–550.

Wehr, M. & Laurent, G., 1996. Odour encoding by temporal sequences of firing in oscillating neural assemblies. *Nature*, 384, pp.356–358.

Whitham, E.M. et al., 2007. Scalp electrical recording during paralysis: Quantitative evidence that EEG frequencies above 20Hz are contaminated by EMG. *Clinical Neurophysiology*, 118(8), pp.1877–1888.

Wilke, M., Logothetis, N.K. & Leopold, D. a, 2006. Local field potential reflects perceptual suppression in monkey visual cortex. *Proceedings of the National Academy of Sciences*, 103(46), pp.17507–17512.

Willard, A. & Lueck, C.J., 2014. Ocular motor disorders. *Current Opinion in Neurology*, 27(1), pp.75–82.

Worden, M.S. et al., 2000. Anticipatory biasing of visuospatial attention indexed by retinotopically specific alpha-band electroencephalography increases over occipital cortex. *Journal of Neuroscience*, 20(RC6), pp.1–6.

Wyart, V. & Tallon-Baudry, C., 2008. Neural Dissociation between Visual Awareness and Spatial Attention. *Journal of Neuroscience*, 28(10), pp.2667–2679.

Xing, D. et al., 2012. Laminar analysis of visually evoked activity in the primary visual cortex. *Proceedings of the National Academy of Sciences*, 109(34), pp.13871–13876.

Yeshurun, Y. & Carrasco, M., 1998. Attention improves or impairs visual performance by enhancing spatial resolution. *Nature*, 396(6706), pp.72–75.

Yuste, R., 2015. From the neuron doctrine to neural networks. *Nature Reviews Neuroscience*, 16(8), pp.487–497.

Yuval-Greenberg, S. et al., 2009. Response to Letter: Melloni et al., “Transient Induced

Gamma-Band Response in EEG as a Manifestation of Miniature Saccades.” Neuron 58, 429–441. *Neuron*, 62(1), pp.10–12.

Yuval-Greenberg, S. et al., 2008. Transient induced gamma-band response in EEG as a manifestation of miniature saccades. *Neuron*, 58(3), pp.429–41.

Yuval-Greenberg, S., Merriam, E.P. & Heeger, D.J., 2014. Spontaneous Microsaccades Reflect Shifts in Covert Attention. *Journal of Neuroscience*, 34(41), pp.13693–13700.

Zuber, B.L. & Stark, L., 1966. Saccadic suppression: Elevation of visual threshold associated with saccadic eye movements. *Experimental Neurology*, 16(1), pp.65–79.

Zuber, B.L., Start, L. & Cook, G., 1965. Velocity-Amplitude Relationship. *Science*, 150(July), pp.1459–1460.

Zumer, J.M. et al., 2014. Occipital Alpha Activity during Stimulus Processing Gates the Information Flow to Object-Selective Cortex. *PLoS Biology*, 12(10), p.e1001965.

Zumer, J.M. et al., 2010. Relating BOLD fMRI and neural oscillations through convolution and optimal linear weighting. *NeuroImage*, 49(2), pp.1479–1489.